UNIVERSITY OF WEST BOHEMIA
FACULTY OF ELECTRICAL ENGINEERING

APPROXIMATE PREDICTIVE CONTROL OF AC ELECTRIC DRIVES

A thesis submitted to the University of West Bohemia, Faculty of electrical engineering, in fulfillment of the requirements for the degree of Doctor of Philosophy

Author:	Ing. Štěpán Janouš
Supervisor:	Prof. Ing. Zdeněk Peroutka, Ph.D.
Expert Adviser:	Doc. Ing. Václav Šmídl, Ph.D.
Date of state doctoral exam:	1.2.2013
Submited on:	May 2, 2017

Declaration

I submit this thesis to the University of West Bohemia, Faculty of electrical engineering, in fulfillment of the requirements for the degree of Doctor of Philosophy. I, declare, that this is my own work, which has been elaborated with the use of literature and sources listed in this thesis.

Pilsen May 2, 2017

. . . . . .
Ing. Štěpán Janouš

Declaration of the project garant

This work was supported by RICE – New Technologies and Concepts for Smart Industrial Systems, project No. LO1607. I, the undersigned, declare that Ing. Štěpán Janouš is the main author of the parts which are used in this thesis.

Pilsen May 2, 2017

. . . . . .
Prof. Ing. Zdeněk Peroutka, Ph.D.

Acknowledgment

I am grateful to my supervisor Prof Zdeněk Peroutka Ph.D. for his support valuable advice's and inspiration, I thank to Doc. Václav Šmídl Ph.D. who introduced me to optimal control theory, for his support, and help with theoretical background of this thesis. My appreciation belongs also to my colleagues.

Finally I would like to thank to my wife and little son and whole my family for their support and love over the years.

Pilsen May 2, 2017

. . . . . .

Ing. Štěpán Janouš

Abstract

This thesis deals with the development of model predictive control of ac electric drives with long prediction horizons and yet with computational cost of the algorithm comparable to conventional cascade control approaches. The basic idea is to approximate the cost to go of dynamic programming on long prediction horizon. For specific cases (linear model and quadratic cost function) the optimization of the control problem can be solved analytically which leads to a dramatic computational cost reduction. However the analytical solution does not consider the hard state and input constraints. Therefore proposed control algorithm combines unconstrained solution with constraint manager. Resulting algorithm is very simple and computationally comparable to conventional control schemes, nonetheless it still preserves excellent control performance of MPC solved on long prediction horizon. Proposed control technique has been implemented in DSP and tested in three practical examples of drive control on laboratory prototype of PMSM drive of rated power 10.7 kW.

The first case is described in chapter four and it is focused on cascade free speed control of PMSM using PWM. In this case, we aim to achieve comparable performance to existing PWM-based solutions of cascade free control at much lower computational cost.

The second case is focused on speed control of PMSM using finite number of admissible control inputs. Existing one step FCS-MPC suffer from high distortion of the stator current. In this case we aim to enhance the current control performance at computational cost comparable to one-step ahead solution of FCS-MPC.

The third Example is focused on designing MPC for control of the traction PMSM drive with input LC filter fed from dc catenary. The control problem is divided in two parts.i) stability of the input LC filter and ii) dynamics of the PMSM drive. Both parts are elegantly combined in the cost function of a simple one step FCS-MPC. The term respecting the input LC filter is designed analytically taking into account long prediction horizons.

Anotace

Tato práce se zabývá vývojem prediktivního řízení střídavých elektrických pohonů s uvažováním dlouhého predikčního horizontu a výpočetními nároky, které jsou srovnatelné s konvenčně používanými metodami řízení. Základní myšlenka navrhovaného řízení vychází z aproximace cost to go funkce Dynamického programování pro dlouhý predikční horizont. Pro speciální případy (tj. lineární matematický model a kvadratická ztrátová funkce) je možné problém řízení vyřešit analyticky což vede na dramatické snížení výpočetních nároků. Problém je však dodržet tvrdá omezení. Navržená technika řízení využívá aproximaci dlouhého horizontu v jednokrokovém MPC, hlavní důraz je přitom kladen na splnění tvrdých stavových a vstupních omezení, která jsou řešena pouze v rámci jednoho kroku MPC. Výsledný algoritmus je velmi jednoduchý a snadno implementovatelný, přesto si ponechává výborné vlastnosti srovnatelné s MPC řešeného na dlouhém predikčním horizontu.

Navrhované algoritmy řízení byly implementovány do DSP a testovány na laboratorním prototypu pohonu s PMSM o jmenovitém výkonu 10,7kW, ve třech praktických případech.

První případ popisovaný v kapitole 4 se zaměřuje na řízení PMSM s využitím pulsně šířkové modulace. Úkolem je navrhnout prediktivní řízení pohonu s PMSM s vlastnostmi srovnatelnými s existujícími metodami řízení bez využití kaskádního řazení lineárních regulátorů, s mnohem nižšími výpočetními nároky algoritmu.

Druhý případ popisovaný v páté kapitole se zaměřuje na prediktivní řízení PMSM bez PWM s využitím přímého výběru napěťového vektoru (FCS-MPC). Navržené řešení má za úkol minimalizovat zvlnění proudu při nízkých spínacích frekvencích s využitím dlouhého predikčního horizontu a překonat existující jednokroková řešení se srovnatelnými výpočetními nároky.

Třetí případ popisovaný v šesté kapitole, se zaměřuje na zvýšení stability trakčního pohonu s PMSM napájeného ze stejnosměrné troleje přes vstupní LC filter. Problém je rozdělen na dvě části: i) stabilita vstupního LC-filteru, která je řešena na dlouhém predikčním horizontu a ii) řízení PMSM, které je řešeno na krátkém horizontu. Obě dvě řešení jsou elegantně zkombinována ve ztrátové funkci jednokrokového FCS-MPC algoritmu.

Annotation

Diese Dissertationsarbeit beschäftigt sich mit der Entwicklung von der Prädiktivregelung der abwechselnden elektrischen Antriebe mit einem langen prädiktiven Horizont und Rechnungsansprüchen, die mit den konventionell angewandten Regelungsmethoden vergleichbar sind. Der elementare Gedanke der entworfenen Regelung geht von der Approximation der Lösung von der cost to go Funktion der Dynamischen Programmierung für einen langen prädiktiven Horizont aus. Bei speziellen Fällen (d.i. das lineare mathematische Modell und die quadratische Verlustfunktion) kann das Regelungsproblem analytisch gelöst werden, was zu einer dramatischen Senkung von Rechnungsansprüchen führt. Die strengen Begrenzungen einzuhalten, ist jedoch ein Problem. Die entworfene Regelungstechnik nutzt die Approximation des langen Horizonts im einschritt MPC. Der größte Akzent wird dabei auf das Einhalten der strengen Zustands- und Eingangsbegrenzungen gelegt, die lediglich im Rahmen eines Schrittes des MPC gelöst werden. Der resultierende Algorithmus ist sehr einfach und leicht implementierbar, trotzdem behält er ausgezeichnete Eigenschaften. Diese sind mit dem MPC, der auf einem langen prädiktiven Horizont gelöst wird, vergleichbar. Die entworfenen Regelungsalgorithmen wurden in DSP implementiert und auf einem Laborprototyp eines Antriebes mit PMSM und der Leistung von 10,7 kW in drei praktischen Regelungsfällen getestet.

Der erste Fall, der im Kapitel 4 beschrieben wird, konzentriert sich auf die Regelung PMSM mit der Nutzung von der Pulsbreitenmodulation. Die Aufgabe ist es, eine Antriebsregelung mit PMSM zu entwerfen, die vergleichbare Eigenschaften mit den bereits existierenden Regelungsmethoden hat, ohne Gebrauch der Kaskadenreihung der linearen Regler und mit viel niedrigeren Rechnungsansprüchen des Algorithmus.

Der zweite Fall, der im fünften Kapitel beschrieben wird, richtet sich auf die prädiktive Regelung PMSM ohne PWM mit der Nutzung von der direkten Auswahl des Spannungsvektors (FCS-MPC). Die entworfene Lösung hat die Aufgabe, die Wellung des Stroms bei niedrigen Schaltfrequenzen mit der Nutzung des langen prädiktiven Horizonts zu minimalisieren. Weiter soll sie existierende Einschritt Lösungen mit vergleichbaren Rechnungsansprüchen überwinden.

Der dritte Fall, der im Kapitel 6 beschrieben wird, richtet sich auf die Stabilitätserhöhung des Traktionsantriebes mit PMSM, der aus einem gleichmäßigen Fahrdraht über einen LC Eingangsfilter gespeist wird. Das Problem ist in zwei Teile eingeteilt: i) die Stabilität des LC Eingangsfilters, die auf dem langen Tranktionsantriebes und ii) die Regelung des PMSM, die auf einem kurzen Horizont gelöst wird. Beide Lösungen sind elegant in einer Verlustfunktion eines Einschritt FCS-MPC Algorithmus kombiniert.

Contents

Abbreviations and symbols

AC	Alternating Current
CCS-MPC	Continues Control Set Model Predictive Control
DC	Direct Current
DP	Dynamic Programming
DSP	Digital Signal Procesor
DTC	Direct Torque Control
FCS-MPC	Finite Control Set Model Predictive Control
FOC	Field Oriented Control
FW	Field Weakening (operational curve)
FPGA	Field Programmable Gate Array
IGBT	Insulated Gate Bipolar Transistor
LQR	Linear Quadratic Regulator
MIMO	Multiple Inputs Multiple Outputs
MPC	Model Predictive Control
MTPA	Maximum Torque Per Ampere (operational curve)
PI/PID	Proportional Integral/Proportional Integral Derivative (controller)
PWA	PieceWise Affine
PWM	Pulse Wide Modulation
SDC	State Dependent Coefficients
SDRE	State Dependent Riccati Equation
THD	Total Harmonic Distortion

1. Introduction

Variable speed ac electric drives in general play a very important role in modern industry and traction. In a standard configuration, the current in electric machine is controlled by input power inverter. The choice of a particular components of a drive, as well as the control algorithm essentially influence the behavior of the drive. Nowadays a lot of attention is dedicated to an improvement of variable speed ac electric drives in order to satisfy increasing demands of a market in quality and reliability. Extremely fast development on the field of power-electronics over the last few decades enabled a use of advanced switches and power inverter topologies, which yield lower THD, higher efficiency, higher reliability, lower costs and significantly improves the overall drive behavior. The need for more accurate control requires to consider not only the drive itself but also its supply (with LC or LCL filters) and load (e.g. with elastic joints or non-symmetries). The complexity of the control algorithms is thus significantly increasing. Therefore, development of a control algorithms can represent equally challenging task as the design of the drive itself.

The control algorithm has to secure not only proper operation of the drive in all operating conditions, but also it needs to satisfy all additional control objectives such us: stability of the supply, satisfaction of hard state constraints, active balancing of the inverter capacitors, improvement of the overall drive efficiency etc. Standard solution often leads to a cascade of linear PI controllers, which offers relatively simple and well understood way how to deal with some special cases of nonlinear multi-variable (MIMO) systems, moreover it handles hard constraints, which are usually inevitably imposed on the drive. However, the performance of such control design is limited. Nonetheless the tuning of PI controllers is often based on empirical guess of a fixed coefficients, which may be inefficient and hard to tune.

Model predictive control (MPC) offers a very attractive alternative to the conventional cascade controllers. The main idea is to formulate control problem as optimization task and solve it numerically on a few steps ahead receding prediction horizon. The solution is found for all possible control actions and all possible objectives, thus there is no need for cascades. Moreover, the MPC allows to consider constraints on the input and state variables on the prediction horizon.

MPC has never reached extensive popularity in electric drives. The potential reason for that might be relatively high computational cost of the algorithm, especially when we consider a long prediction horizons. So far, MPC has been widely used in chemical industry, where the time constants are long and computation of MPC can be easily performed on conventional micro-controllers. Recent advances in computational hardware, however, made MPC available also for electric drives and power-electronics, even thought the computational cost of the algorithm remains one of the limiting factors for wide range MPC implementation.

There has been a lot of work dedicated to a reduction of the computational cost of long horizon MPC. One way how to achieve that, is to pre-compute the solution of the optimal control problem in open loop offline. The controller is than designed in approximated form of the compute solution. Even thought the computational cost of the algorithm is dramatically reduced, it looses its ability to react to parameters changes in a simple and understandable way.

This thesis investigates design and implementation of several approximative forms of MPC for ac electric drives, with focus on extensions of prediction horizons, as a cascade free alternative to the conventionally used cascade structures of PI controllers. Special attention is dedicated to preserving understandable logic and low computational cost of the resulting algorithms such that it could be implemented on conventionally used hardware.

1.1. State of the art analysis

The ac electric drive is a nonlinear multi-variable system with rather high dynamics and hard operating constraints which represent a significant challenge for control. Satisfaction of all control objectives including hard constraint on the state variables is essential for proper operation of the drive. Today, vast majority of ac electric drives is controlled by so called cascade control which is based on cascade structure of PI/PID controllers [1, 2]. The potential reasons for that are i) decomposition of the control problem into several control loops is an intuitive and relatively simple way how to understand the problem, ii) the cascade control schemes represent well understood solution which can be used with conventional control hardware.

In many applications, if well designed, the cascade control provides relatively good performance and can address multiple control objectives including hard constraints [3] and today it represent the industrial standard. On the other hand, the cascade structure of PI/PID controllers has its limits which are given by the constant tuning of the controllers. This becomes even more evident, when the control structure contains multiple control loops and the optimal tuning of particular gains of the controller may become very complicated. In order to fulfill growing de-

mands on modern ac electric drives, researches turn to alternative approaches based on modern optimal control theory using state space models and avoiding cascades and loops [4].

One such approach is MPC [5], which offers extremely flexible solution for control of constraint multi-variable systems. The MPC stands for rather large group of controllers, which are based on solving the optimization of the control problem over receding horizon policy [6].

Despite being well known among the control society since 1960s, most of the particular results with MPC in electric drive control has been only theoretical due to high computational demands of the algorithm, preventing its wider practical application. Nevertheless, rapid development in control hardware over the last few decades made MPC-based algorithms available also for conventional, low cost DSP's [7]. The computational cost of the algorithm, however, still remains one of the limiting factor in control design.

A popular version of MPC, which gained extensive attention over the last few decades in drive control is the finite control set (FCS) MPC [8], which is based on reduction of the number of admissible control action to a limited set. This is a natural choice for example in power electronics [9, 10, 11], where the number of switching combinations is fixed. FCS-MPC is able to handle the control of nonlinear multi-variable (MIMO) systems with constraint on state variables while keeping its low computational demands. It has been successfully applied to induction machine drive control [12, 13] as well as PMSM drive control [14, 15] and control of other types of ac electric drives [16, 10]. Its has also been used to extend the performance of the drive control to additional problems like: improving stability of the drive [9], improving switching losses [17, 18] etc. The key components of a successful FCS-MPC controller is the chosen form of the cost function and the chosen penalization coefficients [11]. If tuned properly FCS-MPC can successfully compete with conventional PWM based solutions [19, 13].

Computational cost of brute force enumeration of all switching combinations grow exponentially with the length of prediction horizon and can thus become too expansive for long prediction horizons. Therefore in most cases, the evaluation of the cost function is done one or two steps ahead only [8]. This may be a significant restriction, when the control action has long term consequences, which needs to be considered by the control algorithm in order to achieve optimal control action [20]. Modern FPGA's can help to extend the prediction horizon of FCS-MPC [21], nevertheless, it may not be sufficient for larger scale problems.

Another solution to minimize the control effort of enumeration of the limited set of control action is Branch and bound [22], where the objective function is restricted by defined bounds. As a result the number of feasible (relevant) control actions is dramatically reduced which lowers the computational burden of the algorithm. In [23] it has been used for one

step ahead optimization. For longer horizon, the branch and bound approach has been used in [24]. A different approach of achieving long prediction horizon with FCS-MPC is based on integer programming and it is called sphere decoding [25]. It was developed for application in communication or cryptography and can be interpreted as a special case of the branch and bound algorithm. The key idea is to solve the least square problem on predetermined discrete lattices. As shown in [26, 27, 28] this technique can be successfully adopted to control of ac electric drives. Despite significant reduction of the computational cost of those control algorithms, they require complex software for online optimization.

Nevertheless, the FCS-MPC also has its weak points, such as variable switching frequency resulting in spread frequency spectrum of the converter currents, and operation at lower switching frequencies resulting in higher current ripple. These can be mitigated by smart techniques [29] or using PWM as a modulator for control designed by the FCS-MPC [18, 30]. The key objective of the latter approach is usually to achieve fixed switching frequency [21]. The simplest approach is however, to solve the optimization problem in continuous action variable. This was done in [31, 32], where a general solver was used. Optimal solution was achieved at high computational cost.

MPC is often formulated as optimal control based on minimization of linear or quadratic criterion. The following procedure can be treated as an quadratic programming [33] or linear programming [34] problem for which numerous effective solvers are available today. Nevertheless solving an optimization task of MPC online is a demanding procedure that is too computationally expensive for the common hardware used in drive control. The possible choice is to solve the quadratic programming offline and approximate it, with piece-wise affine optimal control law [35] . The result is a MPC based controller with long prediction horizon which handles hard constraints on the state variables with acceptable computational cost. However, the resulting solution has no freedom to change any parameter without reevaluation of the full offline optimization.

For special class of control problems with linear model and quadratic criterion, the computational burden of the algorithm can bee dramatically reduced if we are able to solve the control problem analytically, however such solution lack the ability to include hard input and state constraints in a simple way.

An alternative approach to multi-step optimization is based on the idea of dynamic programming [36]. The multi-step optimization problem can be reduced to a one-step ahead optimization if the cost-to-go function (also known as the Bellman function) is known. Since exact evaluation of the cost-to-go function is computationally prohibitive, approximations of the

cost-to-go function has to be used. This technique is known as Limited lookahead policy where the dynamic programming problem over the prediction horizon truncates into optimization of the control problem on limited number of steps ahead [36]. Various approaches to design of the approximate cost-to-go function have been proposed for drive control. For example, off line calculation via multi-parametric toolbox [37], or heuristic approximate of the numerical solution [38]. This is possible when the dimensionality of the cost-to-go function is rather low. In higher dimensions, the computational cost of numerical solutions grow and analytical approximations are harder to find.

A several approaches were developed to combine unconstrained solution with constraints manager that is applied after calculation of the unconstrained solution. This idea has been proved theoretically in [39] and already used in PMSM control e.g. in [40] in simpler settings. The problem is then decomposed into two parts: (i) what unconstrained solution to use, and (ii) what constraints to impose. In some circumstances this approach can be understood as a limited lookahead approach where the unconstrained solution represents the approximation of the cost to go function. The unconstrained solutions were designed using heuristics [38], SDRE approach [41, 42] or non-linear predictive control [43]. The constraints can be addressed by either aforementioned FCS-MPC [38], or in continuous space [44], [45], [31] and [32]. However, the implied computational cost of the solution in continuous space is typically too high.

1.2. Objectives of the thesis

The overall objective of the thesis is to develop MPC-based control algorithms that are suitable for routine application in industry. To compete with existing cascade PI control, the new algorithms have to offer simple implementation, and comparable execution time. At the same time it has to offer some advantage, e.g. in terms of faster performance in transients.

Since it has been well established that existing MPC-based solutions outperform cascade PID controllers in terms of control performance, the main focus of this thesis is on reduction of computational cost of the MPC algorithms. Therefore, our main competitors are one-step and multi-step ahead controllers based on FCS-MPC or numerical solution of the optimization problem by general purpose solvers. In this thesis the main theoretical tool is the limited lookahead strategy combining unconstrained solution with constraint manager.

The proposed algorithms will be tested on PMSM drive. The main aims of the thesis can be summarized into following points as follows:

- Improve cascade free speed control of PMSM drive by better combination of constraint management in transients and exact tracking in steady state. We will focus on both cases with PWM and without PWM.
  - Existing PWM-based solutions of cascade free control are using numerical solvers which are computationally expensive. We aim to achieve the same performance at much lower computational cost.
  - Existing one-step FCS-MPC suffers from high current ripple when required to operate at low switching frequencies. Improvement by multi-steps ahead MPC is too expensive. We aim to lower the current ripple at computational cost comparable to one-step ahead solution.
- Improve stability of traction PMSM drive with input LC filter fed from dc catenary. We aim to improve damping of unwanted oscillation of the filter while preserving as much drive dynamics as possible.

1.3. Applied methodology of the thesis

The thesis is organized into several chapters as follows:

In chapter 2, the theory of MPC is introduced and its key components discussed. Techniques that will be used in subsequent chapters are discussed in detail. In particular, we review the technique of limited lookahead which will be used to achieve the defined aims.

In chapter 3, the problem of cascade free speed control of PMSM is defined and existing solutions for it are reviewed.

In chapter 4, the limited lookahead approach is applied to the cascade free speed control of PMSM drive with PWM. Specifically, the unconstrained solution (obtained by SDRE) is used to approximate the cost-to-go, it is further complemented by constraints and solved by convex optimization. The resulting input voltage is then applied via PWM controlled 3-phase power-converter. The main emphasis is on simplicity of proposed solution in order to be suitable for use with conventional control hardware.

In chapter 5, an extension of the FCS-MPC for control the PMSM drive is presented. The extension is based on the unconstrained solution (SDRE) as the approximate of the cost to go function. The unconstrained solution is then combined with simple one step ahead FCS-MPC as additive term in the cost function. The FCS-MPC does not require any PWM modulator and applies the input voltage via selection of the direct switching combination. We will show

that such extension allows to minimize switching loses at lower current ripples than with conventional one-step ahead FCS MPC.

In chapter 6, the limited lookahead technique is used to improve stability of a traction PMSM drive fed from dc cantenary. The LC filter is almost undamped by design. Thus the control algorithm needs to secure active damping of the input LC filter, as well as the control of PMSM. Conventionally this may be achieved by additive term in the cost function which is usually designed manually. In this chapter, we propose to use the LQR to design the active damping term which takes optimization on long prediction horizon into account.

Conclusions are given in chapter 7 together with proposed directions for future research.

2. Theoretical background of model predictive control

MPC is defined as an optimization task in discrete time on prediction horizon of length h, for which a chosen cost function is minimized. The result is a vector of optimal control actions over selected prediction horizon, although only the first one is used to perform the control action. This procedure is repeated in each control step and it is called receding horizon policy [4]. Formally, we seek solution of problem:

$$\begin{aligned} u^{\text{opt}}_{t:t+h} &= \arg \min_{u_{t:t+h} \in U} \sum_{\tau=t+1}^{t+h} g(x_\tau, u_\tau), \\ \text{subject to: } & u_\tau \in \mathcal{U}, \\ & x_\tau \in \mathcal{X}, \\ & x_\tau = f(x_\tau, u_\tau), \quad \forall \tau = t, t+1, \ldots, t+h. \end{aligned} \tag{2.1}$$

where $g()$ is the chosen cost function, u_τ is the vector of inputs, x_τ is the vector of system states, $\mathcal{U}$ is the set of admissible inputs and $\mathcal{X}$ is the set of allowed system states, $f()$ is the mathematical model of the evolution of the state variable in time. Index τ is a running time on the prediction horizon from the current time t to $t+h$. Star in the upper index denotes requested value of the symbol, e.g. x^* is the requested value of the state vector. The MPC stands for rather large group of controllers, where the designer needs to carefully choose the flowing ingredients, when designing a MPC based controller.

- Mathematical model, $f(.)$
- Cost function, g(.)
- Admissible control action set, $\mathcal{U}$
- Prediction horizon, h
- State constraints,$\mathcal{X}$

We will now briefly outline the possible choices and their use.

2.1. Mathematical model

The mathematical model is used to describe the future behavior of a controlled system. In literature, there is several different model formulations (a good overview of existing models can be seen in [46]). In general, MPC can deal with the nonlinear systems, if proper mathematical model is available. However, the synthesis of the controller for nonlinear systems is rather difficult task, usually requiring great amount of computational power. Contrary to that, a significant simplification of MPC design can be obtained if the system can be described by a linear model. A general formulation in continuous state space form can be written as

$$\frac{dx}{dt} = A_c x + B_c u, \tag{2.2}$$

where, A_c and B_c are constant matrices with appropriate dimensions. Note, that many electrical components can be described by linear first order differential equation.

Modern controllers are implemented in microprocessors, which works in discrete time.We will assume, that all mathematical models, used in this thesis are time invariant, therefore for the sake of readability, in the following text we will use the simplified notation

$$x_{\tau+1} = f(x_\tau, u_\tau) \Leftrightarrow x_{t+1} = f(x_t, u_t) \quad . \tag{2.3}$$

Conversion of the model (2.2) into discrete time form with sampling time Δt is achieved using the conventional discretization formula

$$\begin{aligned} A &= \exp(A_c \Delta t), \\ B &= \int_0^{\Delta t} e^{A_c(\Delta t - \sigma)} B_c d\sigma. \end{aligned} \tag{2.4}$$

Here, A and B are constant matrices of appropriate dimensions. Then the discrete form of state space model is

$$x_{t+1} = Ax_t + Bu_t. \tag{2.5}$$

The formulation (2.5) can be extended to address the nonlinear systems by parametrization of the model resulting in piece-wise linear state dependent structure. Many techniques for local linearization can be used for this task, such as Taylor series method or numerical interpolation

method (see[47],[48]). The resulting formulation can be written as:

$$x_{t+1} = A(x^{\text{op}})x_t + B(x^{\text{op}})u_t. \tag{2.6}$$

Where, $x^{\text{op}}$is an operational point of the linearization, matrices $A(x^{\text{op}})$ and $B(x^{\text{op}})$ are state dependent matrices of appropriate dimensions.

Note, that the linearization of (2.5) is not unique operation and optimality of the close loop performance cannot be always ensured [49]. Moreover for complex MIMO systems where several terms are nonlinear, the parametrization of the model may become too complex and even intractable.

2.2. Cost function

The cost function g is a key component of MPC based control design. It is used to specify all control objectives in the MPC and in general, it may take an arbitrary form.

The performance of the MPC based controller strongly relies on the specific form of the cost function and the way of its minimization. The control problem has typically multiple objectives. For on-line operations, these must be composed into a single objective. This is typically achieved using a weighted sum of all objectives [50][1]

$$g(x_t, u_t) = \sum_{j=1}^{K} g_j(x_t, u_t,)\, \lambda_j, \tag{2.7}$$

$$\lambda_j \geq 0,\, j \in \mathcal{N},$$

where: K is the number of control objectives, $g_j(x_t, u_t)$ are the elements of the cost function representing particular control objectives, and λ_j are the weighting factors, which are used to set the preferences for individual control objectives.

2.2.1. Pareto optimality

The additive form of the cost function has some attractive properties. Specifically, the expected solution of the cost function minimization lies on so called Pareto front [50] (as it can be seen from Fig. 2.1). Pareto optimality principle states, that any solution lying on the Pareto front may not be further minimized without negative impact on other elements of the cost function.

[1]The weighted sum is only one of many existing methods to solve the multi-objective optimization, it may be interesting to compare the others in future research.

One setting of the penalization vector λ defines a point of the Pareto front. Different choice may result in a different point on the Pareto front, thus individual weighting factors have significant influence on the overall behavior of the controller and their correct tuning is very important. In most cases, the weighting factors λ are chosen empirically by the designer. Nonetheless it may not be sufficient especially when single decision variables may be of different units or scale. The process of tuning can be simplified by normalizing the quantities in relation to their nominal values. Some useful guidelines for tuning of the weighting factors has been provided in [51]. The weighting factors can be avoided in some cases by evaluating multiple cost functions independently and the optimized solution is obtained by computation of ranking and using simple sorting algorithm[52], [53]. Further improvement can be achieved by designing the weighting factors by optimizing method [12].

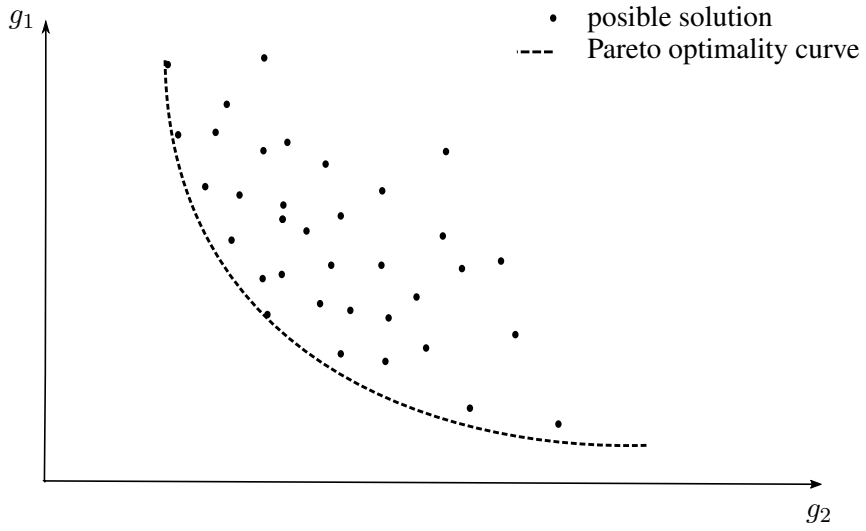

Figure 2.1.: Example of Pareto optimality principle in two dimensions

2.2.2. Quadratic cost function

A special case of (2.7), which is very common in modern control theory, is a quadratic cost function. It is popular choice, which has several advantages, favoring its use among other forms of the cost functions:

- It leads to an analytical solution of the optimization problem (theoretically infinite prediction horizons can be achieved) [4]
- It is convex allowing fast numerical solution even for constraint optimization problem

- It is symmetric (positive and negative control deviations are treated the same)
- Small penalty for small deviations of states from their requested values and quadratically rising penalty for linear increase of the deviation of the states from their requested values.

Quadratic cost function in a standard form can be expressed as

$$g(x_t, u_t) = {x_t}^T Q^{\frac{1}{2}} Q^{\frac{1}{2}} x_t + {u_t}^T R^{\frac{1}{2}} R^{\frac{1}{2}} u_t + 2x_t^T N u_t, \qquad (2.8)$$
$$Q \in Q^T \geq 0,\ R \in \mathcal{R}^{\mathcal{T}} > 0.$$

Where Q, R and N are matrices of appropriate dimensions. For the problem of tracking a predefined state and input trajectory the cost function can be rewritten as

$$g(x_t, u_t, x_t^*, u_t^*) = (x_t - x_t^*)^T Q^{\frac{1}{2}} Q^{\frac{1}{2}} (x_t - x_t^*) + (u_t - u_t^*)^T R^{\frac{1}{2}} R^{\frac{1}{2}} (u_t - u_t^*), \qquad (2.9)$$

where x_t^*, u_t^* are the requested values of the state and the input action. In order to obtained standard form, we augment the state vector $\tilde{x} = [x_t, x_t^*, u_t^*]$. Than (2.9) is

$$g(\tilde{x}_t, u_t) = {\tilde{x}_t}^T Q^{\frac{1}{2}} Q^{\frac{1}{2}} \tilde{x}_t + {u_t}^T R^{\frac{1}{2}} R^{\frac{1}{2}} u_t + 2{\tilde{x}_t}^T N u_t =$$
$$= \begin{bmatrix} \tilde{x_t} & u_t \end{bmatrix} Z_{xu}^T Z_{xu} \begin{bmatrix} \tilde{x_t} \\ u_t \end{bmatrix}, \qquad (2.10)$$

$$Z_{ux} = \begin{bmatrix} Q^{\frac{1}{2}} & -Q^{\frac{1}{2}} & 0 & 0 \\ 0 & 0 & -R^{\frac{1}{2}} & R^{\frac{1}{2}} \end{bmatrix}, N \begin{bmatrix} 0 & 0 & 0 \end{bmatrix},$$
$$Q \in Q^T \geq 0,\ R \in \mathcal{R}^{\mathcal{T}} > 0,\ Z \geq 0.$$

2.3. Admissible control action set

The goal of the optimization of the control problem (2.1) is to find an appropriate control action u_t which drives the system to the required state, while respecting all given objectives and restrictions. The admissible control action set $\mathcal{U}$ is often limited by the physical nature of the system (e.g. maximum available voltage, the quantity of fuel, maximum achievable temperature etc.). MPC can be divided into two main groups according to the admissible control action set to:

CCS-MPC Continuous control set MPC,

FCS-MPC Finite control set MPC ,

This distinction has impact on the technique for solving the optimization problem.

2.3.1. Continuous control set

The MPC with continuous control set covers a large group of controllers. The admissible control set is defined as

$$u_t \in \mathcal{U} \subset \Re^{n_u},\, n_u \geq 1, \tag{2.11}$$

where, n_u is the number of control inputs. Searching for optimal control input in continuous space is often a demanding procedure where the algorithm needs to search over infinite number of possible control actions. The solution to this problem however can be dramatically simplified if the cost function is convex.

Convex optimization

Consider the task of finding a minimum of the convex cost function subject to a set of convex constraints

$$\begin{aligned} x^{\text{opt}} = &\text{arg } \min\, g_0(x), \\ &\text{subject to: } c_m(x),\, m = 1...M, \end{aligned} \tag{2.12}$$

where, $g_0(x)$ is the convex cost function, $c_m(x)$ are convex constraints and M is the number of all constraints. Assume that $g_0(x)$ is differentiable, and $X = \{x | c_m(x)\, m = 1...M\}$ is the set of all x satisfying the defined constraints. Then the x^{opt} is unique and needs to satisfy the condition

$$\nabla\, g_0(x)^T (x - x^{\text{opt}}) \geq 0, \quad \forall x \in X \tag{2.13}$$

This condition is illustrated geometrically in Fig. 2.2. Note, that for solving of the convex optimization problems a various efficient numerical solvers are available (an interested reader may reefer to [54] for more about convex optimization) .

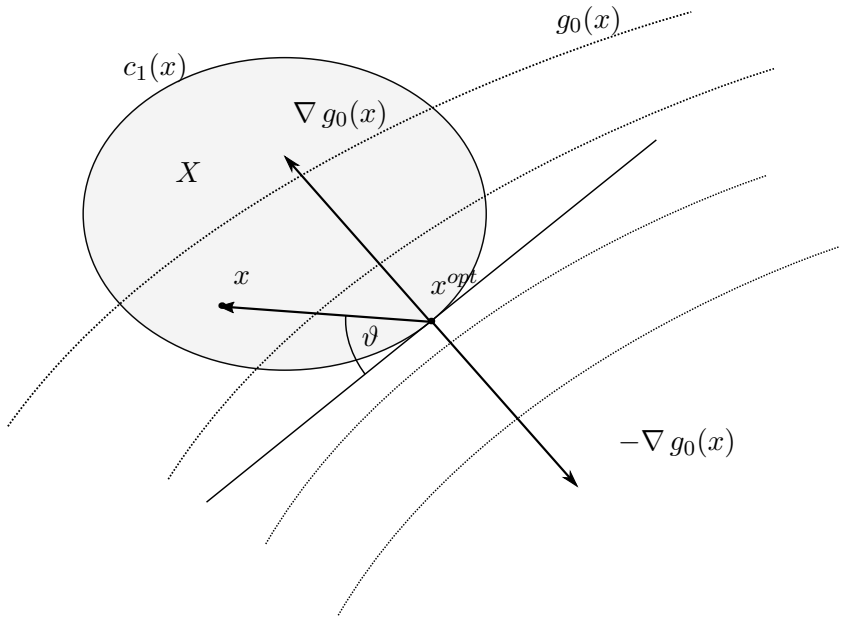

Figure 2.2.: Geometrical illustration of the convex optimality condition.

2.3.2. Finite control set

A special case of a MPC controller arise when only a limited number of admissible control action is available, forming as set $U = [u_t^{(1)}, u_t^{(2)}, \ldots, u_t^{(n)}]$. This approach is known as Finite control set MPC, FCS-MPC.

It has been one of the most successful versions of MPC in industry due to its extremely simple and robust design. The predictive model is run n times, once for each possible control action to yield prediction $x_{t+h}^{(i)}$. The cost function $g(\cdot)$ is evaluated for each prediction and the control input with minimum cost is selected as being optimal.

The FCS-MPC provides a very efficient control approach for various applications which requires very little computations to obtain the optimal control action. However this is true only when the prediction horizon h is short. The computational demands exponentially grow with each extra time step, making the prediction horizon with FCS-MPC restricted to only few steps ahead (see fig. 2.3). Inability to consider long term effects of the control action however may have negative impact on the control quality.

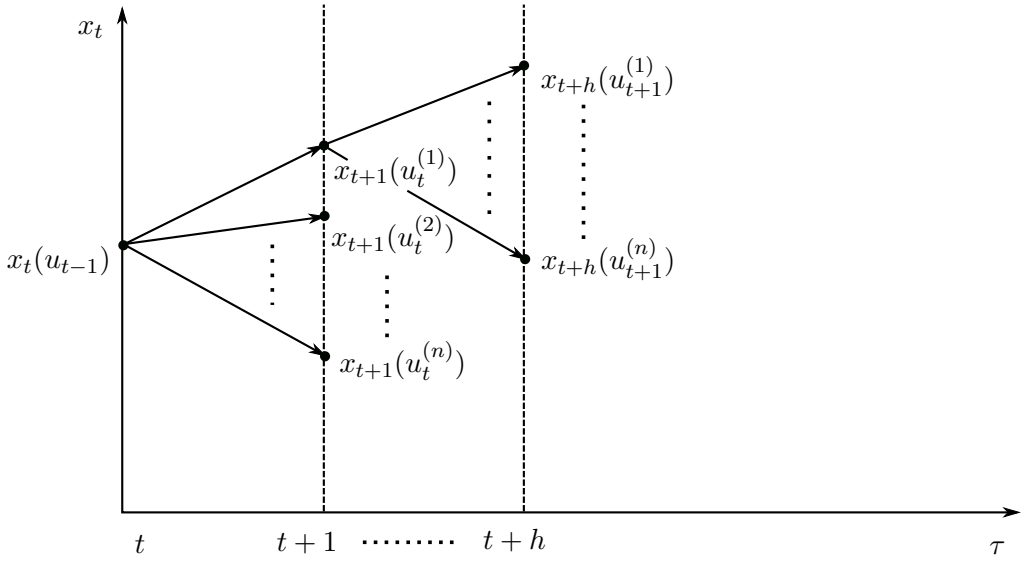

Figure 2.3.: Illustration of combination of control actions of FCS-MPC on longer prediction horizon.

2.4. Prediction horizon

In order to incorporate long term consequences, long prediction horizons h are necessary. However longer prediction horizons implies higher computational costs of the resulting optimization algorithms, often prohibiting its use in real time applications.

One possible approach to address this problem is based on the concept of dynamic programming [36]. Note that the solution of the optimization control problem on long prediction horizons can be expressed recursively

$$u_{t:t+h}^{\text{opt}} = \arg \min_{u_{t:t+h} \in U} \sum_{\tau=t+1}^{t+h} g(\tilde{x}_\tau, u_\tau) =$$

$$= \arg \min_{u_t \in U} \left\{ g(\tilde{x}_{t+1}, u_{t+1}) + \arg \min_{u_{t+1} \in U} \left\{ g(\tilde{x}_{t+2}, u_{t+2}) + \right. \right.$$

$$\left. \left. + \ldots\ldots \arg \min_{u_{t+h} \in U} \{ g(\tilde{x}_{t+h}, u_{t+h}) \} \right\} \right\}, \quad (2.14)$$

where $\tilde{x}_t = [x_t^T, x_t^{*T}, u_t^{*T}]^T$ is the state vector augmented by the vectors of requested values. If

we can find an optimal policy $u^{\text{opt}}(\tilde{x}_{t+h})$, then the last term of (2.14) can be written as

$$V(x_{t+h}) = g(\tilde{x}_{t+h}, u^{\text{opt}}(\tilde{x}_{t+h})).$$

This procedure can be repeated in backward recursion until the complete optimization problem is solved, as in (2.15), and it is generally referred to as Dynamic programming [4]

$$u^{\text{opt}}_{t:t+h} = \arg \min_{u_{t:t+h} \in U} \left\{ g(\tilde{x}_{t:t+h}, u_{t:t+h},) + V(\tilde{x}_{t+h}) \right\}, \tag{2.15}$$

where the prediction horizon h is short as the optimal control problem to be solved, and $V(\tilde{x}_{t+h})$ is the cost to go function defining the optimal policy for the control problems beyond $t + h$.

2.4.1. Lookahead

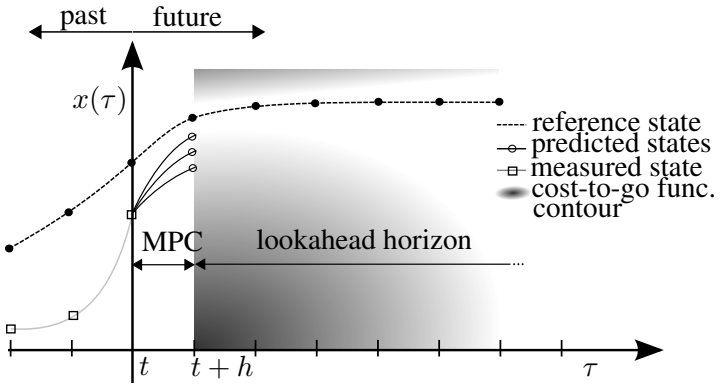

Figure 2.4.: Principle of limited lookahed

The optimal cost to go function $V(\tilde{x}_{t+h})$ can be found numerically or analytically. The numerical solution often requires complete enumeration of the sub-problems involving high computational demands. Thus, it is desirable to find $V(\tilde{x}_{t+h})$ analytically. Nevertheless in some specific cases the analytical solution may be unavailable or hard to find, and therefore, it needs to be approximated. The (2.15) can be then reformulated as lookahead policy [4] as (see fig. 2.4)

$$u^{\text{opt}}_{t:t+h} = \arg \min_{u_{t:t+h} \in U} \left\{ g(\tilde{x}_{t:t+h}, u_{t:t+h}) + \tilde{V}(\tilde{x}_{t+h}) \right\}, \tag{2.16}$$

where the prediction horizon h is as short as possible to allow tractable solution the optimal control problem, and $\tilde{V}(\tilde{x}_{t+h})$ is the approximated cost to go function for the control problems beyond $t + h$.

Lookahead represents an elegant way how to design long range MPC with hard constraints on state variables in a computationally efficient way. This approach will be the main mathematical tool used in this thesis.

Remark 1. Many different approaches can be used to design approximated cost to go function [55],

2.5. State constraint management

Satisfaction of operational constraints on inputs $u_t \in U$, and states $x_t \in \mathcal{X}$, is essentially one of the major requirements imposed on modern controller. While the input saturation is given by the physical capabilities of the system and thus can not be violated, the violation of constraints which are imposed on the states may result in undesirable consequences. We have discussed the problem of limited admissible control set above, so for the clarity in this chapter we focus only on the problem of state constraints.

Contrary to many optimal control approaches, MPC is able to naturally handle the hard constraints, via their explicit statement in (2.1). The set of allowed states may be defined as

$$\mathcal{X} = \{x_t : c_m(x_t) < 0, m = 1, \ldots, M\}, \tag{2.17}$$

The number of constraints M is finite [2]. The solution of the constraint optimization is typically based on introduction of so called penalty functions $g_{lim}()$, that are added into the cost function (2.7)

$$g(x_t, x_t^*, u_t, u_t^*) = \sum_{j=1}^{K} g_j(x_t, x_t^*, u_t, u_t^*)\,\lambda_j + \sum_{m=1}^{M} g_{lim,m}(x_t) \tag{2.18}$$

which are designed to increase the cost over all possible values of the original cost function. Such penalty function will be further used for the FCS-MPC approach:

$$g_{lim,m} \begin{cases} 0 & if\,(c_m(t) < 0) \\ \lambda_{lim,\,m}\, c_m(x_t) & \text{otherwise} \end{cases}, \quad \lambda_{lim\,m} \geq 0,$$

[2] Under certain circumstances the constraint optimization of the control problem in open loop may result in unfeasible behavior of a closed loop. Note, that the feasibility and stability issues in MPC theory is extremely large topic which goes beyond the framework of this thesis and thus it is not discuses in detail (interested reader in this topic may see [56] or [57]). However due to the rather difficult implementation and problems with the feasibility, the hard constraint may be softened [49].

$\lambda_{lim,\,m}$ is a sufficiently large penalization for the violation of particular state constrains. An alternative to $g_{lim,\,m}$with fixed penalty $\lambda_{lim\,m}$, is so called barrier function [58] which introduces near to zero penalty when the system is operating far from the constraint region and as the system is closer to the constraint, the penalty function introduces larger penalty, reducing the dynamics of the controller (see fig. 2.5).

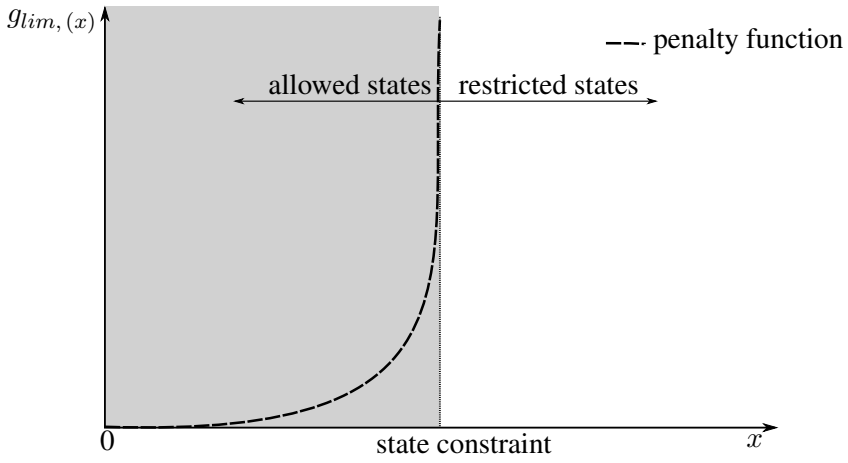

Figure 2.5.: Illustrative example of barier function

2.6. Optimization methods

Solution of the optimization problem in general is a hard task. Many specialized algorithms exist for specific choices of the cost, constraints and prediction models. In this Section we briefly review methods of unconstrained optimization that will be used in this thesis, the LQR and SDRE approaches.

2.6.1. Linear Quadratic Regulator (LQR)

Consider a linear system (2.2) with quadratic cost function (2.8) without any constraints. Based on matrix triangularization [59] and under the assumption of quadratic cost-to-go function in the form

$$\begin{aligned} V(\tilde{x_t}) =& \tilde{x}_t^T S_t \tilde{x}_t, \\ S =& \Psi_t^T \Psi_t, \end{aligned} \tag{2.19}$$

where Ψ_t is a square upper triangular matrix and $\tilde{x}_t = [x_t^T, x_t^{*T}, u_{t-1}^T]^T$ is augmented state vector. One step of the optimization (2.15) can be performed analytically. The cost function inside minimization in (2.15) can be written as

$$g(\tilde{x}_t, u_t) + V(\tilde{x}_{t+1}) = \tilde{x_t}^T Q^{\frac{1}{2}} Q^{\frac{1}{2}} \tilde{x_t} + {u_t}^T R^{\frac{1}{2}} R^{\frac{1}{2}} u_t + \tilde{x}_t^T S_t \tilde{x}_t, \tag{2.20}$$

which can be rewritten in the matrix notation as

$$g(\tilde{x}_t, u_t) + V(\tilde{x}_{t+1}) = \begin{bmatrix} \tilde{x_t} & u_t \end{bmatrix} Z^T Z \begin{bmatrix} \tilde{x_t} \\ u_t \end{bmatrix}, \tag{2.21}$$

$$Z^T = [Z_{xu}, Z_\Psi], \quad Z_{xu} = \begin{bmatrix} Q^{\frac{1}{2}} & -Q^{\frac{1}{2}} & 0 & 0 \\ 0 & 0 & -R^{\frac{1}{2}} & R^{\frac{1}{2}} \end{bmatrix},$$

$$Z_\psi = \Psi_{t+1}^T \begin{bmatrix} A & 0 & 0 & B \\ 0 & \overline{A}_x & 0 & 0 \\ 0 & 0 & \overline{A}_u & 0 \end{bmatrix}.$$

Note that the term with Z_{xu} correspond to $(x_t - x_t^*)^T Q (x_t - x_t^*) + (u_t - u_t^*) R (u_t - u_t^*)$, and the term with Z_Ψ to the cost-to-go function with substitutions $x_{t+1} = Ax_t + Bu_t$, $x_{t+1}^* = \overline{A}_x x_t^*$, $u_{t+1}^* = \overline{A}_u u_t^*$, where $\overline{A}_x$ and $\overline{A}_u$ are matrices of the reference dynamics. Under the assumption of stationary reference values, $\overline{A}_x$ and $\overline{A}_u$ are identity matrices of appropriate dimensions.

Using an arbitrary triangularization procedure, product $Z^T Z$ in (2.21) can be uniquely decomposed into the product of triangular matrices

$$Z^T Z = Y^T Y, \qquad Y = \begin{bmatrix} Y_{uu} & Y_{ux} \\ 0 & Y_{\tilde{x}\tilde{x}} \end{bmatrix}, \tag{2.22}$$

yielding

$$g(\tilde{x}_t, u_t) + V(\tilde{x}_{t+1}) = (Y_{uu} u_t + Y_{ux} \tilde{x}_t)^T (Y_{uu} u_t + Y_{ux} \tilde{x}_t) + \tilde{x}_t^T Y_{xx}^T Y_{xx} \tilde{x}_t. \tag{2.23}$$

which is quadratic in u_t and thus we obtain following optimization problem

$$\begin{aligned} u_t^{\text{opt}} &= \arg\min_{u_t(x_t)} \left\{ (u_t + Lx_t)^T Y (u_t + Lx_t) \right\} \\ L &= Y_{uu}^{-1} Y_{ux}, \\ Y &= Y_{uu}. \end{aligned} \tag{2.24}$$

The (2.24) is minimized for $Y_{uu}u_t + Y_{ux}\tilde{x}_t = 0$, yelling optimal policy $u^{\text{opt}}(x_t)$ in the form

$$u_t^{\text{opt}} = -Lx_t, \tag{2.25}$$

where L is the designed gain matrix.

Remark 2. Note, that, the LQR is a basic technique of control theory with many potential methods of design of the gain matrix L. In this thesis we will follow the standard approach based on solving the algebraic Riccati equation (ARE)[60] (**??**)for matrix variable S, where, the cost to go function is defined as

$$V(\tilde{x}_{t+1}) = \tilde{x}_{t+1}^T S \tilde{x}_{t+1}. \tag{2.26}$$

Many tools such as Matlab `dlqr` are available for this task.

The LQR provides computationally cost efficient solution for the optimization problem on long prediction horizons, which does not take into account any state or input constraints and does apply only to linear systems with quadratic cost.

2.6.2. State-dependent Riccati Equation (SDRE)

Solution via the Riccati equation (**??**) can be used as local approximation of a non-linear model around an operating point. The model is linearized at this point (2.6) (see the section 2.1) and LQR solution for the resulting linear system is designed. The task is how to design the overall control scheme for all operating points. Many approaches based e.g. on Taylor linearization are available [47].

We will follow a simpler approach based on numerical evaluation of the controller on a fixed grid of operating points, i.e.

$$u^{\text{opt}} = -L(x^{\text{op}})x_t. \tag{2.27}$$

where $L(x^{\text{op}})$ is the the designed state dependent matrix of gains. Then, we approximate the controller coefficients using polynomial fitting.

Example: SDRE control design

Consider a nonlinear system with quadratic cost (2.8) in a special form penalizing difference of the input variable (which is used to suppress steady state error of the resulting controller):

$$g(x_t, x_t^*, u_t, u_{t-1}) = (x_t - x_t^*)^T Q(x_t - x_t^*) + (u_t - u_{t-1})^T R(u_t - u_{t-1}), \tag{2.28}$$

To obtain the standard form (2.8) we use augmented state vector $\tilde{x}_t = [x_t^T, x_t^{*T}, u_{t-1}^T]^T$ with state dynamics:

$$\begin{bmatrix} x_{t+1} \\ x_{t+1}^* \\ u_t \end{bmatrix} = \underbrace{\begin{bmatrix} A(x^{\text{op}}) & 0 & 0 \\ 0 & I & 0 \\ 0 & 0 & 0 \end{bmatrix}}_{\tilde{A}} \begin{bmatrix} x_t \\ x_t^* \\ u_{t-1} \end{bmatrix} + \underbrace{\begin{bmatrix} B(x^{\text{op}}) \\ 0 \\ I \end{bmatrix}}_{\tilde{B}} u_t, \tag{2.29}$$

and quadratic cost function:

$$\begin{aligned} g(\tilde{x}_t, u_t) &= \tilde{x}_t{}^T \tilde{Q} \tilde{x}_t + u_t{}^T R u_t + 2\tilde{x}_t^T N u_t, \\ \tilde{Q} &= \begin{bmatrix} Q & -Q & 0 \\ -Q & Q & 0 \\ 0 & 0 & R \end{bmatrix}, \\ N &= [0, 0, -R]. \end{aligned} \tag{2.30}$$

The optimal control is found by solving the state dependent discrete time Riccati equation (2.31),

$$\tilde{A}^T S \tilde{A} S (\tilde{A}^T S \tilde{B} + N)(\tilde{B}^T S \tilde{B} + R)^{-1}(\tilde{B}^T S \tilde{A} + N^T) + \tilde{Q} = 0, \tag{2.31}$$

for matrix variable S.

Since $\tilde{A}$ is state dependent, the resulting S is also state dependent. The matrix $S(x^{\text{op}})$ defines the cost-to-go function of dynamic programming on infinite horizon [4]:

$$V(\tilde{x}_{t+1}) = \tilde{x}_{t+1}^T S(x^{\text{op}}) \tilde{x}_{t+1}, \tag{2.32}$$

The SDRE controller is thus the optimizer of the following optimization problem:

$$\begin{aligned} u_t &= \arg\min_{u_t(x_t)} \left\{(u_t + L\tilde{x}_t)^T Y (u_t + L\tilde{x}_t)\right\} \\ L &= Y^{-1}(\tilde{B}^T S\tilde{A} + N^T), \\ Y &= (\tilde{B}^T S\tilde{B} + R). \end{aligned} \tag{2.33}$$

Which is well known to be

$$u_t^{\text{opt}} = -L(x^{\text{op}})\tilde{x}_t. \tag{2.34}$$

This controller will be evaluated on a grid of state points x_t^{opt} and the coefficients $L(x^{\text{opt}})$ will be interpolated. See Section 4 for details.

.

2.7. Partially observed state

In predictive control, the optimization is often done with the simplifying assumption of perfectly known state. However in some cases, accurate knowledge of the state may not be available. Many observers can be designed for this task.

If the system is linear, the optimal observer can be designed as the standard Kalman filter [61]. We assume that the state space model (2.5) is subject to stochastic error or residues due to model imperfection. Then it can be rewritten as

$$x_{t+1} = Ax_t + Bu_t + \varepsilon_x, \tag{2.35}$$

where, ε_x is the model error, which is assumed to be Gaussian distributed with covariance matrix Σ_x. The state is observed only via observation equation (representing noisy measurement, inaccurate sensors etc.)

$$y_t = Cx_t + \varepsilon_y, \tag{2.36}$$

where, y_t is the observed state, C is the observation matrix of appropriate dimensions and ε_y is the measurement noise with covariance matrix Σ_y. The standard Kalman filter algorithm provides an optimal reconstruction of the state in terms of mean square error.

In this text, we will consider only linear time-invariant systems (2.5). For such system, the observer converges to a linear feedback observer with constant gain [62]:

$$\hat{x}_t = Ax_{t-1} + Bu_{t-1} + K(y_t - Cx_t), \tag{2.37}$$

where K is the matrix of pre-computed Kalman gains. The gain can be obtained using Matlab function `kalmd.m`.

3. Speed control of PMSM drive

In this chapter, we consider speed control of drive with PMSM as an exemplary case of ac machine. However the main principles described here remain valid for other types of ac machines as well.

Nowadays, most of the control algorithms for PMSM are based on Field Oriented Control (FOC) or Direct torque control (DTC). Both techniques are considered to be industrial standards in PMSM drive control. The main principle is based on decoupling the control into the flux and torque control loops, similarly as it is naturally done in DC machines. This may be achieved only when sufficiently accurate knowledge of the rotor position is available. In the case of DTC, the lookup table defines each relevant switching combination of the converter in terms of its effect on torque and flux control, depending on the rotor position. In the case of FOC, the stator current is transformed into a single vector in the rotating coordination frame d, q which is linked with rotor flux vector (rotor flux vector allies with rotor position). Each component of the current vector i_d and i_q is, proportional to the flux or torque respectively. The output of the current controller, is then the required stator voltage vector $u_{d,q}$ which is transformed back to phase coordinates $u_{a,b,c}$ and applied to the drive via PWM.

In both cases it is relatively simple to secure hard current constraint due to the linear nature of the torque and flux control by simply limiting the current references. In speed control, the current reference is given by the speed controller, which forms outer loop of the current control, see Figure 3.1 a).

The basic MPC is based on a different concept, where cascades are replaced by a single mathematical optimization of the full state space model. The block diagram of the control is then very simple (Figure 3.1 b)) and all complexities of the control are solved by the optimization method. Therefore, the block diagrams are not very good description of the MPC approach and we will not make extensive use of them.

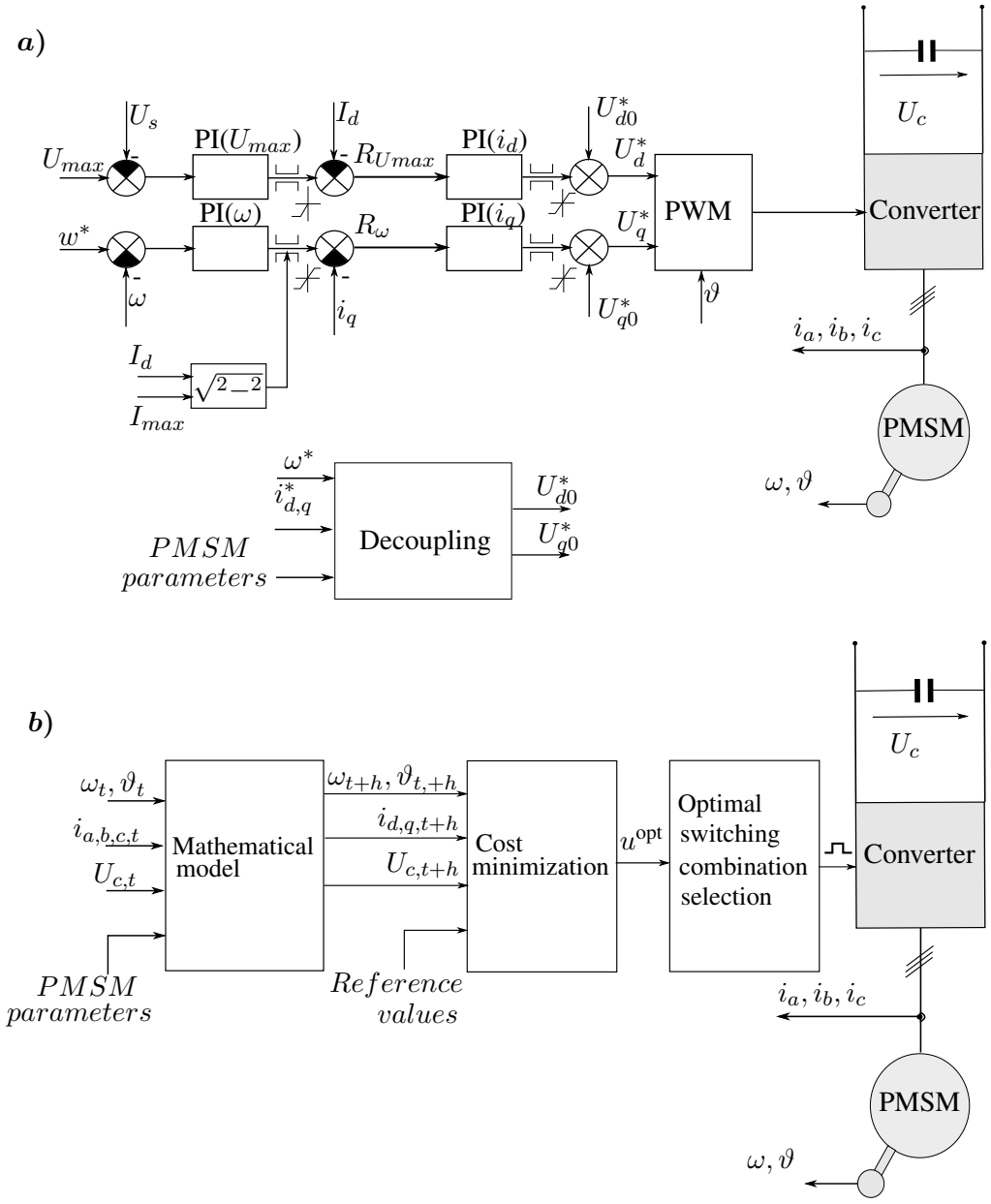

Figure 3.1.: **a)** Block diagram of cascade control of PMSM drive **b)** Block diagram of MPC for PMSM drive

3.1. Aim of control

The behavior of the predictive controller is given by the chosen cost function. In the context of speed control of PMSM drives, the cost function is designed to reach two main objectives: (i)

speed tracking, (ii) drive efficiency. These two requirements can be formulated as minimization of the tracking error

$$g_\omega = (\omega_t - \omega_t^*)^2, \tag{3.1}$$

and minimization of the current amplitude (i.e. Joule losses):

$$g_i = (i_{d,t}^2 + i_{q,t}^2). \tag{3.2}$$

Since these two requirements are contradictory, we need to define a compromise between them, typically in the form of weighted sum (see chapter 2.2). The MPC is then defined as

$$\begin{aligned} u_{t:t+h}^{\text{opt}} = \arg \min_{u_{t:t+h} \in U} \sum_{\tau=t}^{t+h} (\lambda_\omega g_\omega(\omega_\tau, \omega_\tau^*) + \lambda_i g_i(i_{d,\tau}, i_{q,\tau})) \\ \text{subject to: } c_1 : u_\tau \in \mathcal{U}, \\ c_2 : x_\tau \in \mathcal{X}, \\ c_3 : x_\tau = f(x_\tau, u_\tau), \quad \forall \tau = t, t+1, \ldots, t+h, \end{aligned} \tag{3.3}$$

where, λ_ω, λ_i are the penalization's, setting the preferences to particular terms in the cost function. The minimization of the cost function is done with respect to given constraints. The constraints c_1 and c_2 are defined by admissible stator current amplitude I_{max} and admissible control actions which is given by maximum amplitude of the input stator voltage $U_{\text{max}} = \frac{U_{dc}}{\sqrt{3}}$ (where U_{dc} is converter dc-link voltage) :

$$\mathcal{X} = \{i : |i_s| \leq I_{\text{max}}\}, \qquad \mathcal{U} = \{u_t : |u_t| \leq U_{\text{max}}\}. \tag{3.4}$$

The c_3 represents the mathematical model, which describes the behavior of PMSM.

3.2. Model of the drive

The mathematical model of PMSM drive is described by five differential equations:

$$\frac{di_d}{dt} = -\frac{R_s}{L_d} i_d + \frac{L_q}{L_d} i_q \omega + \frac{1}{L_d} u_d, \tag{3.5}$$

$$\frac{di_q}{dt} = -\frac{R_s}{L_q} i_q - \frac{\Psi_{PM}}{L_q} \omega - \frac{L_d}{L_q} i_d \omega + \frac{1}{L_q} u_q, \tag{3.6}$$

$$\frac{d\omega}{dt} = \frac{1}{J}[k_p p_p^2 \left(\Psi_{PM} i_q + (L_d - L_q) i_d i_q\right) - p_p T_L], \tag{3.7}$$

$$\frac{d\vartheta}{dt} = \omega, \tag{3.8}$$

$$\frac{dT_L}{dt} = 0. \tag{3.9}$$

The state vector $x = [i_d, i_q, \omega, \vartheta, T_L]$ is composed of components of the stator current vector of the drive in rotating (d,q) reference frame linked to a rotor flux vector ($i_{d,q}$), the electrical rotor speed ω, the electrical rotor position ϑ, and load torque T_L. Input of the state space model are components of the stator voltage vector $u_{d,q}$. The system parameters are: the components of the stator inductance in d- and q-axis the stator resistance R_s, and the flux linkage excited by permanent magnets on the rotor Ψ_{PM}.

Note that the model (3.5)–(3.9) is non-linear due to products of state variables, $i_d\omega$ in (3.5) $i_d\omega$ in (3.6) and $i_d i_q$ in (3.7). To apply the standard linear system theory, we linearize the model (see chapter 2.1) using a simple method based on two assumptions: (i) the assumption of slowly varying rotor speed ω with respect to the sampling period; and (ii) first order Taylor approximation of the product i_d, i_q. The first assumption allows us to approximate the products $i_d\omega$ and $i_q\omega$ by linear terms $i_d\omega^{\text{op}}$ and $i_q\omega^{\text{op}}$, where ω^{op} is the operational point of the rotor speed. In the resulting algorithm it will be replaced by instantaneous speed. First order Taylor approximation of the nonlinear term in (3.7) is:

$$\begin{aligned} f(i_d, i_q) = f(i_d^{\text{op}}, i_q^{\text{op}}) + (i_{d-} i_d^{\text{op}}) \frac{\partial f(i_d, i_q)}{\partial i_d} + (i_{q-} i_q^{\text{op}}) \frac{\partial f(i_d, i_q)}{\partial i_q} \Rightarrow \\ \Rightarrow i_d i_q \approx i_d^{\text{op}} i_q^{\text{op}} + (i_{d-} i_d^{\text{op}}) i_q^{\text{op}} + (i_{q-} i_q^{\text{op}}) i_d^{\text{op}} = \\ = -i_d^{\text{op}} i_q^{\text{op}} + i_d^{\text{op}} i_q + i_d i_q^{\text{op}}, \end{aligned} \tag{3.10}$$

where i_d^{op} and i_q^{op} are components of stator current vector at the given operational point. They will be also replaced by instantaneous currents.

Under these simplifications, the continuous time model can be rewritten in linear form

$$\frac{dx}{dt} = A_c(x^{\text{op}})x + B_c u, \tag{3.11}$$

where

$$x^{\text{op}} = [i_d^{\text{op}}, i_q^{\text{op}}, \omega^{\text{op}}, 0, 0],$$

$$A_c(x^{\text{op}}) = \begin{bmatrix} -\frac{R_s}{L_d} & -\frac{L_q}{L_d}\omega^{\text{op}} & 0 & 0 & 0 & 0 \\ -\frac{L_d}{L_q}\omega^{\text{op}} & -\frac{R_s}{L_q} & -\frac{\Psi_{PM}}{L_q} & 0 & 0 & 0 \\ \kappa i_q^{\text{op}} & \kappa_\Psi + \kappa i_d^{\text{op}} & 0 & 0 & -\frac{p_p}{J} & -k i_d^{\text{op}} i_q^{\text{op}} \\ 0 & 0 & 1 & 0 & 0 & 0 \\ 0 & 0 & 0 & 0 & 0 & 0 \\ 0 & 0 & 0 & 0 & 0 & 0 \end{bmatrix}, B_c = \begin{bmatrix} \frac{1}{L_d} & 0 \\ 0 & \frac{1}{L_q} \\ 0 & 0 \\ 0 & 0 \\ 0 & 0 \\ 0 & 0 \end{bmatrix}, \tag{3.12}$$

$$\kappa = \frac{3}{2J} p_p^2 (L_d - L_q), \kappa_\Psi = \frac{3}{2J} p_p^2 \Psi_{PM}$$

To accommodate for the constant term $-i_d^{\text{op}} i_q^{\text{op}}$ from (3.10), we assume that the state vector is extended to contain additional constant, i.e. $x = [i_d, i_q, \omega, \vartheta, T_L, 1]$. This is an auxiliary step allowing the use of standard software, that has no impact on physical interpretation of the model.

Conversion of the model into discrete time form (2.5) with sampling time Δt is done using standard formulas for linear systems (2.4) described in Chapter 2.1. The resulting discrete time system is then

$$x_{t+1} = A(x^{\text{op}})x_t + B(x^{\text{op}})u_t. \tag{3.13}$$

3.3. Fundamental consideration of the constraints influence on the drive

Satisfaction of all constraints in the full model on the whole prediction horizon is too complex, hence, we propose to use a problem simplification where, particular solutions are derived for special cases, where only one of the constraints is active.

The first special case is based on consideration of only the maximum stator current limit. It has been shown, that operation on this limit, that maximizes the produced torque implies the

maximum torque per ampere (MTPA) rule:

$$\text{MTPA}: \quad i_d + \frac{L_d - L_q}{\Psi_{PM}}(i_d^2 - i_q^2) = 0. \tag{3.14}$$

The second special case is derived by considering operation on the the maximum supply voltage limit. The result is an equation that can be used as the field weakening curve FW:

$$\text{FW}: \quad \left(\frac{L_q}{L_d} i_q\right)^2 + \left(i_d + \frac{\Psi_{PM}}{L_d}\right)^2 - \left(\frac{\zeta U_{\max}}{|\omega|\, L_d}\right)^2 = 0, \tag{3.15}$$

where $\zeta \in [0, 1]$ is a chosen safety factor. (3.14) and (3.15) may be used to direct the MPC to find the optimal solution on shorter horizon. In [63], those two rules have been used as attraction region in the cost function forcing the the FCS-MPC with one step ahead prediction to operate near to the attraction region. The optimal control input is found by exhaustive search over the finite number of the admissible voltage vectors (switching combinations) one step ahead only, therefore the algorithm is computationally very cheep and the hard state and voltage constraints are easily meet by simply eliminating such switching combination which would lead to their violation.

On the other hand FCS-MPC may results in relatively high current distortion due to constant duty cycles and inconstant switching frequency, which may be prohibitive in some applications (i.e. traction where the inconstant switching frequency may interfere with the railway safety systems).

Therefore an alternative can be found in [31], where rules (3.14) and (3.15) have been used in combination with CCS-MPC using PWM modulator in a feed forward based control design. The PWM modulator has several advantageous over the FCS-MPC direct switching combination selection

- constant switching frequency
- accurate transformation of the input control voltage to the output of the power-converter
- relatively low current ripples.

The aim in [31] is to design current reference which respect all given constraints and follow the MTPA curve. Nevertheless meeting the hard constraints in this case still imposes relatively high demands on computational power which may not be available for PMSM drive control.

Remark 3. The proposed solution of the input constraints is specific to the problem of speed control of the PMSM drive. Similar rules, however, are available for speed control of other ac machines. .

3.3.1. Operation in the field weakening region

To illustrate the benefit of using the explicit rules to reinforce the MPC, we study the conventional MPC formulation in simulation. Speed control of a PMSM drive with parameters from Table A.1 using MPC with cost (3.3) and system model (3.11) has been simulated using numerical toolbox CVX [64]. The results of transient behavior of the step change of the required speed from 1100 to 1102 rad/s is displayed in Figure 3.2 a). For comparison, the i_d current satisfying the field weakening curve (3.15) is displayed as well. Note that even for horizon of length $h = 100$ the numerical solution does not secure steady performance in the steady-state. However, in the transient, the numerical solution is equal to that of the FW equation. If the FW curve is used as an attraction region, the numerical solution follows it exactly even for very low penalization of the attraction region. The use of the FW constraint allows to use much shorter

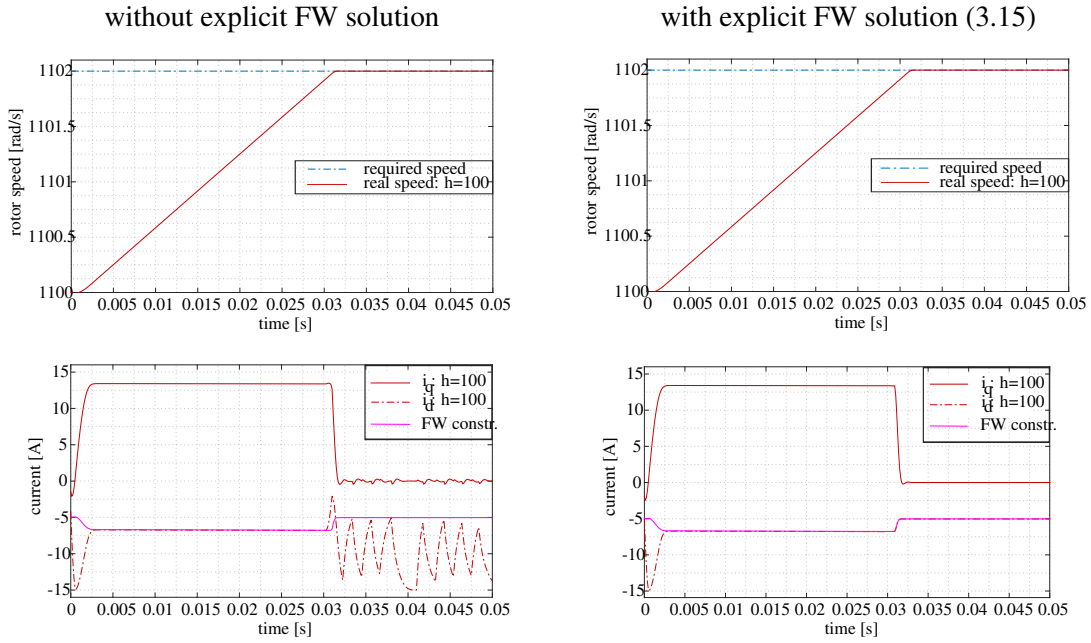

Figure 3.2.: Simulation of step change of electrical rotor speed at field weakening region, from 1100 to 1102 rad/s, without explicit FW constraint (left column) and with explicit constraint on the FW curve (right column). The length of prediction horizon $h = 100$.

horizons.

Remark 4. The field weakening limit (3.15) is based on approximation of the allowed voltage by a circle. More accurate solution is available in [65] which requires more computational resources.

3.4. SDRE for PMSM

Following the approach of [63] of finding approximate solutions with few constraints, we consider a case without any constraint on the voltage or current. Then, the task becomes standard quadratic control of non-linear system for which many techniques exist. One such approach is the state dependent Riccati equation (SDRE) which has been applied to PMSM for example in [41, 42].

The basic idea is to linearize the system at operating point and derive local LQR solution (see section 2.6.2). The state reference vector $x_t^* = [i_{d,t}^*, i_{q,t}^*, \omega_t^*, \vartheta_t^*, T_{L,t}^*, 1]$ is assumed to be constant, the model $f(x_t, u_t)$ is (3.13) and we assume the quadratic cost function2.9, with the substitution of $u_t^* = u_{t-1}$. Than we can rewrite (2.9) as

$$g(x_t, x_t^*, u_t, u_{t-1}) = (x_t - x_t^*)^T Q(x_t - x_t^*) + (u_t - u_{t-1})^T R(u_t - u_{t-1}). \tag{3.16}$$

The term penalizing difference of the input variable $(u_t - u_{t-1})^T R(u_t - u_{t-1})$ is used to penalize too high control inputs. In contrast to the penalization of the control action itself (i.e. $u_t^T R u_t$) it does not introduce a steady state error of the resulting controller[1].

The synthesis of the controller at each point of linearization can be achieved by pole placement or Riccati equation. We will follow the latter approach. Due to the used penalization of the input difference, we need to augment the state vector to obtain the standard form. The augmented vector is $\tilde{x}t = [x_t^T, x_t^{*T}, u_{t-1}^T]^T$ with state dynamics

$$\begin{bmatrix} x_{t+1} \\ x_{t+1}^* \\ u_\tau \end{bmatrix} = \underbrace{\begin{bmatrix} A(x^{\mathrm{op}}) & 0 & 0 \\ 0 & I & 0 \\ 0 & 0 & 0 \end{bmatrix}}_{\tilde{A}} \begin{bmatrix} x_t \\ x_t^* \\ u_{t-1} \end{bmatrix} + \underbrace{\begin{bmatrix} B(x^{\mathrm{op}}) \\ 0 \\ I \end{bmatrix}}_{\tilde{B}} u_t, \tag{3.17}$$

[1] Other causes of steady state error, such as inaccurate model parameters, can be handled by adding an integrator into the system [66]. However, this extension was not necessary in our tests.

and quadratic cost function:

$$\begin{aligned} g(\tilde{x}_t, u_t) &= \tilde{x}_t{}^T \tilde{Q} \tilde{x}_t + u_t{}^T R u_t + 2\tilde{x}_t^T N u_t, \\ \tilde{Q} &= \begin{bmatrix} Q & -Q & 0 \\ -Q & Q & 0 \\ 0 & 0 & R \end{bmatrix}, \\ N &= [0, 0, -R]. \end{aligned} \tag{3.18}$$

The optimal control is found by state dependent discrete time Riccati equation (**??**), where the matrix S defines the cost-to-go function of dynamic programming on infinite horizon (see section 2.6.2).The SDRE controller is then defined as:

$$u_t^{\text{SDRE}} = -L(x^{\text{op}})\tilde{x}_t. \tag{3.19}$$

In order to avoid online evaluation of the gain $L(x^{\text{op}})$ or its approximation by Taylor expansion, we seek explicit parametric form of the gain using the interpolation method. This is typically more accurate approach [48]. Specifically, we solve the LQR problem for a range of operational states $X^{\text{op}} = [x^{\text{op}(1)}, x^{\text{op}(2)}, \ldots, x^{\text{op}(N)}]$.

Illustration of the interpolation for the studied drive parameters is presented in Figure 3.3.

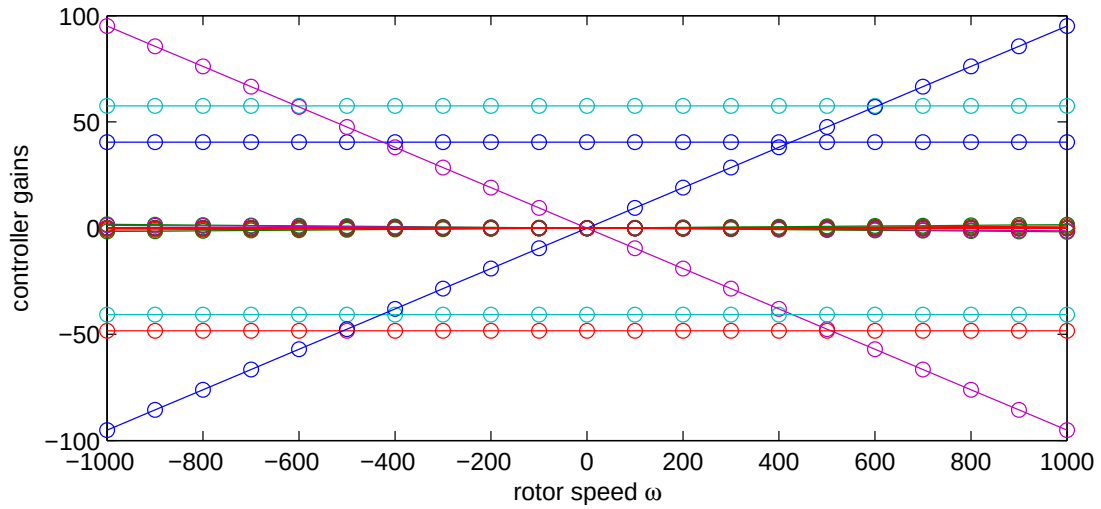

Figure 3.3.: Gains of the SDRE controller evaluated for a grid of $\omega^{\text{op}} \in \langle -1000, 1000 \rangle$ rad/s (circles). The gains are interpolated by a first order polynomial (full line).

3.5. State observer

The MPC controller consider a perfectly known state vector x_t. However the states are usually available through noisy measurement, thus it is desirable to use observer to reconstruct the state vector x_t. We focus on standard Kalman filter for this purpose.

We follow the Kalman filter design from chapter 2.7. We assume that the state model (3.13) is imperfect

$$x_{t+1} = A(x^{\text{op}})x_t + B(x^{\text{op}})u_t + \epsilon_x, \tag{3.20}$$

where ϵ_x is the model error which is assumed to be Gaussian distributed with covariance matrix Σ_x. The state is observed via measurements of the phase currents, $i_{a,t}$, $i_{b,t}$, $i_{c,t}$ and position ϑ_t. Transforming the observed currents into the d-q reference frame, we have an observation equation

$$y_t = \begin{bmatrix} i_{d,t}^{meas} \\ i_{d,t}^{meas} \\ \vartheta_t^{meas} \end{bmatrix} = Cx_t + \epsilon_y, \;\; C = \begin{bmatrix} 1 & 0 & 0 & 0 & 0 \\ 0 & 1 & 0 & 0 & 0 \\ 0 & 0 & 0 & 1 & 0 \end{bmatrix} \tag{3.21}$$

where ϵ_y is the observation error with covariance matrix Σ_y. Using the standard Kalman filter equations for each operational point of linearization x^{op}, we obtain a constant Kalman gain $K(x^{\text{op}})$. In analogy to the SDRE controller, the gain scheduling for the observer is linear

$$K(x^{\text{op}}) = K_0 + x^{\text{op}}K_x, \tag{3.22}$$

with sparse matrices K_0 and K_x. The state reconstruction is then

$$\hat{x}_t = A(x^{\text{op}})x_{t-1} + B(x^{\text{op}})u_{t-1} + K(y_t - Cx_{t-1}). \tag{3.23}$$

Since covariance matrices of the measurement error and especially the model error are not known, they must be tuned. Useful guidelines for contrivances matrices tuning in Kalman filter can be found in [67]. A several work has been done on adaptive tuning of the Kalman filter [68],[69]. This is a promising research direction for tuning of the Kalman filter, however, we are still using manual tuning in this thesis.

The correct tuning of the Kalman filter has been validated in simulation on the data, measured on real laboratory prototype of PMSM drive (The example of the simulation result is shown in fig 3.4).

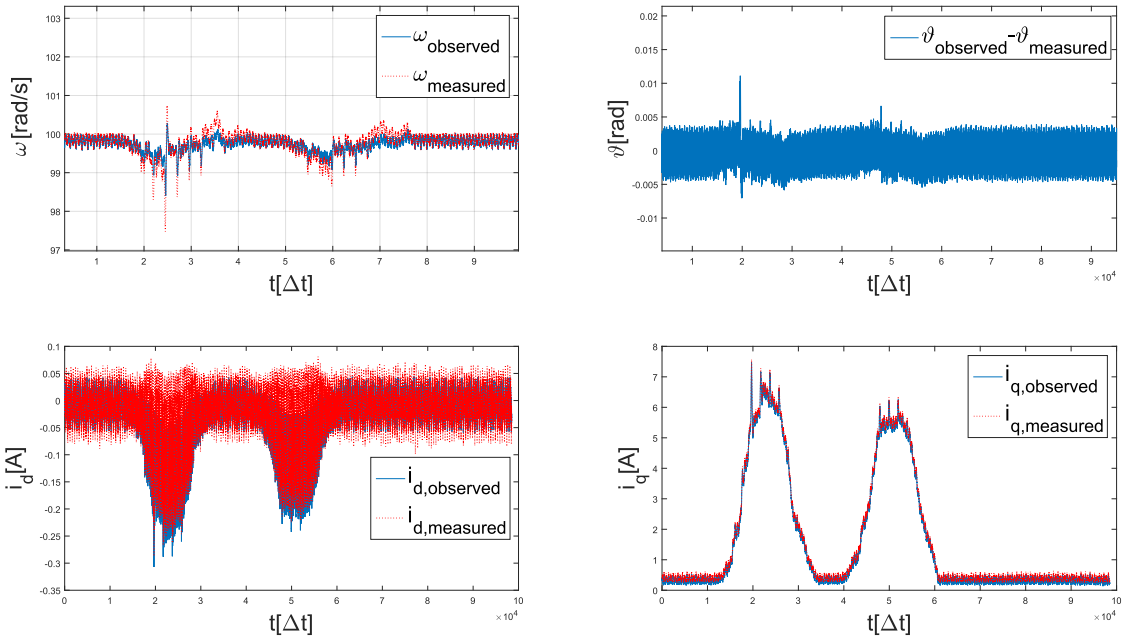

Figure 3.4.: Example of the covariance matrices tuning on set of data measured on laboratory prototype of the PMSM drive with parameters (A.1) and sampling period $125e^{-6}$s.

3.6. Open problems

1. *Efficient evaluation of the constrained MPC with PWM*

   The one of the greatest challenge in the designing of MPC for speed control of PMSM is a simple way of handling the hard state constraints. While the input voltage is limited by the physical nature of the the converter (i.e. maximum available voltage) inclusion of the hard state constraints in the optimization problem over the whole length of the prediction horizon requires extensive computational resources. The approach presented in [31, 32] is based on the use of general purpose solvers that are not useful in practical PMSM drives.

   An algorithm that solves the multi-step ahead MPC with constraints with computational cost comparable to the cost of a PID controller is not available.

2. *Minimization of the average switching frequency of the FCS-MPC*

   An alternative way how to solve the constrained optimization is FCS-MPC with very short sampling period. The shorter the sampling period is, lower the current ripple can

be. However, the optimization is then allowed to switch very often which leads to increase switching losses (since they are not considered in the cost). Penalization of the switching losses can be easily added, however, the solution on the one step ahead horizon is again sub-optimal. Better results can be achieved by multi-step ahead FCS-MPC at much higher computational cost.

An algorithm that provides effective reduction of the switching losses with computational cost of one-step ahead MPC is not available.

4. CCS-MPC for cascade free speed control of PMSM with constraint optimization

In this chapter, the main focus is dedicated to a design of a simple and computationally efficient predictive speed control of PMSM based on CCS-MPC (see section2.3.1), which achieves optimal performance in steady state as well as transients and. Existing solutions (e.g. [31]), usually requires relatively high computational resources.

It has been shown, that analytical solutions of the control problem can be incorporated into the cost function of the MPC formulation which allows to obtain good results even for short prediction horizon. Specifically, in this chapter, SDRE (see section 3.4) is used to solve the unconstrained optimization problem on long prediction horizon which is combined with constrained manager. The unifying principle is the principle of limited lookahead policy (section 2.4.1). The resulting optimization routine forms a convex problem (see section2.3.1) and can be solved using geometrical interpretation of the problem.

4.1. MPC formulation

We propose to solve the speed control of a PMSM drive by optimization of the following control problem

$$
\begin{aligned}
u^{\text{opt}}_{t:t+h} &= \arg \min_{u_{t:t+h} \in U} \sum_{\tau=t}^{t+h} \left(\lambda_\omega g_\omega(\omega_\tau, \omega^*_\tau) + \lambda_i g_i(i_{d,\tau}, i_{q,\tau}) + \lambda_u g_{din}(u_t, u_{t-1}) \right), \\
\text{subject to: } & c_1 : i^2_{d,\tau+1} + i^2_{q,\tau+1} \leq I^2_{\max}, \\
& c_2 : (i^\Psi_d + i_{d,\tau+1})^2 + \xi i^2_{q,\tau+1} \leq I^2_{FW}, \\
& c_3 : x_\tau = f(x_\tau, u_\tau), \quad \forall \tau = t, t+1, \ldots, t+h,
\end{aligned}
\tag{4.1}
$$

where, the c_1 and c_2 are the maximum current constraint and field-weakening constraint lying on the FW curve (3.15), with substitutions $i_d^{\Psi} = \frac{\Psi_{PM}}{L_d}$, $\xi = \frac{L_q^2}{L_d^2}$, and $I_{FW} = \zeta \frac{U_{\max}}{|\omega| L_d}$. In contrast to (3.3), the cost has an additional penalization of the difference of the input voltage $g_{din} = (u_t - u_{t-1})^2$ which is common in SDRE. The constraints c_1 and c_2 are identical to those proposed in [63], with the distinction, that they are used as hard constraints and only for first value on the horizon. This simplification is important for computational cost and we will show, that it has negligible impact on the performance.

Since constraints c_1 and c_2 are active only at time $t+1$, optimization for $t+2$ and further on is unconstrained. Thus we can substitute the SDRE solution derived from (2.24) into the cost function (4.1). This yields the following one step ahead optimization problem

$$u_t^{\text{opt}} = \arg \min_{u_t(x_t)} \left\{ (u_t - u^{\text{sdre}})^T Y (u_t - u^{\text{sdre}}) \right\}, \tag{4.2}$$

subject to:

$$c_1 : i_{d,t+1}^2 + i_{q,t+1}^2 \leq I_{\max}^2, \tag{4.3}$$

$$c_2 : (i_d^{\Psi} + i_{d,t+1})^2 + \xi i_{q,t+1}^2 \leq I_{FW}^2, \tag{4.4}$$

where the simplification of the SDRE solution has a consequence that it does not consider constraint on the torque. This may produce undesired side effects. A solution to this problem was suggested in [38] using modification of the speed tracking error. Specifically, we introduce saturation of the speed tracking error

$$\Delta\omega = \begin{cases} \Delta\omega_{\max} & \text{if } (\omega_t^* - \omega_t) > \Delta\omega_{max}, \\ -\Delta\omega_{\max} & \text{if } (\omega_t^* - \omega_t) < -\Delta\omega_{\max}, \\ \omega_t^* - \omega_t & \text{otherwise.} \end{cases} \tag{4.5}$$

This limit prevents extreme values of the linear controller at step changes. This is a heuristic solution of the operation on the current limit for longer horizon. It was proposed in [38] as one of many heuristics. It is possible to use the full non-linear cost-to-go presented in [38] using local quadratic approximation. However, in our experiments, we found (4.5) to be sufficiently accurate solution of the cost-to-go saturation.

4.2. Convex constrained optimization

The main contribution of this chapter is an efficient and simple algorithm for constrained optimization, solving (4.2-4.4), which is essentially the convex optimization problem (see chapter 2.3). The aim is to achieve accuracy comparable to solvers used in [31] at much lower computational cost. For clarity of explanation, we reformulate the problem to the current space, where most of the constraints are defined. Formulation in the voltage space is also possible, however, it would not be as intuitive.

We note that the stator current vector i_{t+1} is modeled by a first order model:

$$i_{t+1} = A_i(x_t)i_t + B_i u_t, \tag{4.6}$$

where $A_i(x_t)$ and B_t are blocks of the matrices $A(x^{\text{op}})$ and $B(x^{\text{op}})$ from (2.6) corresponding to the current equations and u_t is stator voltage vector. Since matrix B_i is invertible,

$$u_t = B_i^{-1}(i_{t+1} - A_i(x_t)i_t), \tag{4.7}$$

Than projection of the unconstrained control input obtained in 4.2 to the current space as

$$i_{t+1}^{\text{unc}} = A_i(x_t)i_t + B_i u_t^{\text{unc}}. \tag{4.8}$$

Rewriting (2.24) as

$$u_t^{\text{opt}} \quad = \quad \arg\min_{u_t(x_t)} \left\{ (u_t + Lx_t)^T Y (u_t + Lx_t) \right\}, \tag{4.9}$$

and substituting (4.7) and u_t^{unc} in to it we obtain:

$$\begin{aligned} i_{t+1}^{\text{opt}} = \arg\min_{i_{t+1}} \Bigg\{ & \left((B_i^{-1}(i_{t+1} - A_i(x_t)i_t) - (B_i^{-1}(i_{t+1}^{\text{unc}} - A_i(x_t)i_t)^T \right) Y \\ & \left((B_i^{-1}(i_{t+1} - A_i(x_t)i_t) - (B_i^{-1}(i_{t+1}^{\text{unc}} - A_i(x_t)i_t)) \right) \Bigg\} \Rightarrow \\ \Rightarrow \arg\min_{i_{t+1}} \Bigg\{ & \left((B_i^{-1}((i_{t+1}) - (i_{t+1}^{\text{unc}}))) \right)^T Y \left((B_i^{-1}((i_{t+1}) - (i_{t+1}^{\text{unc}}))) \right) \Bigg\}, \end{aligned} \tag{4.10}$$

which yields

$$i_{t+1}^{\text{opt}} = \arg\min_{i_{t+1}} \left\{ (i_{t+1} - i_{t+1}^{\text{unc}})^T \Phi (i_{t+1} - i_{t+1}^{\text{unc}}) \right\} \tag{4.11}$$
$$\text{subject to: } c_1(i_{t+1}), c_2(i_{t+1}),$$

where $\Phi = B_i^{-T} Y B_i^{-1}$ with Choleski decomposition $\Phi^{\frac{1}{2}}$, $\Phi = (\Phi^{\frac{1}{2}})^T \Phi^{\frac{1}{2}}$. Further simplification can be achieved by one-to-one transformation $\bar{i}_{t+1} = \Phi^{\frac{1}{2}} i_{t+1}$ under which the optimization problem becomes:

$$\begin{aligned} \bar{i}_{t+1}^{\text{opt}} &= \arg\min_{i_{t+1}} \left\{ (\bar{i}_{t+1} - \bar{i}_{t+1}^{\text{unc}})^T (\bar{i}_{t+1} - \bar{i}_{t+1}^{\text{unc}}) \right\} \\ \text{subject to: } & |\Phi^{-\frac{1}{2}} \bar{i}_{t+1}| < I_{\text{max}}, \\ & |\Xi \Phi^{-\frac{1}{2}} (\bar{i}_{t+1} - \bar{i}_{t+1}^{\Psi})| < I_{FW}, \end{aligned} \tag{4.12}$$

where $\bar{i}_{t+1}^{\Psi} = \Phi^{\frac{1}{2}} \begin{bmatrix} i_d^{\Psi} \\ 0 \end{bmatrix}$, $\Xi = \begin{bmatrix} 1 & 0 \\ 0 & \sqrt{\xi} \end{bmatrix}$. The optimization problem (4.12) will be solved for $\bar{i}_{t+1}^{\text{opt}}$ and the optimal stator voltage vector found as

$$u_t^{\text{opt}} = B_i^{-1} (\Phi^{-\frac{1}{2}} \bar{i}_{t+1}^{\text{opt}} - A_i(x_t) i_t). \tag{4.13}$$

4.3. Simplified solution of the convex constraint optimization

We derive a simplified optimization algorithm based on the assumptions, that the matrix Φ is diagonal and thus axis of all constraining ellipses are aligned with the d-q coordinate system[1]. Without loss of generality, we assume that the SDRE solution has form $\Phi = \text{diag}([1, \phi^2])$.

Under this assumption, constraints c_1 and c_2 become

$$c_1 : \quad \bar{i}_d^2 + \bar{i}_q^2 \phi^{-2} \leq I_{\text{max}}^2, \tag{4.14}$$

$$c_2 : \quad (\bar{i}_d + i_d^{\psi})^2 + \bar{i}_q^2 \phi^{-2} \xi \leq I_{FW}^2, \tag{4.15}$$

i.e. two ellipsis centers $[0, 0]$, $[-i_d^{\psi}, 0]$ and radii $[I_{\text{max}}, I_{\text{max}}\phi]$, $[I_{FW}, I_{FW}\phi\xi^{-0.5}]$, respectively. Since all variables are in time $t + 1$, we omit its explicit mentioning in the notation for clarity.

[1] Extension to general case is possible but it would involve additional rotations that are not needed in many applications.

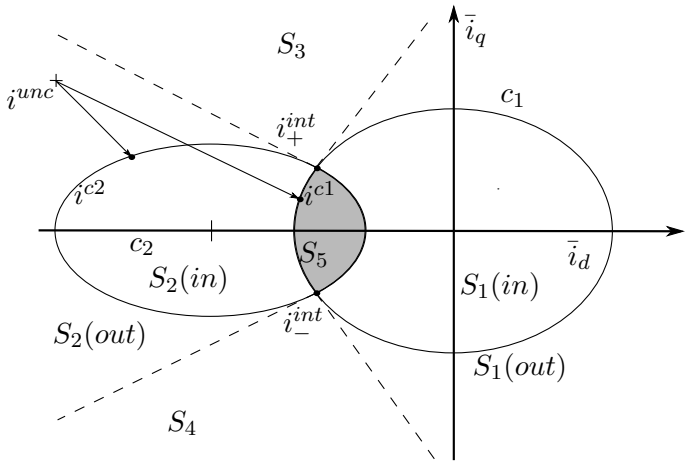

Figure 4.1.: Decomposition of the space for optimal solutions, dashed lines denote normals to the ellipses at their intersection. Feasible set S_5 is denoted by gray area. Illustration of projection of unconstrained solution i^{unc} to ellipse c_1 is denoted by i^{c1} and projection to ellipse c_2 by i^{c2}. Intersection of ellipses is denoted by i_+^{int} and i_-^{int}.

The optimization problem (4.12) is essentially minimization of Euclidean distance to the unconstrained solution i^{unc}, hence the optimum solution is obtained by projection onto the feasible set, as illustrated in Fig. 4.1. This general task of convex optimization can be solved by geometric intuition:

1. In lower speed region, only constraints c_1 can be violated. The optimal solution is then a projection of i^{unc} to ellipse c_1 (), which will be denoted i^{c1}. If the constraint is not violated $i^{\text{c1}} = i^{\text{unc}}$.

2. If only constraint c_2 is violated, the optimal solution is projection of i^{unc} to c_2 which will be denoted i^{c2}.

3. Loaded operation at high speed requires to operate the machine at the intersection of ellipses c_1 and c_2. Efficient algorithm for computing the intersection points i^{int} is given in.

The key question is which of the three cases above is optimal at the current state. Decisions based on comparing speed with reference has been proposed [31], however, they are not optimal in transients. Therefore, we propose a new solution based on convex optimization results.

From Fig. 4.1 it is obvious, that the optimal projection depends on the position of the vector i^{unc} in the current plane. If the unconstrained current vector i^{unc} belongs to S_2, the optimal solution is projection i^{c1}. In such a case, projection i^{c2} will lie outside of constraint

c_1, i.e. $i^{\text{c2}} \notin c_1$. This combination of $i^{\text{c1}} \in c_2$ and $i^{\text{c2}} \notin c_1$ is unique for S_2. The full set of equivalences is then (see chapter 2.3.1) :

$$\begin{aligned}
&i^{\text{unc}} \in S_1 \iff i^{\text{c1}} \notin c_2, \quad i^{\text{c2}} \in c_1, \\
&i^{\text{unc}} \in S_2 \iff i^{\text{c1}} \in c_2, \quad i^{\text{c2}} \notin c_1, \\
&i^{\text{unc}} \in S_3 \iff i^{\text{c1}} \notin c_2, \quad i^{\text{c2}} \notin c_1, \; i^{\text{unc}}_{q,t+1} > 0, \\
&i^{\text{unc}} \in S_4 \iff i^{\text{c1}} \notin c_2, \quad i^{\text{c2}} \notin c_1, \; i^{\text{unc}}_{q,t+1} < 0, \\
&i^{\text{unc}} \in S_5 \iff i^{\text{c1}} \in c_2, \quad i^{\text{c2}} \in c_1.
\end{aligned} \tag{4.16}$$

When none of the projections satisfy both constraints (sets S_3 and S_4), the solution is at the intersection of both ellipses, denoted i^{int}_+ and i^{int}_-. The sign of the q component is equal to the sign of the q component of the unconstrained solution. Note that the ellipses can be also disjoint, e.g. when dc-link voltage suddenly drops in field weakening regime. In such case, constraint c_1 has higher priority and the optimal solution is $i^{\text{opt}} = [-I_{max}, 0]$.

Conditions on the right hand side of (4.16) allow to design a very efficient control design presented in algorithm 4.1.

4.4. Simulations

The proposed control approach was tested on a system (PMSM drive prototype) with sampling time $\Delta t = 125\mu s$, dc-link voltage U_{dc} =100V and parameters (see Table A.1)

Since the main contribution of this chapter is the constrained optimization algorithm, we present the simulation results with perfect state information for clarity. The controller for state reference $x^*_t = [0, 0, \omega^*_t, 0, 0, 0]$ and penalization matrices

$$\begin{aligned}
Q^{\frac{1}{2}} &= \text{diag}([0.4, 0.4, 1, 0, 0]), \\
R^{\frac{1}{2}} &= 2 \times 10^{-4}\,\text{diag}([1, 1]).
\end{aligned} \tag{4.17}$$

was designed using the SDRE approach. The penalization of the currents in d and q axis is identical since the resistive losses are also identical. The penalization for the u_d and u_q differences is also chosen as symmetric.

Using (4.17) and model (2.6) in the SDRE design procedure with polynomial interpo-

Algorithm 4.1 Simplified solution of the convex constraint optimization with SDRE lookahead.

Off-line (SDRE):

1. Design approximate linear model of the controlled system 3.13with matrices $A(x^{\text{op}})$, $B(x^{\text{op}})$.
2. Choose quadratic loss function (3.18) with appropriate penalization matrices Q, R.
3. Design the unconstrained solution of the optimization problem by solving the SDRE (4.2).
4. Validate results of the optimized closed loop. If not successful GOTO 2.

On-line (Simplified constrained one-step optimization):

1. Project the unconstrained optimal control input u_t^{opt} to the current space (4.8)
2. Project i^{unc} to c_1 and c_2 (see fig 4.1) and select the optimal constrained current i^{opt} found by simple procedure as follows:

```
1: i^c1 := projection(i^unc, c1)
2: i^c2 := projection(i^unc, c2)
3: if (i_d^c1 + i_d^Ψ)^2 + (i_q^c1)^2 φ^-2 ξ ≤ I_FW^2 thenComment S2 or S5
4:     i^opt := i^c1
5: else                                                          ▷ S1, S3, S4
6:     if (i_d^c2)^2 + (i_d^c2)^2 φ^-2 ≤ I_max then              ▷ S1 or S5
7:         i^opt := i^c2
8:     else                                                      ▷ S3, S4
9:         if I_FW + I_max > i_d^Ψ then                          ▷ Intersection exists
10:            i^int := intersect(c1, c2)
11:            i_d^opt := i_d^int
12:            i_q^opt := sgn(i_q^unc) i_q^int
13:        else                                                  ▷ Secure c1, ignore c2
14:            i^opt := [−I_max, 0]
15:        end if
16:    end if
17: end if
18: return i^opt
```

3. Compute the optimal control action u^{opt} (4.13) corresponding to the i^{opt}
4. Apply the optimal control action u^{opt} via PWM

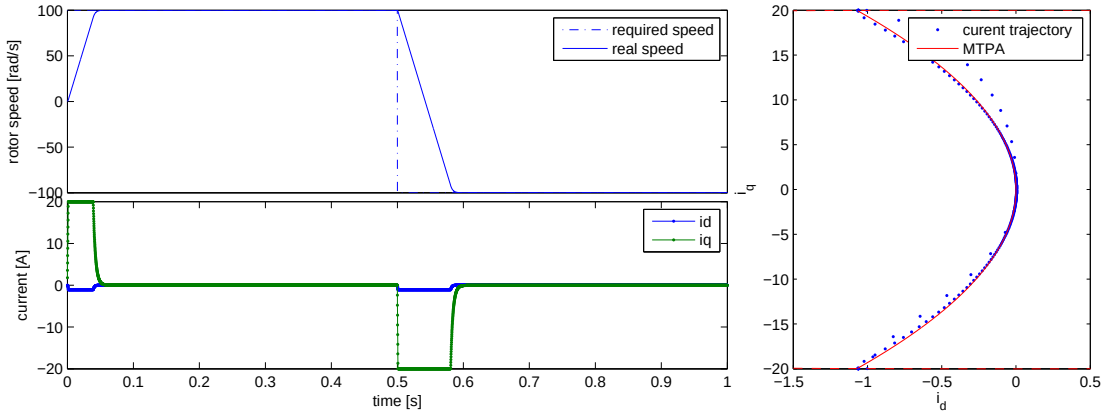

Figure 4.2.: Comparison of the current trajectory of the proposed SDRE controller with the MTPA trajectory on speed control of PMSM drive at startup and speed reversal of el. rotor speed of $\omega = \pm 100 rad/s$ under current limit $I_{\max} = 20A$. **Top left:** simulated speed of the drive and speed reference. **Bottom left:** flux and torque component of the stator current current vector in the dq reference frame (i_{dq}). . **Right**: trajectory of the current vector in the dq plane and its comparison with MTPA trajectory.

lation, we obtain controller in form (2.34):

$$\begin{aligned} u_{d,t}^{\text{unc}} =& -27 i_{d,t} - (1.9e - 3\omega_t + 1.8e - 3 i_{q,t}) i_{q,t} && (4.18)\\ & - (-6.5e - 3\omega_t - 0.2 i_{q,t}) \Delta\omega + 2e - 4 i_{d,t} i_{q,t} \\ & - (1.7e - 3\omega_t + 0.064 i_q) T_{L,t} + 3e - 4 u_{d,t-1}. \\ u_{q,t}^{\text{unc}} =& -32 i_{q,t} + 1.7e - 3\omega_t - 8.5e - 2 i_{q,t} i_{d,t} + && (4.19)\\ & - (79 + 3.9e - 3 i_{d,t} - 2.9e - 4 - i_{q,t}^2) \Delta\omega_t + && (4.20)\\ & + (27 + 7.2e - 2 i_{d,t} + 2e - 4 i_{d,t}^2 - 2e - 4 i_{q,t}^2) T_L + \\ & - 2.3e - 4 i_{d,t}^2 i_{q,t} + 2.5e - 4 u_{q,t-1}, \end{aligned}$$

where the only requested value is ω^* entering the equation via $\Delta\omega$ given in (4.5). Substitution $i_d^{\text{op}} = i_{d,t}$, $i_q^{\text{op}} = i_{q,t}$ and $\omega^{\text{op}} = \omega_t$ was already made.

The second output of the Riccati equation is matrix $Y = \begin{bmatrix} 1.16 & 0.01 \\ 0.01 & 0.96 \end{bmatrix}$ with state-dependent variations lower than 1% of the values which will be neglected. Due to low values of off-diagonal elements, the approximation of the matrix Φ proposed in Section 4.3 is well justified with ϕ^2 =1.05.

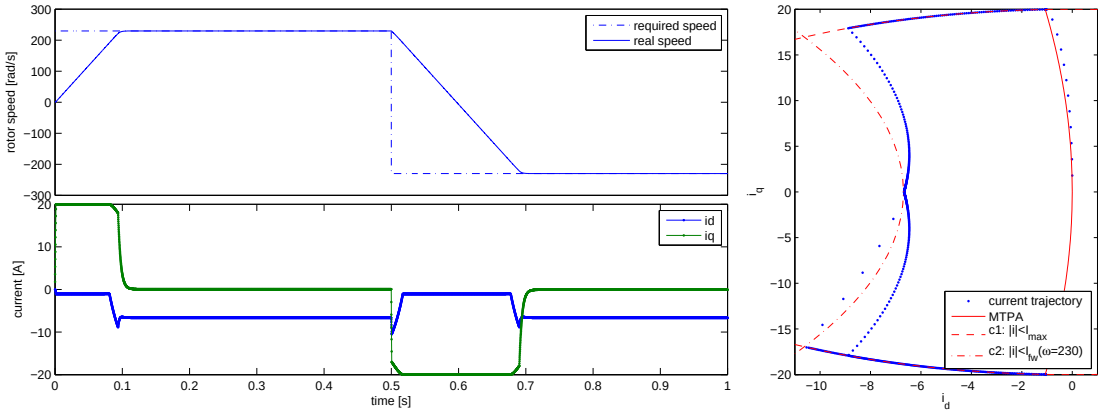

Figure 4.3.: Comparison of the current trajectory of the proposed SDRE controller with the MTPA trajectory and FW constraints on speed control of PMSM drive at startup and speed reversal of el. rotor speed of $\omega = \pm 230$rad/s under current limit $I_{\max}$ =20A. **Top left:** simulated speed of the drive and speed reference. **Bottom left:**flux and torque component of the stator current vector in the dq reference frame (i_{dq}). **Right**: trajectory of the current vector in the dq plane and its comparison with the MTPA trajectory and FW constraints.

4.4.1. SDRE solution follows the MTPA curve

Validation of efficiency of the SDRE solution with respect to non-linearities is presented by comparison of the current trajectory under SDRE control and the MPTA rule (3.14). The results of simulation of the proposed control strategy for step change of the requested rotor speed from 0 to $100rad/s$ and reversal to $-100rad/s$ is displayed in Figure 4.2. We note that the current vector follows the MTPA trajectory very accurately when the current is decreasing from the limit to zero. Slight deviation from the MTPA is notable when the current is increasing from zero to the limit (isolated dots right from the MTPA curve in Figure 4.2 right). We conjecture that this is due to the local linearization that is inherent in the SDRE approach.

4.4.2. Field weakening operation

The results of simulation of the proposed control strategy for a step change of the requested speed from 0 to $230rad/s$ and reversal to $-230rad/s$ is displayed in Figure 4.3. The current vector in dq reference frame follows the MTPA trajectory at the beginning. When the current limit constraint is reached, the trajectory is kept at the intersection of the current limit and MTPA. With increasing speed, the current vector is moved to intersection of the current limit (curve c1) and FW constraints. As the speed approaches the reference, the torque is decreas-

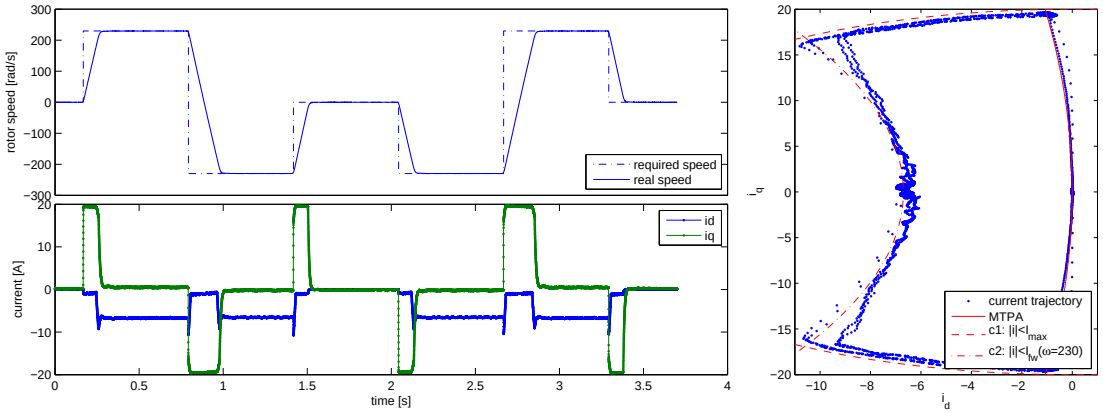

Figure 4.4.: Speed control of PMSM drive at startup and speed reversal of el. rotor speed of $\omega = \pm 230$rad/s under current limit $I_{\max} = 20A$. **Top left:** measured speed of the drive and speed reference. **Bottom left:** flux and torque component of the stator current current vector in the dq reference frame (i_{dq}). **Right**: trajectory of the current vector in the dq plane and its comparison with the MTPA trajectory and FW constraint.

ing and the current follows the FW curve at the actual speed. The current vector leaves c_1 at $\omega = 221 rad/s$ and ends at the requested $\omega = 230 rad/s$, Figure 4.3.

4.5. Experimental results

A laboratory prototype of the PMSM drive with the same parameters as in the simulation (see TableA.1) was used to verify the approach experimentally. The proposed algorithm was implemented in digital signal processor Texas Instruments TMS320F28335. Computational times of individual blocks of the controller are displayed in Table 4.1. The computational time of the constraint manager corresponds to the worst case scenario, i.e. computation of the ellipse intersection Since the most expensive operation of the constraint manager is inverse square root, further computational savings can be achieved using its approximation [70].

Tuning of the controller was identical to that in simulation, i.e. (4.18) and (4.20). However, the perfect state values were replaced by the output of the Kalman observer which was designed with covariance matrices $\Sigma_x = \text{diag}(1, 1, 1\text{e}{-8}, 5\text{e}{-6})$ and $\Sigma_y = \text{diag}(0.01, 0.01, 0.0001)$. However, all variables in the subsequent Figures are displayed before any filtering to visualize real conditions as close as possible. The rotor speed is obtained by moving average filter of numerical differentiation of the rotor position. Therefore, quantization effect of the rotor position encoder are visible as a ripple on the unfiltered speed.

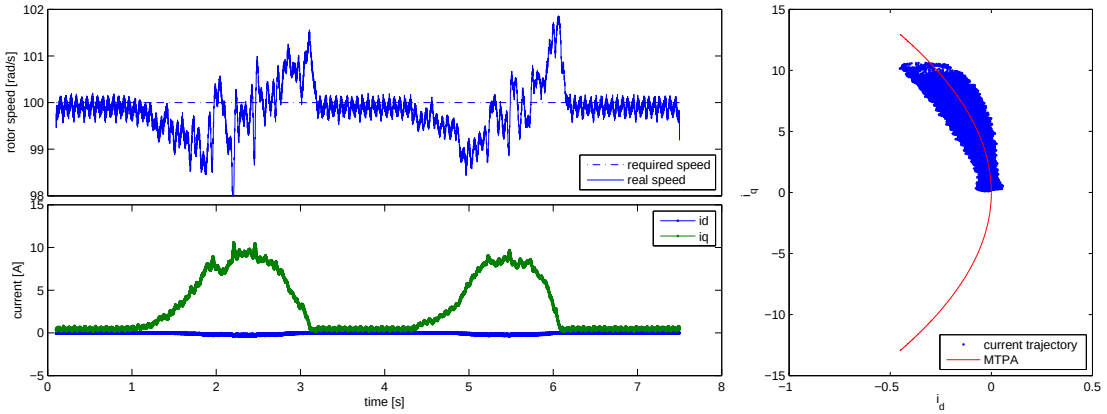

Figure 4.5.: Speed control of PMSM drive under load at el. rotor speed of $\omega = 100$rad/s. **Top left:** measured speed of the drive and speed reference. **Bottom left:** flux and torque component of the stator current current vector in the dq reference frame (i_{dq}). **Right**: trajectory of the flux and torque component of the stator current (i_{dq}) and its comparison with the MTPA trajectory.

Table 4.1.: Execution times of steps of the algorithm

operation	exec. time
data acquisition	$3.3\mu s$
Kalman filter	$3.1\mu s$
delay compensation	$0.9\mu s$
SDRE controller evaluation	$3\mu s$
constraint manager	$< 7\mu s$
total	$17.3\mu s$

Results of the startup and speed reversal $\pm 230 rad/s$ are displayed in Figure 4.4 for repeated runs. Note that the current vector operates within the constraints in the same manner as in simulations. Slight fluctuations of the current are caused by minor fluctuations of the dc-link voltage.

Response of the drive to load is displayed in Figure 4.5. Note that even in the loading scenario, the current also follows the MTPA trajectory.

4.6. Conclusion

In this chapter we have proposed an algorithm for cascade-free speed control of a PMSM drive. It combines results of unconstrained control strategies with explicit constraints on the stator current and input voltage. The focus of the solution is on efficient implementation. Therefore, we implement the unconstrained SDRE solution using gain scheduling approach. The main contribution is computationally efficient constraint manager. We show that it is sufficient to compute only two projections to ellipses and one ellipse intersection to obtain optimal solution. The resulting algorithm provides optimal behavior of the drive comparable to expensive predictive control strategies at the computational cost comparable to cascade PID control.

5. FCS-MPC with limited lookahead to reduce switching frequency in speed control of PMSM

In electric drive the power converter has limited number of admissible switching combinations. Thus FCS-MPC (see chapter 2.3.2) is a natural approach to control of power converters and ac drives. Evaluation of FCS-MPC is computationally efficient on one step ahead horizon. Extension to longer prediction horizons improves the performance but at the expense of increased computational cost. The benefits of the extended prediction horizon, however, becomes obvious, when we deal with the control objectives with long time constants where the control action influences the behavior of the drive very slowly. This is the case of PMSM speed control, where the speed is changing relatively slowly compared to the stator current.

We propose to lower the computational burden of the brute force search over the sequence of control inputs $u_t, u_{t+1}, \dots u_{t+h}$, by approximation of the longer horizon using continuous control set. Similarly to the previous CCS-MPC approach (chapter 4), only optimal control input in time t is constrained ($u_t^{\text{opt}} \in \mathcal{U}$) and the optimal inputs beyond u_{t+1}^{opt} are unconstrained. The resulting algorithm is computationally as cheap as the conventional one step FCS-MPC, however it provides the solution respecting long prediction horizons. A similar solution has been presented in [71] where the approximation of the solution of the optimal control on long prediction horizon has been used as region of the attractions in combination with explicitly given constraints.

FCS-MPC provides an elegant solution to the managing the state and input voltage constraints, moreover, unlike the PWM based approaches, the switching of the power converter is directly influenced by the controller. From the efficiency point of view, we wish to reduce the switching of the power converter and so decrease the switching losses to its minimum. On the other hand, the lower switching frequency results in increase of the current distortion. Thus the control needs to consider both criteria. This phenomenon has been addressed for example in [7]

In this chapter, we intend to minimize the average switching frequency of the FCS-MPC which is used for speed control of PMSM, while keeping the stator current distortion as low as possible. The SDRE has been used to approximate the cost to go function which is then added to the one step FCS-MPC as an additional term in the cost function.

5.1. MPC formulation

Consider a speed control of PMSM defined as (3.3) with the mathematical model (3.13). In this case, the control action is selected from limited set $u_t \in \{u_t^{(1)}, \ldots, u_t^{(7)}\}$, which is defined by admissible switching combinations of the converter $\{000, 001, 010, 100, 011, 101, 110\}$ (Fig. 5.1), where 1 or 0 defines the states of respective switches. Finding the optimal control action is

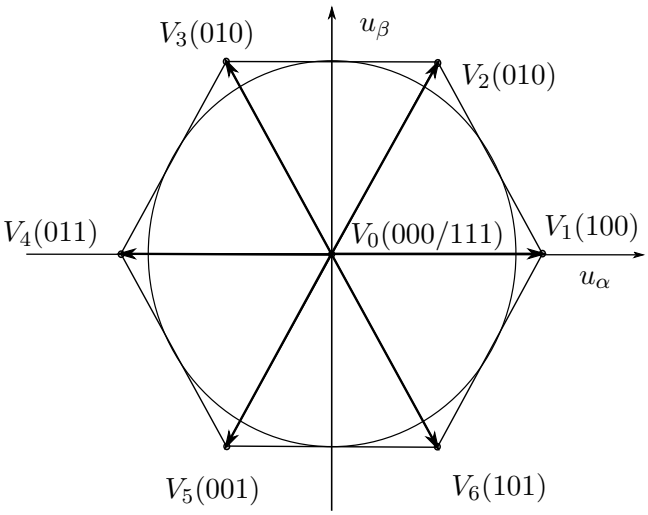

Figure 5.1.: Admissible switching combination of three-phase inverter and corresponding output voltage vectors

achieved by brute-force search over the admissible u_t and finite prediction horizon, thus the hard state constraints can be simply addressed by additional terms in the cost function, penalizing the violation of those constraints (see chapter2.5) The FCS-MPC for speed control of PMSM can be, then, formulated as,

$$u_{t:t+h}^{\text{opt}} = \arg \min_{u_{t:t+h} \in U} \sum_{\tau=t+1}^{t+h} (\lambda_\omega g_\omega(\omega_\tau, \omega_\tau^*) + \lambda_i g_i(i_{d,\tau}, i_{q,\tau}) + \lambda_L g_L(i_{d,\tau}, i_{q,\tau}) + \lambda_{fw} g_{fw}(i_{d,\tau}, i_{q,\tau}) + g_{din}(u_\tau, u_{\tau-1})) \quad (5.1)$$

$$\text{subject to: } x_\tau = f(x_\tau, u_\tau),$$
$$\forall \tau = t, t+1, \ldots, t+h,$$

where, g_ω and g_i are defined as in (3.1) and (3.2), g_L is a penalty function respecting the hard stator current constraints defined as

$$\begin{aligned} g_L &= \chi(\sqrt{i_{d,t}^2 + i_{q,t}^2}) - I_{max}), \\ \chi &= \begin{cases} 0 & \text{if } (\sqrt{(i_{d,t}^2 + i_{q,t}^2)} \leqq I_{max}) \\ 1 & \text{if } (\sqrt{(i_{d,t}^2 + i_{q,t}^2)} > I_{max}) \end{cases}, \end{aligned} \tag{5.2}$$

and g_{fw} is used to respect the limited input voltage vector u_t and it is derived from (3.15) as

$$\begin{aligned} g_{fw} &= \gamma\sqrt{(L_q i_{q,t})^2 + (L_d i_{d,t} + \Psi_{pm})^2} - \frac{\zeta U_c}{\sqrt{3}\omega}, \\ \gamma &= \begin{cases} 0 & \text{if } (\sqrt{(L_q i_{q,t})^2 + (L_d i_{d,t} + \Psi_{pm})^2} - \frac{\zeta U_c}{\sqrt{3}\omega}) < 0 \\ 1 & \text{otherwise} \end{cases}. \end{aligned} \tag{5.3}$$

The last term $g_{din} = \lambda_{u,d} du_d + \lambda_{u,q} du_q$, $du_d = (u_{d,t} - u_{d,t-1})^2$, $du_q = (u_{q,t} - u_{q,t-1})^2$ is used to penalize the difference of the input voltage similarly as in (4.1). However, here it has a distinct meaning. Note that due to discrete nature of the action set, this penalization is either zero, if the same combination is preserved but rather high when the switching combination is changed. This allows to penalize the change of the switching combination and therefore minimize the switching effort of the converter. In order to evaluate the the switching effort of the converter we define the average switching frequency as

$$f_{aw,t+1} = f_s \left(0.99 f_{aw,\tau} + 0.01 \left(\frac{s_a + s_b + s_c}{3} \right) \right), \tag{5.4}$$

where f_s is a sampling frequency of the algorithm and $s_{a,b,c}$ defines the switching transition in corresponding phases of the converter during one sampling period of the algorithm.

Since extensive part of (5.1) is quadratic, we can apply the same idea of approximating the horizon of the unconstrained control problem using SDRE, as in (4.1). This yields the following one step FCS - MPC

$$u_t^{\text{opt}} = \arg\min_{u_t(x_t)} \left\{ g_{unc}(\tilde{x_t}, u_t) + \lambda_L g_L(i_{d,t}, i_{q,t}) + \lambda_{fw} g_{fw}(i_{d,t}, i_{q,t}) \right\}, \tag{5.5}$$

where g_{unc} is derived from (2.33) using the model (3.12) and quadratic cost function

$$g_{SDRE,t} = (\lambda_{q\omega} g_\omega(\omega_t, \omega_t^*) \ \lambda_{qi} g_i(i_{d,t}, i_{q,t}) + \lambda_{qu} g_{din}(u_t, u_{t-1}))\,. \tag{5.6}$$

The final FCS-MPC can be then written as

$$u_t^{\text{opt}} = \arg\min_{u_t(x_t)} \left\{ (u_t - u^{\text{sdre}})^T Y (u_t - u^{\text{sdre}}) + \lambda_l g_{L,t} + \lambda_{fw} g_{fw,t} \right\} \tag{5.7}$$

Note, that the constraints are addressed only in the FCS-MPC cost function on one step of the prediction horizon. Further on the control does not consider hard constraints. The proposed control design is summarized in Algorithm 5.1.

Algorithm 5.1 FCS-MPC with SDRE lookahead.

Off-line (SDRE):

1. Design approximate linear model of the controlled system 3.13 with matrices $A(x^{\text{op}})$, $B(x^{\text{op}})$.
2. Choose quadratic loss function (5.6) with appropriate penalization,
3. Design the unconstrained solution of the optimization problem by solving the SDRE (2.33) in the form $(u_t - u^{\text{sdre}})^T Y (u_t - u^{\text{sdre}})$.
4. Validate results of the optimized closed loop. If not successful GOTO 2.

On-line (FS-MPC):

1. For all admissible control inputs $u_t^{(i)} \in U, i = 1, \ldots, I$ evaluate cost function in (5.7)
2. Apply optimal- control input $u_t^{(i)}$ which minimize (5.7)

5.2. Simulations

The proposed control approach was tested on a PMSM drive system with parameters (see Table A.1) and sampling time $\Delta t = 50\mu s$. The penalization of the input voltage of the q axis is higher than that of the d axis. We conjecture that this is because the q current has higher influence on the speed which is also penalized (see below).

5.2.1. Influence of input penalization

Direct comparison of the conventional and the SDRE lookahead cost functions is difficult due to different effect of the tuning parameters. The most notable difference is however, the effect of penalizations of the input differences $(u_t - u_{1-t})$. With increasing penalization of the change of the switching combination, the switching frequency is decreasing which results in current distortions (current ripple). The current ripple is also propagated into the speed ripple which has an impact on the speed tracking error.

Tracking error of the state was evaluated using the cumulative quadratic cost function

$$G = \sum_{\tau=t_1}^{t_2} (x_\tau - x_\tau^*)^T Q (x_\tau - x_\tau^*) \tag{5.8}$$

where τ is a running index on a window of samples starting at time t_1 and ending at time t_2 and Q is the penalization matrix which set the importance to a specific terms in the cost function. Distortion of the phase current was evaluated numerically using the total harmonic distortion plus noise (THDn), [72], of the phase current i_a :

$$THD_n(i_a) = \frac{\sqrt{\sum_{j \neq j_{nom}} I_j^2}}{I_{j_{nom}}}. \tag{5.9}$$

evaluated on the same recorded time window $\langle t_1 \dots t_2 \rangle$ (which was $0.25s$) as the tracking error. Its distinction from the classical THD is that indexes j in the numerator are not only multipliers of the nominal frequency, but all frequencies in the spectrum typically excluding the dc and the nominal frequency of the current. This measure is more informative than the classical THD in the context of FCS-MPC [73].

Simulation studies using one step FCS-MPC with conventional cost (5.6) and proposed cost SDRE (5.7) were performed using single penalization of $Q = \text{diag}([0.01, 0.01, 1, 0, 0])$ and a range of penalization of $\lambda_u \in \left\langle 10^{-8}, 4 \times 10^{-6} \right\rangle$. Note, that the Q penalization has non-zero penalization for tracking of reference currents i_q^* and i_d^*. We chose the same value 0.01 for both currents for simplicity. For higher penalizations of the currents, the control problem is approaching the current control and the differences between the cost functions become smaller. In general, penalizations of the currents lower the current ripple.

Two scenarios were tested: i) steady state operation at electrical rotor speed of 100 rad/s with load torque of 6.25 Nm, and ii) steady state operation at electrical rotor speed of $800 rad/s$, i.e. field weakening with $i_d^* = -15.7$A. Since the penalizations are not directly comparable,

we plot the speed tracking error (5.8) and the THDn of the phase current (5.9) as a function of the average switching frequency in Fig. 5.2. Both methods were tuned to provide comparable results. Note that for low penalizations λ_u (which are numerically different for each method), both methods provide very similar results. However, with growing penalization of λ_u, the FCS-MPC with the SDRE lookahead cost achieves significantly better results for the same average switching frequency. We conjecture that this is due to the ability of the SDRE lookahead to consider longer horizons.

Remark 5. As low penalization region we understand such penalization tuning, which results in operation at 1.6-4 kHz of the average switching frequency.

5.2.2. Length of the receding horizon

To verify this conjecture, we run an experiment on multi steps optimization of the FCS-MPC part of the horizon. The cost-to-go function of the SDRE lookahead approach is applied in the original form (2.32), i.e. as an additional term after $k \in \{1, 2, 3, 4\}$ optimization steps. The optimization on the k steps of the FCS-MPC block is done by brute force search over all possible switching combinations.

The mean square error of the speed control of a PMSM drive with parameters (see Table A.1) running at 100 rad/s and 6.25 Nm load torque is displayed in Fig. 5.3 for $Q = ([0.01, 0.01, 1, 0, 0])$ and two values of penalization λ_u: low (10^{-8}) and high (10^{-6}). The performance of the FCS-MPC without and with the SDRE lookahead cost-to-go are compared in Fig. 5.3 via cumulative sum of cost functions $g()$. As expected, the control error of all algorithms improves with the length of the FCS-MPC optimization horizon k. The improvement of the conventional FCS-MPC is more significant, which is given by challenging properties of the control task. The control with the SDRE lookahead cost also improves with the horizon length. This is due to the fact, that SDRE is sub-optimal solution on the horizon because of incorrect assumption of continuous control inputs.

The relative improvement of both approaches heavily depends on the penalization of the input. For low penalization, the performance of FCS-MPC with conventional cost is comparable for $k = 3$ and actually better for $k = 4$. For high penalization, the SDRE lookahead cost at $k = 1$ is still better than the conventional cost at $k = 4$. This behavior can be understood from evolution of the gains of the SDRE controller with increasing lookahead horizon, Fig. 5.3 right. For low penalization, only two elements of the controller gain change significantly with increasing length of the lookahead horizon. Thus, the one step ahead optimal controller is rather similar to that with infinite lookahead horizon. For high penalization, the controller

a) normal operation at 100 rad/s with $T_L = 6.25\mathrm{Nm}$

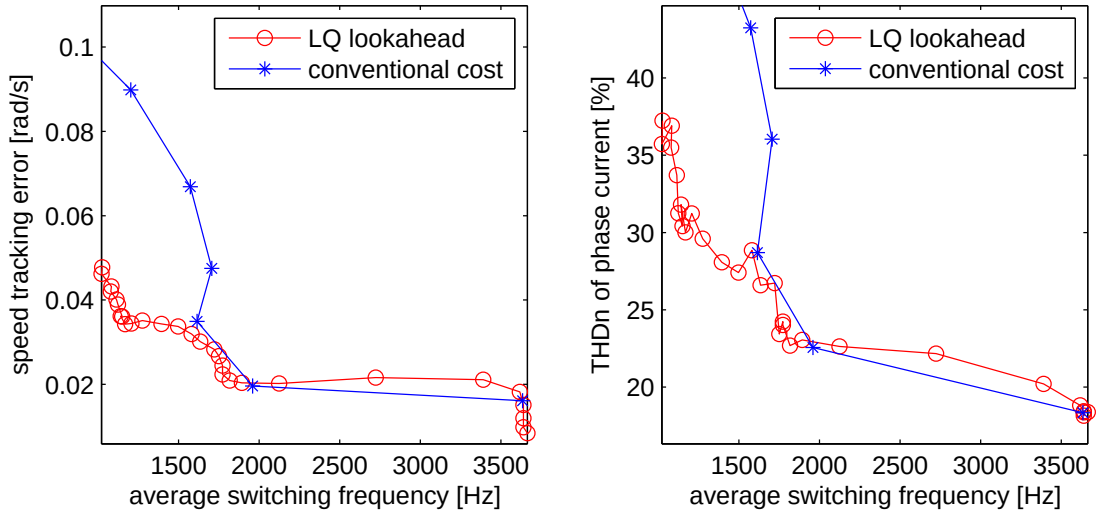

b) field-weakening operation at 800 rad/s with $i_d^* = -15.7\mathrm{A}$ and with $T_L = 6.25\mathrm{Nm}$

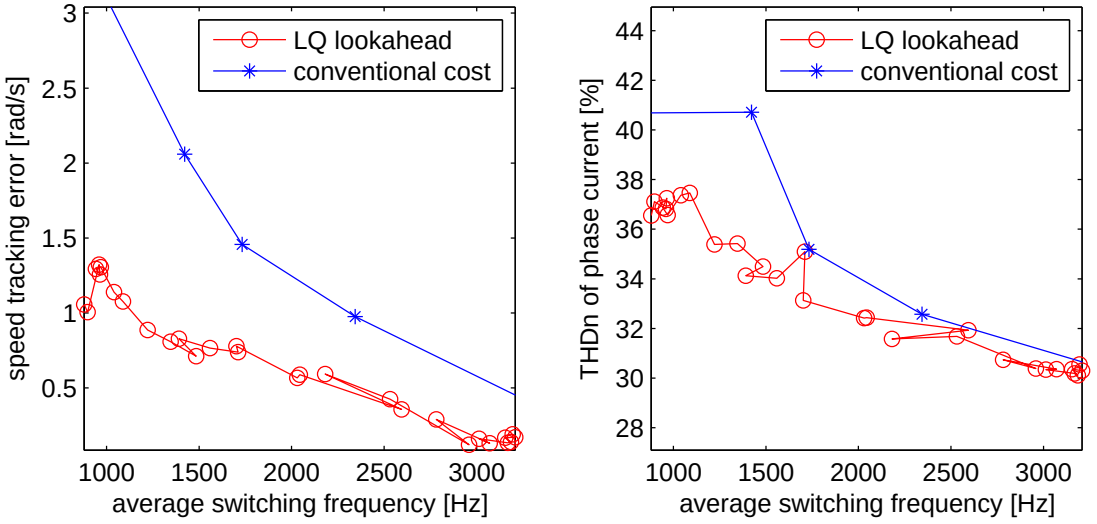

Figure 5.2.: The effect of switching loss minimization for the FCS-MPC with the conventional cost and with the SDRE lookahead cost for normal operation and field weakening operation. The average speed tracking error (left) and total harmonic distortion with noise (THDn) were evaluated.

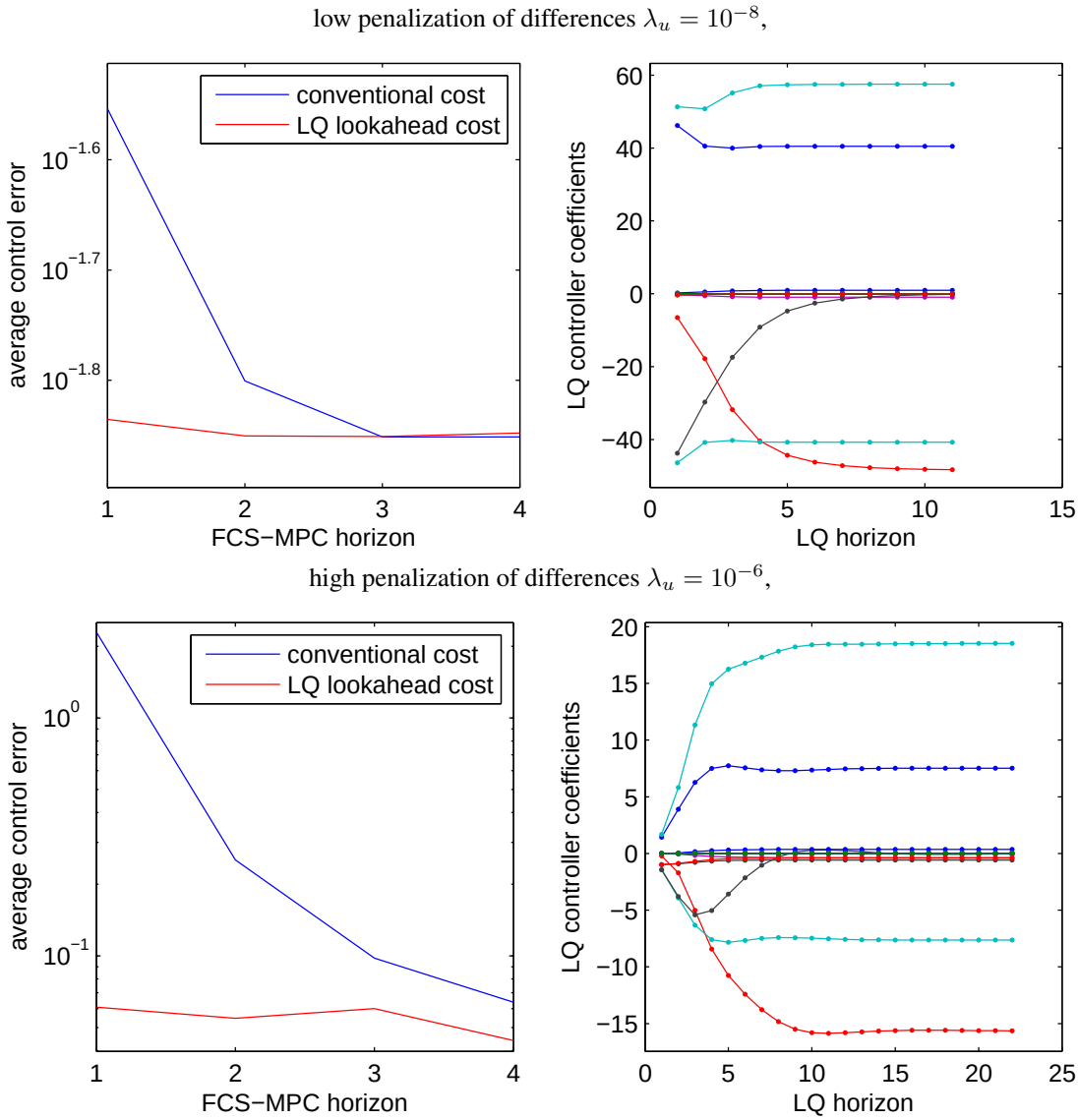

Figure 5.3.: Comparison of influence of the optimization horizon on the control cost of FCS-MPC for speed control of PMSM running at 100 rad/s and 6.25 Nm load torque for $Q = \text{diag}([0.01,0.01,1,0,0])$ and different penalization of the input $\lambda_u = 10^{-8}$ (top row) and $\lambda_u = 10^{-6}$ (bottom row). Each result is composed of comparison of the control cost for FCS-MPC with and without the SDRE lookahead term (left column) and gains of the SDRE for different lookahead horizon (right column). The display of SDRE coefficients is zoomed to show smaller coefficients, the two largest coefficients converge within few steps.

Table 5.1.: Execution times of steps of the FCS-MPC algorithm

	conventional	SDRE
data acquisition	$4.3\mu s$	$4.3\mu s$
delay compensation	$0.7\mu s$	$0.7\mu s$
model prediction (Ax_t)	$0.4\mu s$	
SDRE controller evaluation		$0.7\mu s$
cost evaluation for all combinations	$11.7\mu s$	$11.1\mu s$

gains change more significantly with longer horizon, reaching steady state values for lookahead horizons longer than 10 steps. In both graphs, we omit the SDRE gain of the $(\omega - \omega^*)$ term, which has much higher value. It behaves similarly for both penalizations, reaching convergence after 5 steps.

Remark 6. The same approach was applied to torque control operation of the drive. The difference between one step ahead approach and the SDRE extension was completely negligible.

5.3. Experimental results

A laboratory prototype of the PMSM drive with the same parameters as in the simulation (TableA.1) was used to verify the approach experimentally. The control algorithm was implemented in digital signal processor TMS320F28335.

We compared the classical one-step ahead FCS-MPC with the conventional cost and the LQ lookahead cost. Both algorithms were run with control sampling period of $50\mu s$. The algorithm follows the conventional FCS-MPC timing [71] with execution times listed in Table 5.1.

Penalizations of both approaches were tuned to obtain as close performance in dynamic operation as possible. Specifically, the penalization of the speed error in the conventional cost (λ_ω in (3.3)) has to be higher than that of the version with SDRE lookahead to achieve the same dynamic behavior. For penalization of the switching combinations yielding average switching frequency (5.4) of $2kHz$, the behavior is almost equivalent, Fig. 5.4. In this rapid step change, the dynamics is limited by the maximum allowed current, which is $20A$, Fig. 5.4 lower row.

With growing penalization of the switching frequency, the distortion of the phase currents increases. In agreement with simulation, the SDRE lookahead cost exhibits much lower distortion of the phase currents than the conventional cost. For average switching frequency of $550Hz$ the distortion (current ripple) becomes very visible, Fig. 5.5. Note that the switching frequency rises to $2kHz$ during the transient for both methods, thus the current ripple is lower

a) FCS-MPC with conventional cost

b) FCS-MPC with the SDRE lookahead cost

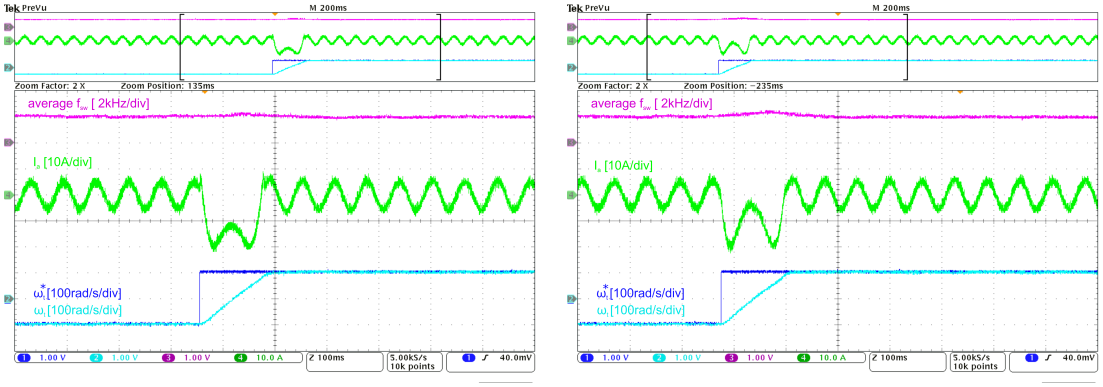

ch1: ω_t^* (100rad/s/div), ch2: ω_t (100rad/s/div), ch3: average switching frequency (2kHz/div), ch4: i_a (10A/div),

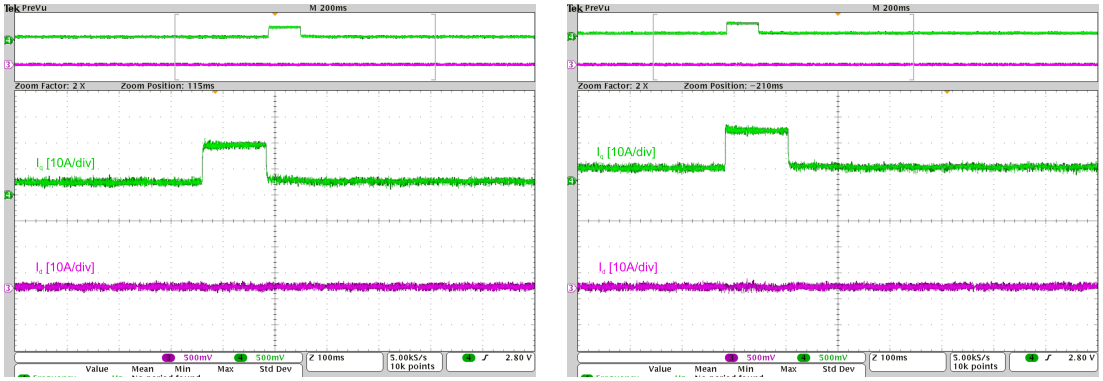

ch4: i_q (10A/div), ch3: i_d (10A/div),

Figure 5.4.: Comparison of FCS-MPC with conventional (left) and with the SDRE lookahead cost (right) for step change of speed of PMSM drive from -100 to $100 rad/s$ at $6.25 Nm$ of load torque. Penalization λ_u was tuned to average switching frequency $2000 Hz$ in steady state.

a) FCS-MPC with conventional cost b) FCS-MPC with the SDRE lookahead cost

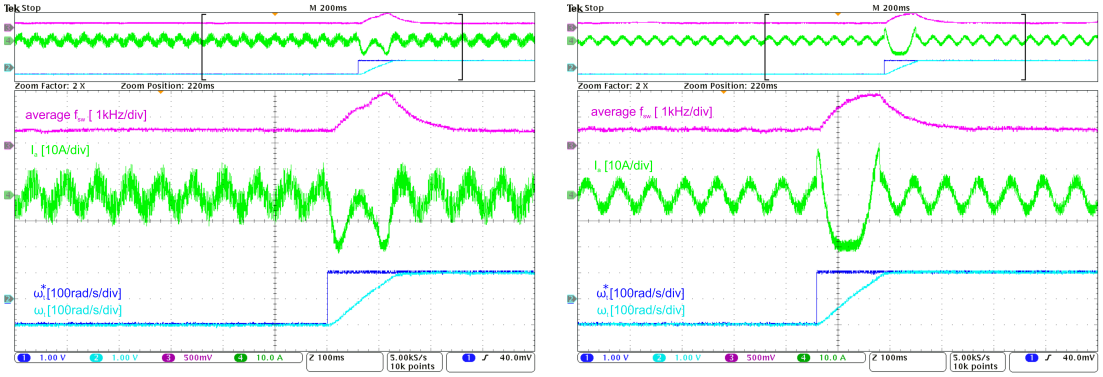

ch1: $\omega^*{}_t$ (100rad/s/div), ch2: ω_t (100rad/s/div), ch3: average switching frequency (1kHz/div), ch4: i_a (10A/div),

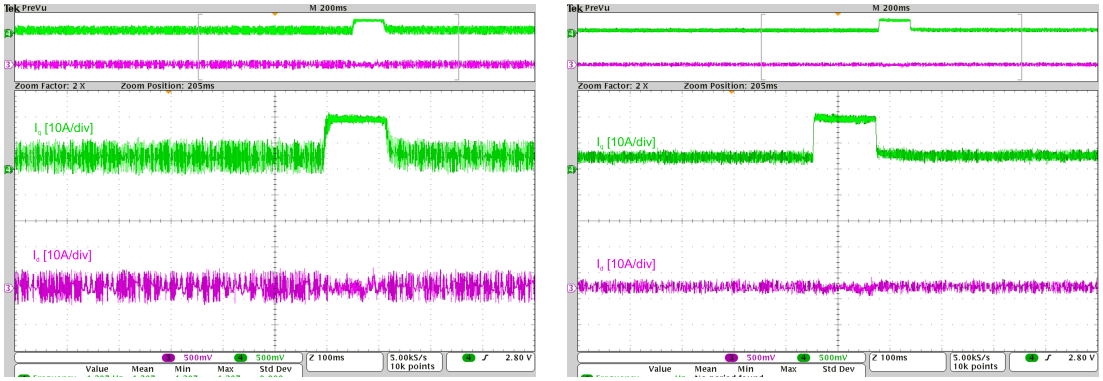

ch4: i_q (10A/div), ch3: i_d (10A/div),

Figure 5.5.: Comparison of FCS-MPC with conventional cost (left) and with the SDRE lookahead cost (right) for step change of speed of PMSM drive from -100 to 100 rad/s at 6.25 Nm of load torque. Penalization λ_u was tuned to average switching frequency of 550Hz in steady state.

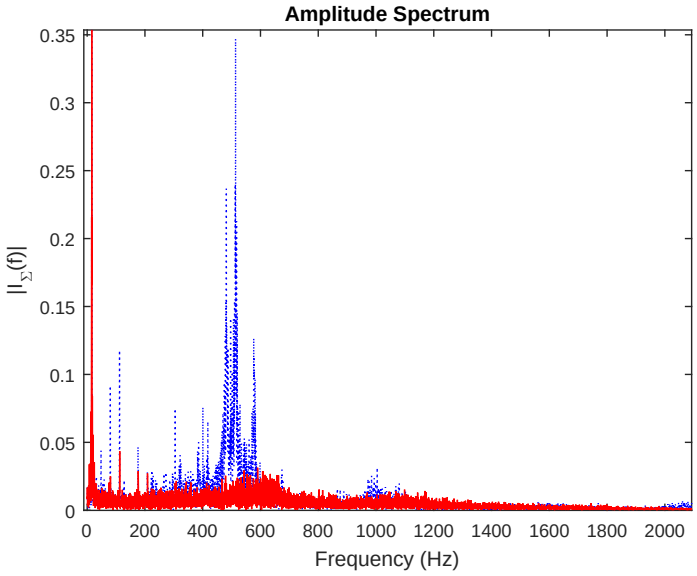

Figure 5.6.: Frequency spectrum of the phase current of the FCS-MPC of PMSM drive running at 100rad/s and 6.25 Nm load torque for conventional and lookahead cost function, both tuned approximately to $f_{aw} = 550\,Hz$. (The window of FFT is $1s$)

Table 5.2.: Total harmonic distortion with noise, $THD_n(i_a)$, for steady state operation of the drive at 100rad/s with 6.25 Nm nominal load.

average switching frequency	2000Hz	550Hz
$THD_n(i_a)$ conventional cost	32%	94%
$THD_n(i_a)$ SDRE lookahead cost	29%	44%

than that in the steady state. Frequency spectrum of the phase current in the steady state is displayed in Fig. 5.6 for both methods.

Numerical evaluation of the THDn (5.9) of the phase current for the steady state operation of the drive is presented in Table 5.2. In agreement with simulation in Fig. 5.2, the improvement of the SDRE lookahead is minor for low penalization, however, it becomes more significant with increasing penalizations of the switching losses.

Naturally, performance of the classical FCS-MPC can be improved by expert chosen terms of the cost function. For example, the current ripple would be reduced by the additional term with filtered value of the i_q as proposed in [8]. However, the SDRE lookahead achieves the same result without additional on-line computation and without additional tuning.

5.4. Conclusion

In this chapter, we propose to extend the horizon of the FCS-MPC via approximation obtained from an unconstrained solution on the infinite prediction horizons. Specifically, this approach results in combination of two well known techniques, the SDRE control and the FCS-MPC approach. The idea is that the SDRE controller provides an approximate cost-to-go on the extended horizon of the FCS-MPC optimization. In effect, the SDRE methodology is used to design a cost function that will be evaluated by the FCS-MPC. Advantages of this approach were demonstrated on speed control of the PMSM drive, where the SDRE controller can be computed off-line. Moreover, model of the system allows to simplify the cost function such that its evaluation is very fast. The resulting FCS-MPC control is then used to handle the phase currents constraints.

In order to highlight the benefits of long prediction horizon the conventional one step FCS-MPC has been compared with with proposed solution with extended prediction horizon by approximated cost to go function. For high switching frequencies, both approaches can be tuned to obtain almost identical dynamic properties of the drive. However, with increasing penalization of the switching effort, the SDRE lookahead term results in much lower distortion of the phase currents.

The proposed approach is very simple and computational cost is relatively low thus it can be easily implemented into conventionally used control hardware.

6. Improved stability of DC catenary fed traction drives using FCS-MPC with lookahead

This chapter is concerned with control of a traction drive with PMSM fed from a DC catenary. Contrary to the chapter 5, the control has to consider not only the the control of the PMSM drive, but also needs to consider behavior of the dc catenary and input LC-filter. Specifically, the catenary voltage is subject to short circuits, fast changes, harmonics and other disturbances which can vary in very wide range. Therefore, the drive is equipped by the catenary input LC filter. The filter is almost undamped by design in order to achieve maximum efficiency and the control strategy needs to secure active damping of the filter to guarantee the drive stability. This represents nonlinear MIMO control problem which is difficult to solve. Thus most of the existing solutions approach each sub-problem (PMSM control and damping of the LC-filter) separately, significantly simplifying the optimization problem. The crucial property of the control algorithm is to actively damp the LC-filter as well as provide excellent dynamic properties, however those objectives are contradictory. In order to effectively resolve this problem, we design cost function for active damping of the LC filter using approximation of the cost-to-go function of the limited lookahead approach, which is used as an additional term in the one step ahead FCS-MPC cost. The dynamic properties of the drive are guaranteed by optimization on one step ahead horizon using the FCS-MPC.

6.1. Theoretical background of the phenomenon

One of the main constraints of design of traction vehicles control fed from a dc catenary are the oscillations of an input catenary LC filter and the resulting instability of the traction drive. This problem is even more complicated in multi-motor propulsion units which operate many drives with their naturally almost undamped dc-link LC filters in parallel. The problems with the input

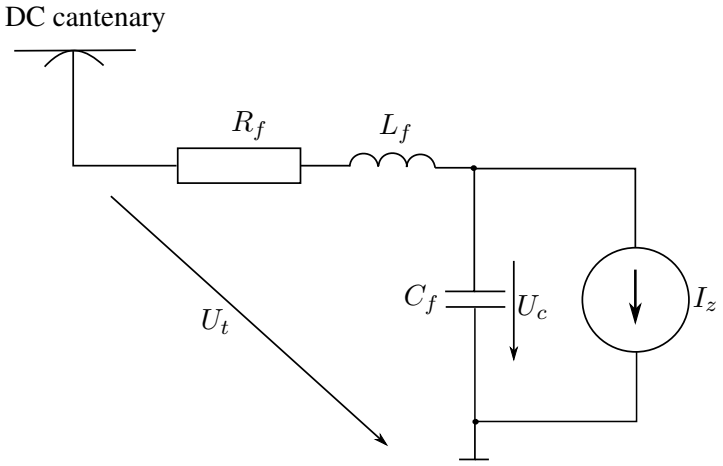

Figure 6.1.: Equivalent circuit of the dc catenary supplied traction drive with input LC filter

LC filter are closely linked with frequency characteristics of the whole drive and so-called "drive resonant frequency", e.g. [74].

The problem of oscillations of the catenary LC filter in dc catenary supplied traction drives is known for many years, e.g. [75, 76]. Traction drives use an input LC filter and not only a C-filter for the following reasons: (i) an effective limitation of the catenary current (due to fast changes of the catenary voltage and short-circuit of the catenary), and (ii) EMC issues. Thus, the LC filter is necessary for proper operation of the drive. On the other hand, the dc-link LC filter has negative impact on the traction drive stability.

The specifics of the traction drive are: i) excellent dynamic properties of its control, ii) the drive has a very high moment of inertia, i.e. the change of the vehicle speed is slow in comparison with electrical time constants, and iii) the input to the drive controller is often the maximum achievable torque command, which will be considered as a constant for the stability analysis.

Under the above stated conditions, the drive consumes constant active power from the dc-link filter under steady-state conditions. The equivalent circuit of the drive used for the description of the LC filter resonance is shown in Fig. 6.1. Voltage-source converter and ac motor can be replaced by an equivalent current source which models the filter load. The LC filter resonance can be excited by many events – by the drive itself (e.g. unsuitable control commands or drive harmonics) or from the outside. One of the most common effects from outside which can excite the filter oscillations is the change of the catenary voltage which can vary very fast due to different reasons. If the catenary voltage increases then the drive still takes the constant power from the dc-link filter (constant torque command and negligible speed change within

the time interval of investigated transient phenomenon). This may act as a positive feedback (or negative-resistance effect) which results in dangerous oscillations of the dc-link filter. This phenomenon can be also explained using frequency characteristics of the drive.

The resonant frequency of the drive is clearly changing with the change of the position of the vehicle within the feeding section (change of the catenary parameters with varying distance from the static substation). However, the drive resonance properties are also changing with the drive operating point (for more details see [74]). A dangerous situation also occurs when the resonance loop is composed of a two or more traction drives [77]. It is obvious that the explained phenomenon significantly impacts the stability of the traction drive and must be carefully considered during the drive design.

6.1.1. Possible solutions for mitigation of dc-link LC filter oscillations

Stability of the traction drive can be improved by either passive or active damping of the dc-link LC filter. The passive damping requires addition of a damping resistor to the LC filter circuit or detailed design of the filter [78]. Passive damping is a bulky and expensive solution which moreover reduces the drive efficiency. Active damping of the dc-link LC filter is the preferred solution in the modern traction drives. However, suitability of active damping of the LC filter heavily depends on operating conditions of the drive. Active damping of the LC filter is much more difficult in the low speeds where the drive power has smaller impact on damping of the dc-link filter. These specific conditions are one of the operating states which needs to be addressed by a braking chopper. The most common techniques of active damping has been reported e.g. in [77, 79, 76]. In order to suppress only the resonant frequency, the dc-link voltage is filtered using a band-pass filter. The band-pass filtering is one of the constraints of these techniques, because the drive resonant frequency is significantly changing as described in the previous section. Moreover, the band-pass filtering is further complicated in the drive of locomotives and suburban units where the cut-off frequency of the LC filter is usually very low in order to reinforce the damping of the danger drive harmonics which can disturb the railway track circuits. We seek a general method that does not require a band-pass filter, or it is able to tune the filter on-line.

6.1.2. Relation to other active damping approaches

Active oscillation damping is a common problem of many applications with rich literature and many possible approaches. The applications range from stabilization of LC filter of a converter [80, 81] or including model of the grid of network [82, 83, 84] to active suppression of bearing

oscillations [85, 86] and two mass systems [87]. Since the root cause of the problem is similar in all applications, the approaches are often closely related.

When LC filter is used in the drive application it is between the converter and the motor [88, 89], where the chance of unstable oscillations is quite limited. Stability of the input filter is much harder problem [90].

In this chapter, we investigate application of the model predictive control for improvement of traction drive stability, specifically active damping of the catenary input LC filter.

Methodology of systematic design of appropriate cost functions is still an open problem of the MPC approach, as well as its extension for longer prediction horizons [11]. Approaches based on dynamic optimization [91] or polynomial approximations [92] have been investigated. In this paper, we propose to use The FCS-MPC with limited lookahead to address both the control of the LC-filter as well as traction drive control.

6.2. MPC formulation

The control problem is divided into two parts i) the torque control of PMSM and ii) active damping of the LC filter.

6.2.1. Torque control of PMSM

Consider the mathematical model of PMSM in the form (3.5) - 3.6). For the sake of simplicity we assume slowly varying speed and therefore $\frac{d\omega}{dt} \approx 0$. Then the mathematical model becomes linear and torque control of PMSM can be defined as minimization of the cost function

$$g_T = \left(i_{d,t} - i^*_{d,t}\right)^2 + (i_{q,t} - i^*_{q,t})^2 + g_L^2 + \lambda_S g_s, \tag{6.1}$$

where

$$g_L = \chi\,(\sqrt{i^2_{d,t} + i^2_{q,t}}) - I_{max}), \tag{6.2}$$

$$\chi = \begin{cases} 0 & \text{if}(\sqrt{(i^2_{d,t} + i^2_{q,t})} \leqq I_{max}) \\ 1 & \text{if}(\sqrt{(i^2_{d,t} + i^2_{q,t})} > I_{max}) \end{cases} \tag{6.3}$$

where $g_L$is the same as in (5.2) χ is the penalty function which imposes high penalty for violation of the condition in its argument (see section2.5). The last term g_s is used to minimize the

switching effort in order to reduce the switching losses,[1]

$$g_s = \sum_{x=a,b,c} (S_{x,t} - S_{x,t-1}), \tag{6.4}$$

where $S_{a,b,c} \in \{0, 1\}$ indicates the states of particular switches in each phase leg of the power converter (i.e. 1 if the upper switch is open and 0 if the upper switch is closed) .

6.2.2. Input LC filter control

The equivalent circuit of the drive used for the description of the LC filter resonance is shown in Fig. 6.1. The voltage-source converter and an ac motor can be replaced by an equivalent current source which models the filter load. The associated LC filter can be modeled as:

$$\frac{di_l}{dt} = -\frac{R_f}{L_f} i_l + \frac{1}{L_f}(U_T - U_c), \tag{6.5}$$

$$\frac{dU_c}{dt} = \frac{1}{C_f}(i_l - i_z), \tag{6.6}$$

$$\frac{dU_T}{dt} = 0, \tag{6.7}$$

where R_f, L_f and C_f are the resistance, inductance and capacitance of the LC filter; i_l is the catenary current, U_T is the catenary voltage and U_c is the voltage on the dc-link filter capacitor; i_z is the current consumed from the dc-link capacitor by the voltage-source converter and it is considered to be the control input of the LC filter. The whole system interacts via current equation

$$i_z = i_a S_a + i_b S_b + i_c S_c, \tag{6.8}$$

where $S_{a,b,c}$ is a switching function indicating open or close state of the upper power switch in the given inverter leg and i_a, i_b, i_c are the stator phase currents of PMSM.

Approximation of the full system (3.5)–(3.6) and(6.5)–(6.8) by a linear model is very demanding due to non-stationary input voltage of the PMSM drive. Therefore, we neglect the PMSM model and consider only the input LC filter in this part.

Note that the model of the LC filter (6.5)–(6.7) is linear with state vector $x_f = [i_l, \Delta U_c]$,

[1] Other terms can be added to achieve desired properties of the drive.

$\Delta U_c = U_T - U_c$,

$$\frac{dx_f}{dt} = \underbrace{\begin{bmatrix} -\frac{R_f}{L_f} & \frac{1}{L_f} \\ -\frac{1}{C_f} & 0 \end{bmatrix}}_{A_{cf}} \begin{bmatrix} i_l \\ \Delta U_c \end{bmatrix} + \underbrace{\begin{bmatrix} 0 \\ \frac{1}{C_f} \end{bmatrix}}_{B_{cf}} i_z, \tag{6.9}$$

The mathematical model (6.9) is discretized for sampling time Δt (reminder from chapter2.1)

$$\begin{aligned} A_f &= \exp(A_{cf}\Delta t), \\ B_f &= \int_0^{\Delta t} e^{A_{cf}(\Delta t - \sigma)} B_{cf} d\sigma. \end{aligned} \tag{6.10}$$

Here, $A_f$and B_f are constant matrices of appropriate dimensions. Then the discrete form of state space model is

$$x_{f,t+1} = A_f x_{f,t} + B_f x_{f,t}. \tag{6.11}$$

The cost function for active damping is designed to penalize differences from a steady state solution, which will be denoted by x^*, i.e.

$$g_{f,t} = (x_{f,t} - x^*_{f,t}) Q_f (x_{f,t} - x^*_{f,t}) + (i_{z,t})^2 \lambda_z^2, \tag{6.12}$$

where $Q_f = \mathrm{diag}(\lambda_l, \lambda_C)$ and λ_z are chosen penalizations. We use standard constant reference model for state and input variables $f_{x^*} : x^*_{t+1} = x^*_t$, $f_u : i_{z\,t+1}^* = i_{z,t}$.

The requested value of the current i_l^* is obtained from the power balance equation of the drive. Specifically, we want the energy flowing from the catenary through the LC filter to match the energy consumed by the drive:

$$i^*_{l,t} U_{T,t} = i^*_{q,t} u^*_{q,t} + i^*_{d,t} u^*_{d,t}, \tag{6.13}$$

where $u^*_{q,t}$ and $u^*_{d,t}$ are given by the steady state solution of the drive

$$u^*_{d,t} = R_s i^*_{d,t} - L_{sq} i^*_{q,t} \omega_t, \tag{6.14}$$

$$u^*_{q,t} = R_s i^*_{q,t} + \Psi_{pm} \omega_t + L_{sd} i^*_{sd,t} \omega_t, \tag{6.15}$$

for the requested current $i^*_{q,t}$ and the field weakening current $i^*_{d,t}$, which is either zero when the drive operates in the region from zero to nominal speed or it is given by a solution of equality

in (3.15) (see e.g. [71] for details). The remaining steady state solutions are:

$$i^*_{z,t} = i^*_{l,t}, \qquad \Delta U^*_{C,t} = R_f i^*_{l,t}. \tag{6.16}$$

Here, the first equality follows from the steady state solution of (6.6) and the second equality from the steady state solution of (6.5).

6.3. FCS-MPC with lookahead

Since the model of LC filter (6.9) is linear, with quadratic cost function (6.12) we propose to use LQR (see Chapter 2.6.1) for design of control of the LC filter. The input of the LC filter is the current i_z, hence the optimal input is obtained by linear feedback

$$i^{\text{LQ}}_{z,t} = -L_f \tilde{x}_{f,t},$$

where L_f is designed using matlab function `dlqr.m` and $\tilde{x}_{f,t} = [i_{l,t}, \Delta U_{c,t}, i^*_{l,t}, i^*_{z,t}]$ denotes the augmented state vector. This implies cost-to-go function

$$\tilde{V}_f(\tilde{x}_{f,t}) = \lambda_{LC}(i_{z,t} + L_f \tilde{x}_{f,t})^2, \tag{6.17}$$

where λ_{Lc} is a result of optimization (see 2.24), however it can be also tuned manually due to its direct dependence on penalization Q_f.

Using methodology from Section 2.4.1, active damping of the LC filter and torque control of PMSM can be elegantly combined in one step ahead optimization of FCS-MPC. The optimization problem is defined as follows

$$u^{\text{opt}}_t = \arg \min_{u_t \in U_{FCS}} (g_{T,t+1} + \tilde{V}_f(\tilde{x}_{f,t+1})), \tag{6.18}$$

In effect, the resulting control algorithm acts as a cascade controller, where the LQR provides a set point $i^*_{z,t}$ for the FCS-MPC controller, see Fig. 6.2The proposed algorithm is described in algorithm 6.1.

Algorithm 6.1 Design procedure of the FCS-MPC with LQ lookahead for control of the traction PMSM drive fed from DC cantenary.

Off-line (LQR):

1. Design approximate linear model of input LC-filter with matrices A_f, B_f6.11.
2. Choose quadratic cost function $g_{f,t}$ with penalization matrices Q, R (6.12).
3. Design the approximate cost to go function in the form $\tilde{V}_f(\tilde{x}_{f,t}) = \lambda_{LC}(i_{z,t} + L_f\tilde{x}_{f,t})^2$ (6.17), where L_f is designed using matlab function `dlqr.m`. Note that the cost to go function $\tilde{V}_f(\tilde{x}_{f,t})$ is designed only for the input LC-filter .
4. Validate results of the optimized closed loop. If not successful GOTO 2.

On-line (FS-MPC):

1. For all admissible control inputs $u_t^{(i)} \in U, i = 1, \ldots, I$ evaluate $(g_{T,t+1} + \tilde{V}_f(\tilde{x}_{f,t+1}))$ in (6.18)
2. Apply optimal control input $u_t^{(i)}$ which solves (6.18)

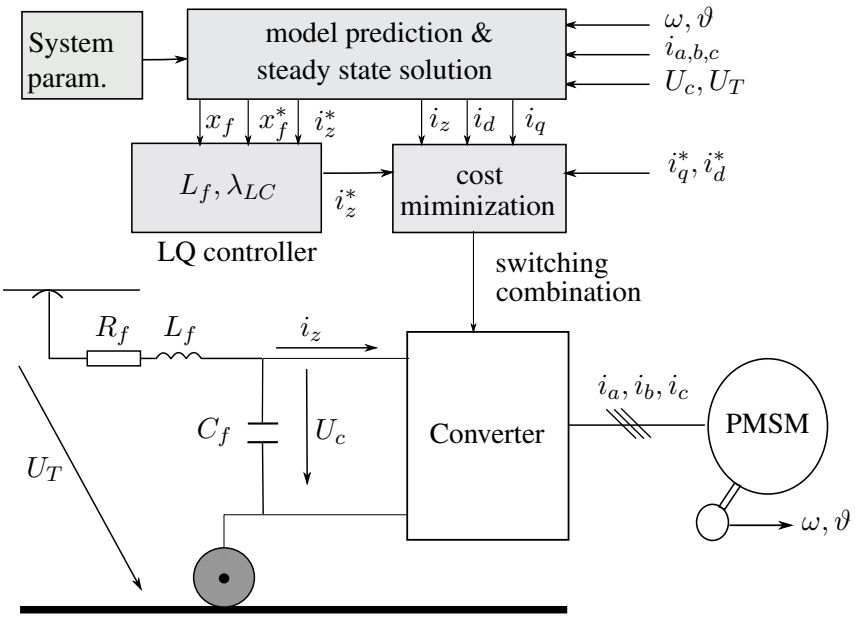

Figure 6.2.: Control scheme of the two stage predictive controller, where FCS-MPC is used in the first stage (short horizon) and LQR in the second stage (long horizon).

6.4. Simulations

The proposed control approach was tested on a system with parameters in Table A.3 and sampling period$\Delta t = 50\mu s$, In the first experiment, we compare properties of the LC filter. Substituting parameters of the filter Table A.3 into (6.9), we obtain linear model with eigenvalues at $[0.99998, 0.99998]$, i.e. almost at the stability boundary. Any disturbance can thus cause undamped or even unstable oscillations.

Since the LQR design yields linear controller, the properties of the closed loop can be tested using standard linear systems theory. This can be helpful for tuning of the penalization terms λ_C, λ_l and λ_z. We may design controllers for different penalization values and check the closed loop properties.

It remains to tune the relative penalizations, denoted by $\bar{\lambda}_*$, starting from a natural choice $\bar{\lambda}_* = 1$. For better intuition of the penalization matrices, we use penalizations inversialy proportional to the range of the variable, e.g.

$$\lambda_C = \frac{\bar{\lambda}_C}{(U_{C,min} - U_{C,max})^2},$$

where variable ranges for the system are:

$$U_T = U_C \in \langle 400, 900 \rangle\, V, \qquad i_l \in \langle -125, 125 \rangle\, A,$$
$$i_q \in \langle -212, 212 \rangle\, A, \qquad i_d \in \langle -212, 0 \rangle\, A.$$

Tuning of the penalizations is done in three steps:

1. Penalizations of the PMSM drive ($\bar{\lambda}_d$, $\bar{\lambda}_q$ and $\bar{\lambda}_S$) are tuned in ideal conditions with stable catenary supply. The aim is maximum dynamic performance of the drive. $\bar{\lambda}_S$ is tuned to reach the required average switching frequency (see 5.4) of 5kHz.

2. Penalizations of the LC filter ($\bar{\lambda}_C$, $\bar{\lambda}_L$ and $\bar{\lambda}_z$) are chosen using properties of the closed loop of the LC filter such as damping ratio of resonance frequency, see Figure 6.3. Note that: i) the penalization term $\bar{\lambda}_C$ has the greatest influence on damping of the oscillations, and ii) increase in $\bar{\lambda}_l$ is increasing the resonance frequency of the closed loop, while $\bar{\lambda}_C$ has negligible effect in this range.

3. Final check of the full system using simulations. It is necessary to check that the contribution of the LQR term is always lower than the limits for the hard constraints on the current in (6.1).

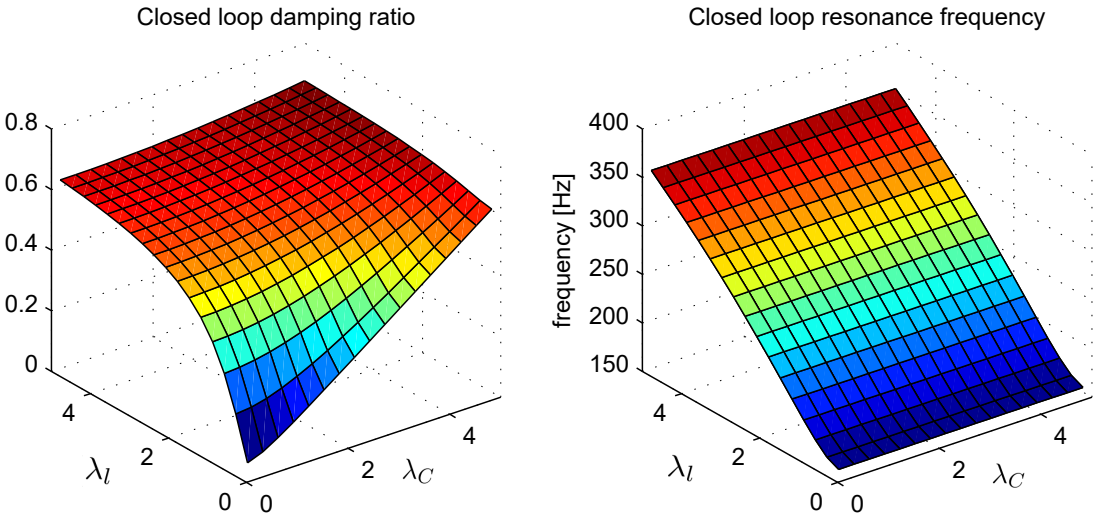

Figure 6.3.: Theoretical properties of the closed loop of the LC filter controlled by the LQR for different values of relative penalizations $\bar{\lambda}_l$ and $\bar{\lambda}_C$ and constant $\bar{\lambda}_z = 1$.

A suitable tool for final tuning of both components of the controller is the coefficient λ_{LC}in (6.17). Multiplying this value by a chosen constant c correspond to multiplication of all penalization matrices in cost function of the LC filter by the same constant. Thus by modifying λ_{LC} we preserve the closed loop performance of the LC filter and only tune the importance of LC-filter damping term in the cost function relative to the torque command tracking.

As a first scenario, we simulated acceleration and deceleration of the tram with fixed torque current command of $150\,\mathrm{A}$ (motor mode) and $-150\,\mathrm{A}$ (braking mode), respectively. We neglected the torque command ramp and considered an extreme step change of the torque current command. The cost function of the PMSM drive was same for all controllers with relative penalizations $\bar{\lambda}_d = \bar{\lambda}_q = 1$. Penalization of the switching of IGBTs was chosen as $\bar{\lambda}_S = 0.002$ for which the average switching frequency of the converter is the requested $5kHz$. Without active damping, the capacitor voltage oscillates uncontrollably (6.4 a)). Two active damping terms were tested: i) the LQ controller designed with relative penalizations $\bar{\lambda}_l = \bar{\lambda}_z = \bar{\lambda}_c = 1$ and with relative weight $\lambda_{LC} = 500$; and ii) the conventional damping

$$g_{UC,t} = g_{T,t} + (U_{c,t+1} - U_{c,f,t})^2 \frac{\bar{\lambda}_{uc}}{(U_{T,min} - U_{T,max})^2}, \tag{6.19}$$

where $U_{c,f,t}$ is the capacitor voltage filtered by a low-pass filter with cutoff frequency of 100Hz and relative penalization $\bar{\lambda}_{uc} = 1$. This method is closely related to the approach of [93]. The

results are displayed in Figure 6.4. Note that performance of both active damping terms is

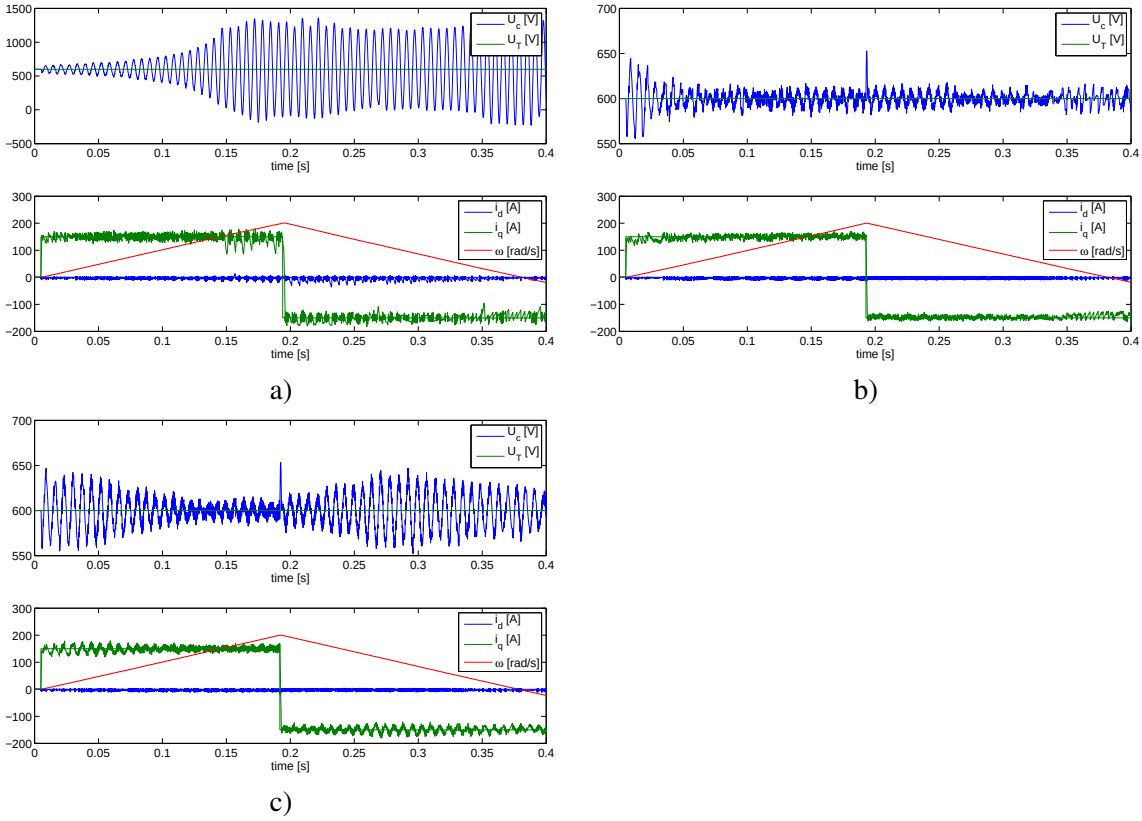

Figure 6.4.: Start-up, tram acceleration to $10km/h$ and deceleration to zero speed under FCS-MPC: a) without active damping, b) active damping using the proposed LQ approach, and c) conventional damping with filtered U_c; step change of torque current command to $150A$ (motor mode) and $-150A$ (braking mode), respectively. **Top rows**: catenary and filter capacitor voltage. **Bottom rows**: torque (i_q) and flux (i_d) components of the stator current vector and electrical rotor speed (ω).

comparable, with LQR resulting in lower dc-link voltage oscillations and smaller differences from the requested torque current command.

More demanding scenario is the step change of the catenary voltage from $600V$ to $550V$. The torque current command i_q^* was kept constant at 150A for the whole time of the simulation. If the drive was controlled by the FCS-MPC controller with only the PMSM cost (6.1), the reference current was followed exactly, however, the drop of the catenary voltage resulted in undamped oscillations (Figure 6.5a). Results of the same test with active damping terms designed with the same penalizations as in the previous scenario are displayed in Figure 6.5 b) and c), respectively. Note that in this case, the active damping based on LQR lookahead

approach (left) secures significantly better damping of the oscillations of the filter capacitor voltage and the control intervention in the torque current is also evidently smaller than in case of the conventional approach (right). In this simulation, the LQR active damping results in slightly lower switching frequency ($4.7kHz$) than without the LQR lookahead term (5kHz).

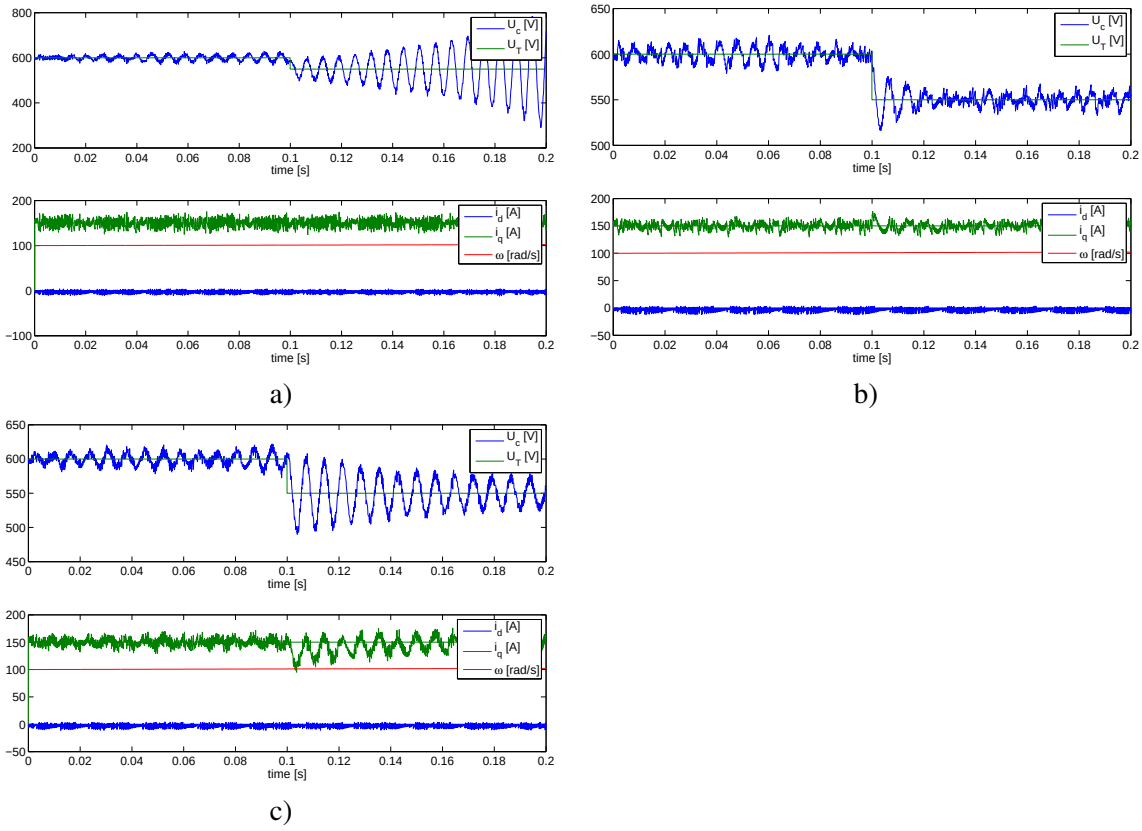

Figure 6.5.: Effect of a step change of the catenary voltage from 600 to $550V$ under FCS-MPC: a) without active damping, b) with active damping designed via LQR lookahead, and c) via conventional approach; fixed electrical rotor speed of $100rad/s$ and torque current command of $150A$. **Top rows**: catenary and filter capacitor voltage. **Bottom rows**: torque (i_q) and flux (i_d) components of the stator current vector and electrical rotor speed (ω).

6.4.1. Stability of the closed loop

Since parameters of the input catenary filter vary with position of the vehicle at supply section, it is necessary to study properties of the closed loop for different values of the input filter total inductance which is the sum of the fixed filter inductance (Table A.3) and varying equivalent inductance of the catenary. Therefore, we investigate properties of the closed loop with constant

controller, but varying L_f of the controlled system. Specifically we study the damping ratio and resonance frequency, [2], which characterize the frequency properties of the second order system. A Matlab function `damp.m` can be used for this purpose. Results of the sensitivity study to the increase of the total filter inductance is displayed in Figure 6.6.

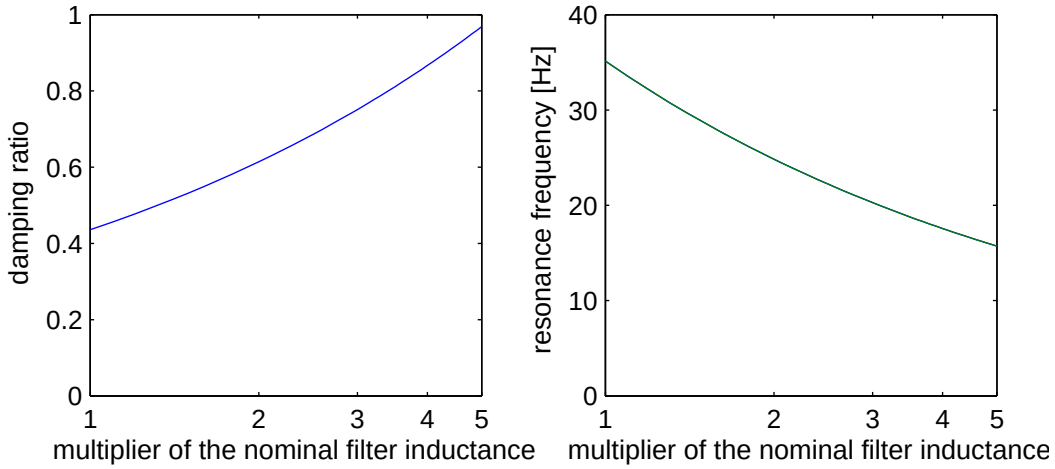

Figure 6.6.: Sensitivity study of the closed loop of the LC filter to increase of the total filter inductance.

Note that the less damped closed loop behavior is expected for the minimal filter inductance, which is achieved when the vehicle is close to the supply station, where the equivalent catenary inductance is very small. Therefore, it is recommended to tune the controller for such conditions.

6.5. Experimental results

A laboratory prototype of the traction PMSM drive (Figure A.3) was used to verify the proposed control approach experimentally. The test rig consists of intelligent power source by AMETEK emulating the catenary, the input LC filter which is connected to voltage source inverter supplying the PMSM. The proposed control algorithm was implemented in DSP Texas Instruments TMS320F28335. The parameters of experimental system are in table (A.2) yielding open-loop eigenvalues $[0.9998, 0.9998]$, i.e. about ten times farther from the stability boundary than the simulated tram drive.

Drive response to a step change of the catenary voltage from $200V$ to $150V$ was explored under constant electrical rotor speed of f_{me}=$20Hz$. The drive was operated in torque

[2] An interested reader may refer to [94] for more about resonance frequency and dumping ratio of the system.

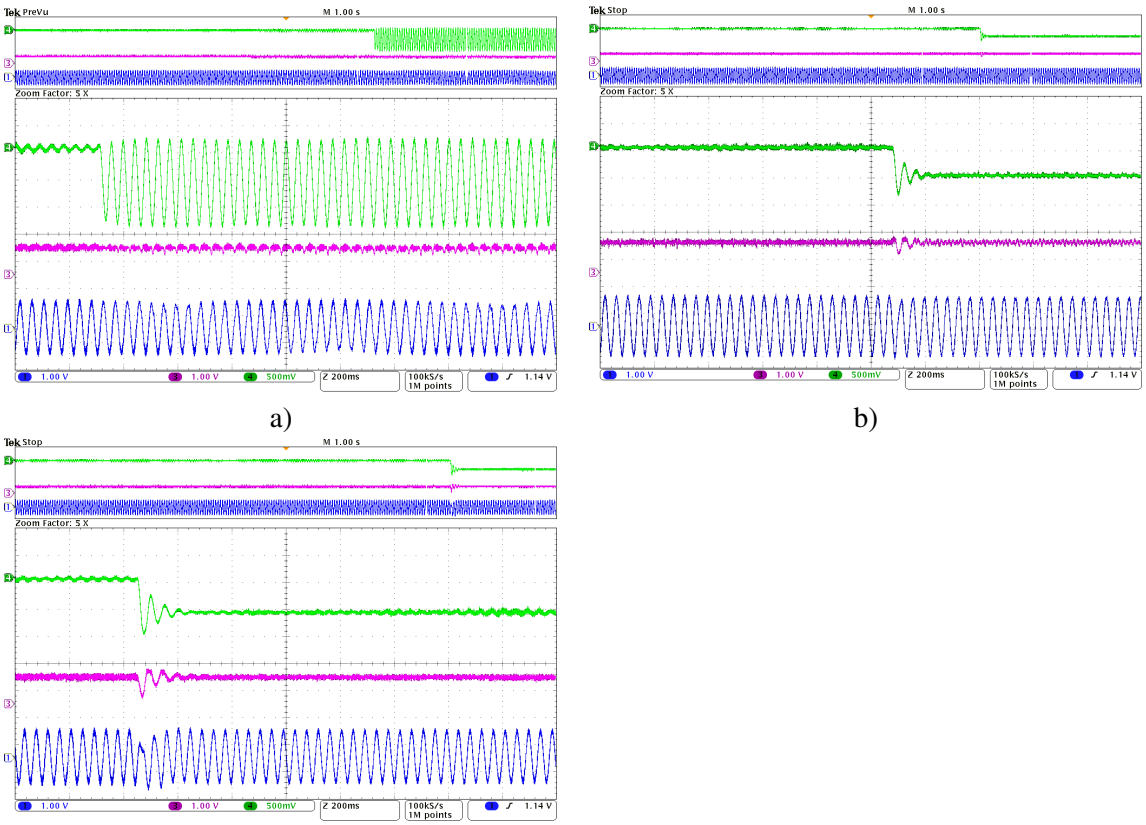

Figure 6.7.: Step change of the catenary voltage from 200 to 150V under FCS-MPC control: a) without active damping, b) with active damping using LQR lookahead, and c) conventional active damping; fixed el. rotor speed of 20Hz, constant torque current command 30A. ch1: i_a (30A/div), ch3: i_q (30A/div), ch4: U_c (50V/div).

control mode and the torque current command $i_q^*= 30A$ was kept constant during the experiment.

If the drive controller does not use any active damping method, the behavior of the drive under the tested conditions may results in undamped (or very lightly damped) oscillations of the input LC-filter as demonstrated in Figure 6.7 a). This behavior may result in emergency shutdown of the drive.

Next, we evaluated performance of two penalization terms of the basic FCS-MPC controller, the proposed LQR and the simple active damping (6.19) under the same test conditions, see Figure 6.7 b) and c), respectively. Both controllers were tuned to yield comparable performance. Note that in agreement with the simulation, the LQR damping term was able to stabilize the drive faster and with smaller deviation from the requested torque and flux currents.

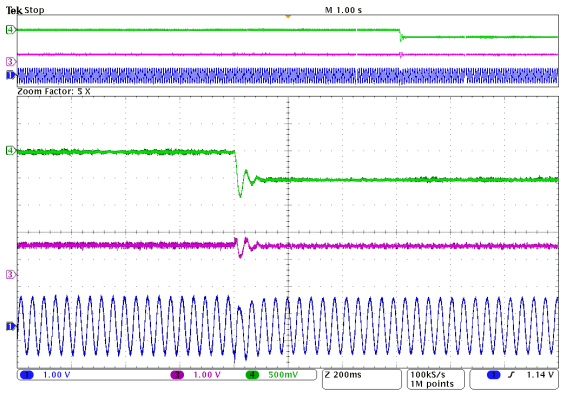

Figure 6.8.: Sensitivity of proposed control to the variation of total filter inductance – step change of the catenary voltage from 200 to 150V; FCS-MPC with active damping using LQR lookahead; mismatch in the filter inductance in the design and in the test rig, $L_{f,LQRdesign} = 0.1 L_{f,RIG}$, fixed el. rotor speed of $20Hz$, constant torque current command $30A$: ch1: i_a (30A/div), ch3: i_q (30A/div), ch4: U_c (50V/div).

An important problem of dc catenary fed traction vehicles is the change of the total input filter inductance with changing distance of the vehicle from the supply station. To investigate sensitivity of the control algorithm to the value of the total filter inductance, we tested performance of the control with LQR term designed under ten times lower filter inductance than the real inductance used in experiment. The controller was tuned with the same relative penalization $\lambda_* = 1$, and $\lambda_{LC} = 2$. Response of the resulting controller to the step change of the catenary voltage is displayed in Figure 6.8.

6.6. Conclusion

The problem of stability of the dc catenary fed traction drives was addressed using two stage model predictive control. In the first stage (short horizon), we used the FCS-MPC approach and in the second stage (long horizon) we used the LQR to approximate the cost to go function. The resulting control algorithm can be interpreted as a cascade of LQR and FCS-MPC controllers.

Stability of proposed traction drive controller to an extreme step change of the catenary voltage was tested in simulation and experiment. The proposed controller was shown to damp the resulting oscillation faster than conventional active damping terms and with smaller deviation of the requested torque and flux currents. This was achieved even in demanding situations such as low speed of the drive and varying inductance of the input filter due to the change of the vehicle position within the supply section.

The proposed control design methodology offers a range of attractive properties such as ability to change resonance frequency of the controlled LC filter. Full exploration of these advantages offers a lot of space for further research.

7. Conclusion

Model predictive control is one of the most promising research direction in control of drives and power converters. Due to its mathematical formulation it offers the possibility to operate the devices at maximum possible dynamics, considering maximum possible efficiency and robustness. It has already been successfully applied to a key components of the drive as well as the whole drive itself.

The MPC is defined as an optimization problem on a chosen prediction horizon. It has been shown that for longer prediction horizons the performance of MPC tends to improve however the computational cost may grow above the limits given by the capability of the control hardware. That is one of the potential reasons why MPC haven't been extensively used in industry so far. A standard solution is to pre-compute the optimal control law offline and approximate it as an explicit piece-wise affine control low for real time implementation. This way the computational cost can be reduced by order of magnitudes. However, an intuitive insight is lost and tuning of the controller via change of the cost function is computationally expensive. An alternative to this approach may be found by approximation of the cost function on the long horizon using simplified model. In this work, we have studied the use of linear/linearized model with quadratic cost, which allows to use the theory of state dependent Riccati equation (SDRE). This way the resulting control algorithm take into account long prediction horizon (possibly infinite) in computationally inexpensive way. However this solution does not consider hard constraints on the input variables nor the state variables which are important in speed control of an AC drive. Thus, we proposed several cost functions using combination of constraints and cost-to-go approximation to achieve the desired performance of the drive control. This approach has been elaborated into to three special cases of drive control.

- *Cascade free speed control of PMSM using PWM modulation (chapter*4*).* A well known SDRE has been used to approximate the solution of the optimization on long prediction horizon. It has been shown, that unconstrained SDRE solution accurately follows the MTPA curve. The main contribution of this chapter, however, is in design of a computationally efficient constraint manager, which is able to follow hard constraints. We

propose to use simplified convex optimization based on geometrical operations. The proposed solution provides near to optimal performance as the expensive solution of [31] but the computational demands are comparable with conventionally used cascade control schemes with PI/PID controllers.

- *FCS-MPC for speed control of PMSM drive with optimized switching losses (chapter*5*).* Contrary to PWM based approaches, FCS-MPC is characterized by limited set of control inputs which drastically simplifies the algorithm. However absence of the PWM leads to inconstant switching frequency. Very short sampling times are preferred to minimize the current ripple, which may imply frequent switching and thus high switching loses. Penalization of the switching on one-step-ahead horizon yields sub-optimal solution. In this chapter, we have showed, that a better solution can be obtained by the use of SDRE approach for design of the cost to go function that is optimized using one step FCS-MPC. The computational cost of the resulting algorithm is comparable to the conventional one step FCS-MPC. The proposed approach has been tested on speed control of PMSM drive and improvements were demonstrated on better harmonic distortion of the stator currents.

- *Improved Stability of DC Catenary Fed Traction Drives using FCS-MPC with lookahead (chapter*6*).* The stability of the LC input filter of the traction PMSM drive represent a challenging task for MPC design. It is essentially highly nonlinear control problem where the designer expects high-quality torque control and at the same time mitigation of the oscillations of trolley-wire input LC filter. The proposed approach is based on decomposition of the control problem to a control of the LC filter and torque control of the PMSM. The LQR is used to design the required current taken from the DC link i_z^*. It is than used as an additional term in one step ahead FCS-MPC which is used for torque control of PMSM drive. The proposed control algorithm has been tested on laboratory prototype of the traction PMSM drive. The results show, that proposed control approach achieved better results in comparison with existing active damping strategies in terms of the quality of both the torque control and stability of the dc- link filter. We have demonstrated the capability of this method on the extreme step change of the catenary voltage resulting in fast damping of the LC filter oscillations with eligible impact to the torque response. The proposed cost function can be further extended or modified to incorporate other control objectives. The resulting algorithm is computationally cheep as conventional one step FCS-MPC while providing the performance which takes into account long prediction horizons.

7.1. The main contribution of this research

- The detailed state of the art analysis of the MPC applied in ac electric drives has been provided together with the definition of the main existing problems.
- In the chapter 2 the basic theory of MPC has been provided
- The main focus of this thesis is on predictive control of ac electric drives specifically PMSM. The main contribution of this thesis is in design of MPC techniques considering long prediction horizons with low computational cost, suitable for real time implementation.

7.2. Perspective directions of future research

This thesis presented a possible way how to make the model predictive control accessible for electric drives using conventional control hardware. This was achieved by aproximating the cost to go function of the dynamic programming, which represents very simple way how to extend the prediction horizon of MPC while preserving very simple and computationaly cheap nature of the algorithm. The electric drives are, in most cases, considered to be linear or linearized systems for which an aproximation of the cost to go function may be easily find by analytical solution of the control problem. A more challenging task however is when the control needs to consider additional components of the drive which makes the whole system highly nonlinear and the linearization may not bee traceable. Therefore, approximation of the cost to go for complex nonlinear systems provides a lot of space for future research.

Another promising direction of further research of MPC, is the design of a cost function itself. We may enhance the control performance, extend the control objective, include the hard constraints satisfaction and even extend the prediction horizon of MPC by simply adjusting the cost function. In addition, if the cost function contains multiple control objectives, the optimization is more complex and often requires a difficult penalization tuning. This phenomenon is still widely unresolved.

List of Figures

List of Tables

References

[1] T. A. Lipo, *Vector control and dynamics of AC drives*, vol. 41. Oxford university press, 1996.

[2] D. Casadei, F. Profumo, G. Serra, and A. Tani, "Foc and dtc: two viable schemes for induction motors torque control," *IEEE transactions on Power Electronics*, vol. 17, no. 5, pp. 779–787, 2002.

[3] Z. Peroutka, K. Zeman, F. Krus, and F. Kosten, "New generation of trams with gearless wheel pmsm drives: From simple diagnostics to sensorless control," in *Power Electronics and Motion Control Conference (EPE/PEMC),*, pp. S10–31 –S10–36, 2010.

[4] D. Bertsekas, *Dynamic Programming and Optimal Control*. Nashua, US: Athena Scientific, 2001. 2nd edition.

[5] C. E. Garcia, D. M. Prett, and M. Morari, "Model predictive control: theory and practice—a survey," *Automatica*, vol. 25, no. 3, pp. 335–348, 1989.

[6] D. Clarke and R. Scattolini, "Constrained receding-horizon predictive control," in *IEE Proceedings D-Control Theory and Applications*, vol. 138, pp. 347–354, IET, 1991.

[7] T. Geyer, G. Papafotiou, and M. Morari, "Model predictive direct torque control – part i: Concept, algorithm, and analysis," *Industrial Electronics, IEEE Transactions on*, vol. 56, no. 6, pp. 1894–1905, 2009.

[8] J. Rodriguez and P. Cortes, *Predictive Control of Power Converters and Electrical Drives*. Wiley - IEEE, Wiley, 2012.

[9] M. Rivera, P. Correa, J. Rodriguez, I. Lizama, J. Espinoza, and C. Rojas, "Predictive control with active damping in a direct matrix converter," in *Energy Conversion Congress and Exposition, 2009. ECCE 2009. IEEE*, pp. 3057–3062, 2009.

[10] S. Kouro, P. Cortes, R. Vargas, U. Ammann, and J. Rodriguez, "Model predictive control a simple and powerful method to control power converters," *IEEE Transactions on Industrial Electronics*, vol. 56, pp. 1826–1838, June 2009.

[11] J. Rodriguez, M. Kazmierkowski, J. Espinoza, P. Zanchetta, H. Abu-Rub, H. Young, and C. Rojas, "State of the art of finite control set model predictive control in power electronics," *Industrial Informatics, IEEE Transactions on*, vol. 9, no. 2, pp. 1003–1016, 2013.

[12] S. A. Davari, D. A. Khaburi, and R. Kennel, "An improved fcs–mpc algorithm for an induction motor with an imposed optimized weighting factor," *IEEE Transactions on Power Electronics*, vol. 27, no. 3, pp. 1540–1551, 2012.

[13] C. S. Lim, E. Levi, M. Jones, N. Rahim, and W. Hew, "Fcs-mpc-based current control of a five-phase induction motor and its comparison with pi-pwm control," *Industrial Electronics, IEEE Transactions on*, vol. 61, pp. 149–163, Jan 2014.

[14] M. Preindl and S. Bolognani, "Model predictive direct speed control with finite control set of pmsm drive systems," *IEEE Transactions on Power Electronics*, vol. 28, no. 2, pp. 1007–1015, 2013.

[15] A. Formentini, A. Trentin, M. Marchesoni, P. Zanchetta, and P. Wheeler, "Speed finite control set model predictive control of a pmsm fed by matrix converter," *IEEE Transactions on Industrial Electronics*, vol. 62, no. 11, pp. 6786–6796, 2015.

[16] M. Salehifar and M. Moreno-Equilaz, "Fault diagnosis and fault-tolerant finite control set-model predictive control of a multiphase voltage-source inverter supplying bldc motor," *ISA transactions*, vol. 60, pp. 143–155, 2016.

[17] M. Preindl, E. Schaltz, and P. Thogersen, "Switching frequency reduction using model predictive direct current control for high-power voltage source inverters," *Industrial Electronics, IEEE Transactions on*, vol. 58, pp. 2826–2835, July 2011.

[18] R. Ramirez, J. Espinoza, F. Villarroel, E. Maurelia, and M. Reyes, "A novel hybrid finite control set model predictive control scheme with reduced switching," *Industrial Electronics, IEEE Transactions on*, vol. 61, pp. 5912–5920, Nov 2014.

[19] T. Geyer, "A comparison of control and modulation schemes for medium-voltage drives: Emerging predictive control concepts versus field oriented control," in *Energy Conversion Congress and Exposition (ECCE), 2010 IEEE*, pp. 2836–2843, Sept 2010.

[20] S. Vazquez, C. Montero, C. Bordons, and L. G. Franquelo, "Model predictive control of a vsi with long prediction horizon," in *2011 IEEE International Symposium on Industrial Electronics*, pp. 1805–1810, IEEE, 2011.

[21] Z. Ma, S. Saeidi, and R. Kennel, "Fpga implementation of model predictive control with constant switching frequency for pmsm drives," *Industrial Informatics, IEEE Transactions on*, vol. 10, pp. 2055–2063, Nov 2014.

[22] E. L. Lawler and D. E. Wood, "Branch-and-bound methods: A survey," *Operations research*, vol. 14, no. 4, pp. 699–719, 1966.

[23] M. J. Duran, J. Prieto, F. Barrero, and S. Toral, "Predictive current control of dual three-phase drives using restrained search techniques," *IEEE Transactions on Industrial Electronics*, vol. 58, no. 8, pp. 3253–3263, 2011.

[24] T. Geyer, "Computationally efficient model predictive direct torque control," *Power Electronics, IEEE Transactions on*, vol. 26, pp. 2804–2816, Oct 2011.

[25] B. Hassibi and H. Vikalo, "On the sphere-decoding algorithm i. expected complexity," *IEEE transactions on signal processing*, vol. 53, no. 8, pp. 2806–2818, 2005.

[26] T. Geyer and D. Quevedo, "Multistep finite control set model predictive control for power electronics," *Power Electronics, IEEE Transactions on*, vol. 29, pp. 6836–6846, Dec 2014.

[27] P. Karamanakos, T. Geyer, and R. Kennel, "Reformulation of the long-horizon direct model predictive control problem to reduce the computational effort," in *Energy Conversion Congress and Exposition (ECCE), 2014 IEEE*, pp. 3512–3519, Sept 2014.

[28] T. Geyer and D. Quevedo, "Performance of multistep finite control set model predictive control for power electronics," *Power Electronics, IEEE Transactions on*, vol. 30, pp. 1633–1644, March 2015.

[29] W. Xie, X. Wang, F. Wang, W. Xu, R. M. Kennel, D. Gerling, and R. D. Lorenz, "Finite-control-set model predictive torque control with a deadbeat solution for pmsm drives," *IEEE Transactions on Industrial Electronics*, vol. 62, pp. 5402–5410, Sept 2015.

[30] M. Gendrin, J.-Y. Gauthier, and X. Lin-Shi, "An improved model predictive control for online pwm sequence selection applied on converter," in *Industrial Electronics Society, IECON 2014-40th Annual Conference of the IEEE*, pp. 1233–1239, IEEE, 2014.

[31] M. Preindl and S. Bolognani, "Optimal state reference computation with constrained mtpa criterion for pm motor drives," *Power Electronics, IEEE Transactions on*, vol. 30, no. 8, pp. 4524–4535, 2015.

[32] M. Preindl, "Robust control invariant sets and lyapunov-based mpc for ipm synchronous motor drives," *IEEE Transactions on Industrial Electronics*, vol. 63, pp. 3925–3933, June 2016.

[33] P. E. Gill and W. Murray, "Numerically stable methods for quadratic programming," *Mathematical programming*, vol. 14, no. 1, pp. 349–372, 1978.

[34] A. Bemporad, F. Borrelli, M. Morari, *et al.*, "Model predictive control based on linear programming˜ the explicit solution," *IEEE Transactions on Automatic Control*, vol. 47, no. 12, pp. 1974–1985, 2002.

[35] T. Besselmann, J. Lofberg, and M. Morari, "Explicit mpc for lpv systems: Stability and optimality," *Automatic Control, IEEE Transactions on*, vol. 57, pp. 2322–2332, Sept 2012.

[36] R. Bellman, "Dynamic programming and lagrange multipliers," *Proceedings of the National Academy of Sciences of the United States of America*, vol. 42, no. 10, p. 767, 1956.

[37] P. Stolze, M. Tomlinson, R. Kennel, and T. Mouton, "Heuristic finite-set model predictive current control for induction machines," in *ECCE Asia Downunder (ECCE Asia), 2013 IEEE*, pp. 1221–1226, June 2013.

[38] E. Fuentes, D. Kalise, J. Rodriguez, and R. Kennel, "Cascade-free predictive speed control for electrical drives," *Industrial Electronics, IEEE Transactions on*, vol. 61, pp. 2176–2184, May 2014.

[39] D. Limón, I. Alvarado, T. Alamo, and E. F. Camacho, "Mpc for tracking piecewise constant references for constrained linear systems," *Automatica*, vol. 44, no. 9, pp. 2382–2387, 2008.

[40] T. Tarczewski and L. M. Grzesiak, "Constrained state feedback speed control of pmsm based on model predictive approach," *IEEE Transactions on Industrial Electronics*, vol. 63, pp. 3867–3875, June 2016.

[41] T. D. Do, H. H. Choi, and J.-W. Jung, "Sdre-based near optimal control system design for pm synchronous motor," *Industrial Electronics, IEEE Transactions on*, vol. 59, pp. 4063–4074, Nov 2012.

[42] T. D. Do, S. Kwak, H. H. Choi, and J.-W. Jung, "Suboptimal control scheme design for interior permanent-magnet synchronous motors: An sdre-based approach," *Power Electronics, IEEE Transactions on*, vol. 29, pp. 3020–3031, June 2014.

[43] R. Errouissi, M. Ouhrouche, W.-H. Chen, and A. M. Trzynadlowski, "Robust nonlinear predictive controller for permanent-magnet synchronous motors with an optimized cost function," *Industrial Electronics, IEEE Transactions on*, vol. 59, no. 7, pp. 2849–2858, 2012.

[44] A. Damiano, G. Gatto, I. Marongiu, A. Perfetto, and A. Serpi, "Operating constraints management of a surface-mounted pm synchronous machine by means of an fpga-based model predictive control algorithm," *Industrial Informatics, IEEE Transactions on*, vol. 10, pp. 243–255, Feb 2014.

[45] J. Lemmens, P. Vanassche, and J. Driesen, "Pmsm drive current and voltage limiting as a constraint optimal control problem," *Industrial Electronics, IEEE Transactions on*, 2014.

[46] A. Linder, R. Kanchan, R. Kennel, and P. Stolze, *Model-based predictive control of electric drives*. Cuvillier, 2010.

[47] T. Cimen, "State-dependent riccati equation (sdre) control: a survey," *IFAC Proceedings Volumes*, vol. 41, no. 2, pp. 3761–3775, 2008.

[48] H. Banks, B. Lewis, and H. Tran, "Nonlinear feedback controllers and compensators: a state-dependent riccati equation approach," *Computational Optimization and Applications*, vol. 37, no. 2, pp. 177–218, 2007.

[49] M. Morari and J. H. Lee, "Model predictive control: past, present and future," *Computers & Chemical Engineering*, vol. 23, no. 4, pp. 667–682, 1999.

[50] R. T. Marler and J. S. Arora, "Survey of multi-objective optimization methods for engineering," *Structural and multidisciplinary optimization*, vol. 26, no. 6, pp. 369–395, 2004.

[51] P. Cortés, S. Kouro, B. La Rocca, R. Vargas, J. Rodríguez, J. I. León, S. Vazquez, and L. G. Franquelo, "Guidelines for weighting factors design in model predictive control of power converters and drives," in *Industrial Technology, 2009. ICIT 2009. IEEE International Conference on*, pp. 1–7, IEEE, 2009.

[52] C. A. Rojas, J. Rodriguez, F. Villarroel, J. R. Espinoza, C. A. Silva, and M. Trincado, "Predictive torque and flux control without weighting factors," *IEEE Transactions on Industrial Electronics*, vol. 60, no. 2, pp. 681–690, 2013.

[53] F. Villarroel, J. R. Espinoza, C. A. Rojas, J. Rodriguez, M. Rivera, and D. Sbarbaro, "Multiobjective switching state selector for finite-states model predictive control based on fuzzy decision making in a matrix converter," *Industrial Electronics, IEEE Transactions on*, vol. 60, no. 2, pp. 589–599, 2013.

[54] S. Boyd and L. Vandenberghe, "Convex optimization," 2004.

[55] E. Ostertag, *Mono-and Multivariable Control and Estimation: Linear, Quadratic and LMI Methods*, vol. 2. Springer, 2011.

[56] D. Q. Mayne, J. B. Rawlings, C. V. Rao, and P. O. Scokaert, "Constrained model predictive control: Stability and optimality," *Automatica*, vol. 36, no. 6, pp. 789–814, 2000.

[57] A. Zheng and M. Morari, "Stability of model predictive control with mixed constraints," *IEEE Transactions on Automatic Control*, vol. 40, no. 10, pp. 1818–1823, 1995.

[58] A. G. Wills and W. P. Heath, "Barrier function based model predictive control," *Automatica*, vol. 40, no. 8, pp. 1415–1422, 2004.

[59] V. Peterka, "Predictor-based self-tuning control," *Automatica*, vol. 20, no. 1, pp. 39–50, 1984.

[60] P. Lancaster and L. Rodman, *Algebraic riccati equations*. Clarendon press, 1995.

[61] R. Kalman, "A new approach to linear filtering and prediction problem," *Trans. ASME, Ser. D, J. Basic Eng.*, vol. 82, pp. 34–45, 1960.

[62] M. Grewal and A. Andrews, *Kalman filtering: theory and practice using MATLAB*. Wiley-IEEE Press, 2008.

[63] M. Preindl and S. Bolognani, "Model predictive direct torque control with finite control set for pmsm drive systems, part 1: Maximum torque per ampere operation," *Industrial Informatics, IEEE Transactions on*, vol. 9, pp. 1912–1921, Nov 2013.

[64] I. CVX Research, "CVX: Matlab software for disciplined convex programming, version 2.0." `http://cvxr.com/cvx`, Aug. 2012.

[65] Z. Mynar, L. Vesely, and P. Vaclavek, "Pmsm model predictive control with field weakening implementation," *IEEE Transactions on Industrial Electronics*, vol. PP, no. 99, pp. 1–1, 2016.

[66] K. Aström, "Theory and applications of adaptive control," *Automatica*, vol. 19, no. 5, pp. 471–486, 1983.

[67] S. Bolognani, L. Tubiana, and M. Zigliotto, "Extended kalman filter tuning in sensorless pmsm drives," *IEEE Transactions on Industry Applications*, vol. 39, no. 6, pp. 1741–1747, 2003.

[68] D. Loebis, R. Sutton, J. Chudley, and W. Naeem, "Adaptive tuning of a kalman filter via fuzzy logic for an intelligent auv navigation system," *Control engineering practice*, vol. 12, no. 12, pp. 1531–1539, 2004.

[69] C. Hide, T. Moore, and M. Smith, "Adaptive kalman filtering for low-cost ins/gps," *The Journal of Navigation*, vol. 56, no. 01, pp. 143–152, 2003.

[70] C. Lomont, "Fast inverse square root," tech. rep., West Lafayette, Indiana, 2003.

[71] M. Preindl and S. Bolognani, "Model predictive direct torque control with finite control set for pmsm drive systems, part 2: field weakening operation," *Industrial Informatics, IEEE Transactions on*, vol. 9, no. 2, pp. 648–657, 2013.

[72] W. A. Kester, *Data conversion handbook*. Newnes, 2005.

[73] M. R. Arahal, M. Castilla, J. D. Álvarez, and J. A. Sánchez, "Subharmonic content in finite-state model predictive current control of im," in *Industrial Electronics Society, IECON 2013-39th Annual Conference of the IEEE*, pp. 5866–5872, IEEE, 2013.

[74] T. Glasberger, M. Janda, and Z. Peroutka, "Frequency domain evaluation of a traction pmsm drive with direct torque control including field weakening area," in *Power Electronics and Applications (EPE), 2013 15th European Conference on*, pp. 1–8, IEEE, 2013.

[75] B. Delemontey, C. Iung, B. Jacquot, B. De Fornel, and J. Bavard, "Nonlinear decoupling of an induction motor drive with input filter," in *Control Applications, 1995., Proceedings of the 4th IEEE Conference on*, pp. 1004–1009, IEEE, 1995.

[76] S. Sudhoff, K. Corzine, S. Glover, H. Hegner, and H. Robey Jr, "Dc link stabilized field oriented control of electric propulsion systems," *Energy Conversion, IEEE Transactions on*, vol. 13, no. 1, pp. 27–33, 1998.

[77] B.-H. Bae, B.-H. Cho, and S.-K. Sul, "Damping control strategy for the vector controlled traction drive," in *Proc. 9th Eur. Conf. Power Electron. and Appl*, 2001.

[78] V. Dzhankhotov and J. Pyrhonen, "Passive lc filter design considerations for motor applications," *Industrial Electronics, IEEE Transactions on*, vol. 60, pp. 4253–4259, Oct 2013.

[79] H. Mosskull, J. Galic, and B. Wahlberg, "Stabilization of induction motor drives with poorly damped input filters," *Industrial Electronics, IEEE Transactions on*, vol. 54, no. 5, pp. 2724–2734, 2007.

[80] Z. Bai, H. Ma, D. Xu, B. Wu, Y. Fang, and Y. Yao, "Resonance damping and harmonic suppression for grid-connected current-source converter," *Industrial Electronics, IEEE Transactions on*, vol. 61, pp. 3146–3154, July 2014.

[81] M. Tomlinson, T. Mouton, R. Kennel, and P. Stolze, "Model predictive control of an ac-to-ac converter with input and output lc filter," in *Industrial Electronics and Applications (ICIEA), 2011 6th IEEE Conference on*, pp. 1233–1238, June 2011.

[82] B. Bahrani and A. Rufer, "Optimization-based voltage support in traction networks using active line-side converters," *Power Electronics, IEEE Transactions on*, vol. 28, no. 2, pp. 673–685, 2013.

[83] A. Houari, H. Renaudineau, B. Nahid-Mobarakeh, J.-P. Martin, S. Pierfederici, and F. Meibody-Tabar, "Large signal stability analysis and stabilization of converters connected to grid through lcl filters," *Industrial Electronics, IEEE Transactions on*, vol. PP, no. 99, pp. 1–1, 2014.

[84] L. Wang and D.-N. Truong, "Stability enhancement of a power system with a pmsg-based and a dfig-based offshore wind farm using a svc with an adaptive-network-based fuzzy inference system," *Industrial Electronics, IEEE Transactions on*, vol. 60, pp. 2799–2807, July 2013.

[85] A. Looser and J. Kolar, "An active magnetic damper concept for stabilization of gas bearings in high-speed permanent-magnet machines," *Industrial Electronics, IEEE Transactions on*, vol. 61, pp. 3089–3098, June 2014.

[86] S. Zheng, B. HAN, and L. Guo, "Composite hierarchical anti-disturbance control for magnetic bearing system subject to harmonic drive resonance and gyroscopic torque," *Industrial Electronics, IEEE Transactions on*, vol. PP, no. 99, pp. 1–1, 2014.

[87] K. Erenturk, "Fractional-order PI$^{\lambda}$D$^{\mu}$ and active disturbance rejection control of nonlinear two-mass drive system," *Industrial Electronics, IEEE Transactions on*, vol. 60, pp. 3806–3813, Sept 2013.

[88] J. Guzinski, "Closed loop control of ac drive with lc filter," in *Power Electronics and Motion Control Conference, 2008. EPE-PEMC 2008. 13th*, pp. 994–1001, Sept 2008.

[89] K. Hatua, A. Jain, D. Banerjee, and V. T. Ranganathan, "Active damping of output lc filter resonance for vector-controlled vsi-fed ac motor drives," *Industrial Electronics, IEEE Transactions on*, vol. 59, pp. 334–342, Jan 2012.

[90] D. Marx, S. Pierfederici, and B. Davat, "Nonlinear control of an inverter motor drive system with input filter – large signal analysis of the dc-link voltage stability," in *Power Electronics Specialists Conference, 2008. PESC 2008. IEEE*, pp. 498–503, June 2008.

[91] J. Stumper, A. Dotlinger, R. Kennel, *et al.*, "Loss minimization of induction machines in dynamic operation," *Energy Conversion, IEEE Transactions on*, vol. 28, no. 3, pp. 726–735, 2013.

[92] N. Ameen, B. Galal, R. Kennel, and R. Kanchan, "The polynomial approximation of the explicit solution of model-based predictive controller for drive applications," in *Predictive Control of Electrical Drives and Power Electronics (PRECEDE), 2011 Workshop on*, pp. 76–81, IEEE, 2011.

[93] S. Mastellone, G. Papafotiou, and E. Liakos, "Model predictive direct torque control for mv drives with lc filters," in *Power Electronics and Applications, 2009. EPE '09. 13th European Conference on*, pp. 1–10, 2009.

[94] D. G. Alciatore, *Introduction to mechatronics and measurement systems*. Tata McGraw-Hill Education, 2007.

[95] T. Kosan, M. Jara, D. Janik, and Z. Peroutka, "Complete development platform for multilevel converters and complex control algorithms," in *Proceedings of the 16th International Conference on Mechatronics - Mechatronika 2014*, pp. 152–157, Dec 2014.

List of Author's publications

Jurnal papers

[A1] ŠMÍDL, V., JANOUŠ, Š., PEROUTKA, Z. Improved stability of DC catenary fed traction drives using two stage predictive control. IEEE Transactions on industrial electronics, 2015, roč. 62, č. 5, s. 3192-3201. ISSN: 0278-0046

[A2] ŠMÍDL, V., JANOUŠ, Š., PEROUTKA, Z. Fast Algorithm for Predictive Control of PMSM Drive Using SDRE and Convex Optimization, IEEE Transactions on industrial electronics, 2017 (currently under review)

International conference papers

[A3] ŠMÍDL, V., MÁCHA, V., JANOUŠ, Š., PEROUTKA, Z. Analysis of cost functions and setpoints for predictive speed control of PMSM drives. In Proceedings of the 18th European Conference on Power Electronics and Application (EPE ECCE Europe 2016). Piscataway: IEEE, 2016. s. 1-8. ISBN: 978-9-0758-1524-5

[A4] JANÍK, D., KOŠAN, T., JANOUŠ, Š., SADSKÝ, J., PEROUTKA, Z. The SVPWM modulation technique with active voltage balancing control for 3-level ANPC inverter. In Proceedings of the 20th International Conference on Applied Electronics 2015 (APPEL 2015). Piscataway: IEEE, 2015. s. 81-84. ISBN: 978-80-261-0385-1 , ISSN: 1803-7232

[A5] ŠMÍDL, V., JANOUŠ, Š., PEROUTKA, Z. Frequency spectrum shaping using finite control set MPC with LQ lookahead. In Proceedings of the 3rd Symposium on Predictive Control of Electrical Drives and Power Electronics (PRECEDE 2015). Piscataway: IEEE, 2015. s. 1-5. ISBN: 978-1-5090-1717-1

[A6] ŠMÍDL, V., MÁCHA, V., JANOUŠ, Š., PEROUTKA, Z. Predictive current limiter for LQ based control of AC drives. In Proceedings of the 3rd Symposium on Predictive Control

of Electrical Drives and Power Electronics (PRECEDE 2015). Piscataway: IEEE, 2015. s. 1-6. ISBN: 978-1-5090-1717-1

[A7] JANOUŠ, Š., DJANÍK, D., KOŠAN, T.,KAMENICKÝ,P. and PEROUTKA, Z., "Comparative study of vector PWM and FS-MPC for 3-level Neutral Point Clamped converter," Proceedings of the 16th International Conference on Mechatronics - Mechatronika 2014, Brno, 2014, pp. 158-163. doi: 10.1109/MECHATRONIKA.2014.7018252

[A8] ŠMÍDL, V., JANOUŠ, Š., PEROUTKA, Z. Extending horizon of finite control set MPC of PMSM drive with input LC filter using LQ lookahead. In Proceedings of IECON 2014 : 40th Annual Conference of the IEEE Industrial Electronics Society. Piscataway: IEEE, 2014. s. 581-586. ISBN: 978-1-4799-4033-2 , ISSN: 1553-572X

[A9] JANOUŠ, Š., ŠMÍDL, V., PEROUTKA, Z. "Feed-forward guided generalized predictive control of PMSM drive," 2013 IEEE International Symposium on Industrial Electronics, Taipei, Taiwan, 2013, pp. 1-6. doi: 10.1109/ISIE.2013.6563785

[A10] JANOUŠ, Š., PEROUTKA, Z. Analysis of Open-Loop Model-Based Sensorless Control of PMSM Drive. In 2011 International Conference on Applied Electronics. Plzeň: Západočeská univerzita v Plzni, 2012. s. 123-127. ISBN: 978-80-261-0038-6 , ISSN: 1803-7232

Czech conference papers

[A11] JANOUŠ, Š., ŠMÍDL, V., PEROUTKA, Z. Prediktivní regulátor pro řízení rychlosti pohonu s PMSM. In Elektrické pohony : XXXIV. konference (ELPO 2015). Plzeň: Česká elektrotechnická společnost, 2015. s. 1-7. ISBN: 978-80-02-02592-4

[A12] JANOUŠ, Š., JANÍK, D., KOŠAN, T. FCS-MPC pro vícehladinové měniče. In Elektrotechnika a informatika 2014, část druhá, Elektronika. Plzeň: Západočeská univerzita v Plzni, 2014. s. 29-32. ISBN: 978-80-261-0366-0

[A13] JANOUŠ, Š. Využití algoritmů prediktivního řízení při stabilizaci napětí na vstupním kondenzátoru trakčního pohonu s PMSM. In Elektrotechnika a informatika 2013. Část 1., Elektrotechnika. Plzeň: Západočeská univerzita v Plzni, 2013. s. 49-52. ISBN: 978-80-261-0233-5

[A13] JANOUŠ, Š. Návrh a optimalizace prediktivního regulátoru pro PMSM. In Elektrotechnika a informatika 2012. Část 1., Elektrotechnika. Plzeň: Západočeská univerzita v Plzni, 2012. s. 41-44. ISBN: 978-80-261-0120-8

[A15] JANOUŠ, Š. Bezsenzorové řízení PMSM. In Elektrotechnika a informatika 2011. Část druhá. Elektronika.. Plzeň: Západočeská univerzita, 2011. s. 43-46. ISBN: 978-80-261-0015-

Research reports

[A16] TALLA, J., JANOUŠ, Š. Stavové DQ modely LCL filtrů. Západočeská univerzita v Plzni, 2015.

[A17] JANÍK, D., JANOUŠ, Š., KOŠAN, T. Návrh modulátoru pro 3úrovňový měnič s aktivním clampingem. ČKD ELEKTROTECHNIKA, a.s., 2014.

[A18] JANÍK, D., JANOUŠ, Š., KOŠAN, T. Návrh a implementace FS-MPC regulátoru pro řízení vícehladinových měničů. ČKD Elektrotechnika, 2014.

[A19] JANOUŠ, Š., GLASBERGER, T. Software analysis of sensored and sensorless drive control algorithms (DV006). Západočeská univerzita v Plzni, 2014.

[A20] JANÍK, D., JANOUŠ, Š. Implementace modulátoru SVPWM pro měnič 3L-ANPC. ČKD ELEKTROTECHNIKA, a.s., 2014.

[A21] JANOUŠ, Š., ŠMÍDL, V., PEROUTKA, Z. Stavový regulátor založený na algoritmech prediktivního řízení doplněný dopředným modelem. Plzeň : Západočeská univerzita, 2013. 24 s.

[A22] JANOUŠ, Š., JÁRA, M. Analýza možných topologických struktur pro pomocné pohony a nabíječe vozové baterie - analýza nabíječe ZIVAN NG3. Plzeň : Škoda Electric, a.s., 2011. 13 s.

[A23] JANOUŠ, Š., JÁRA, M. Analýza možných topologických struktur pro pomocné měniče a nabíječe vozové baterie –nanokrystalické materiály. Plzeň : Škoda electric, 2011. 40 s.

Functional prototypes and softwares

[A24] JANOUŠ, Š., CIBULKA, J. Prototype of a new induction motor based servodrive. 2016.

[A25] UZEL, D., ŠMÍDL, V., VOŠMIK, D., JANOUŠ, Š. Software library of estimator and soft sensors. 2016.

[A26] JANÍK, D., JANOUŠ, Š. Modulátor pro řízení 3úrovňového měniče typu ANPC implementovaný v obvodu FPGA. 2014.

[A27] FOŘT, J., PITTERMANN, M., KŮS, V., JANOUŠ, Š. Regulační systém pro generování řídicích signálů pro simulaci přechodových jevů asynchronního motoru napájeného z napěťového střídače. 2012.

Appendix A.

The test rig - traction drive prototype

A.1. Parameters of the PMSM machine

Table A.1.: Parameters of PMSM

Nominal voltage	$3x400V$
Nominal frequency	$100Hz$
Rated power	$10.7kW$
Number of pole-pairs	4
Stator resistance	$R_s = 0.2\Omega$
Stator inductance in d axe	$L_{sd} = 0.35H$
Stator inductance in q axe	$L_{sq} = 0.4H$
Permanent magnet flux	$\Psi_{PM} = 0.2Wb$
Rated power	$P_{pmsm} = 10.7kW$

A.2. Parameters of the input LC filter (laboratory prototype)

Table A.2.: Parameters of PMSM

Filter resistance	$R_f = 0.15\Omega$
Input inductance	$L_f = 0.01H$
Input capacitor	$C_f = 0.004F$

A.3. Parameters of the traction drive and input LC filter (low floor tram Škoda ForCity)

Table A.3.: Parameters of of the low floor tram Škoda ForCity used in simulation of the traction PMSM drive:

Nominal voltage (effective)	$230V$
Nominal frequency	$73Hz$
Rated power	$58kW$
Number of pole-pairs	22
Stator resistance	$R_s = 0.2085\Omega$
Stator inductance	L_{sd}=$L_{sq} = 0.0025H$
Permanent magnet flux	$\Psi_{PM} = 0.398Wb$
Filter resistance	$R_f = 0.005\Omega$
Input inductance	$L_f = 0.001H$
Input capacitor	$C_f = 0.001F$

A.4. Control hardware

This control hardware was developed by Ing. Tomáš Košan Ph.d., for the purpose of testing advanced algorithms and drive topologies. It combines DSP TMS320F28335 which supports floating point calculation and FPGA Altera Cyclon III on a single control unit design with sufficiently large number of peripherals (PWM outputs, A/D converters, etc.) which allows to control extremely complex drive topologies, including drives with various multilevel converter designs. The detailed description can be found in [95].

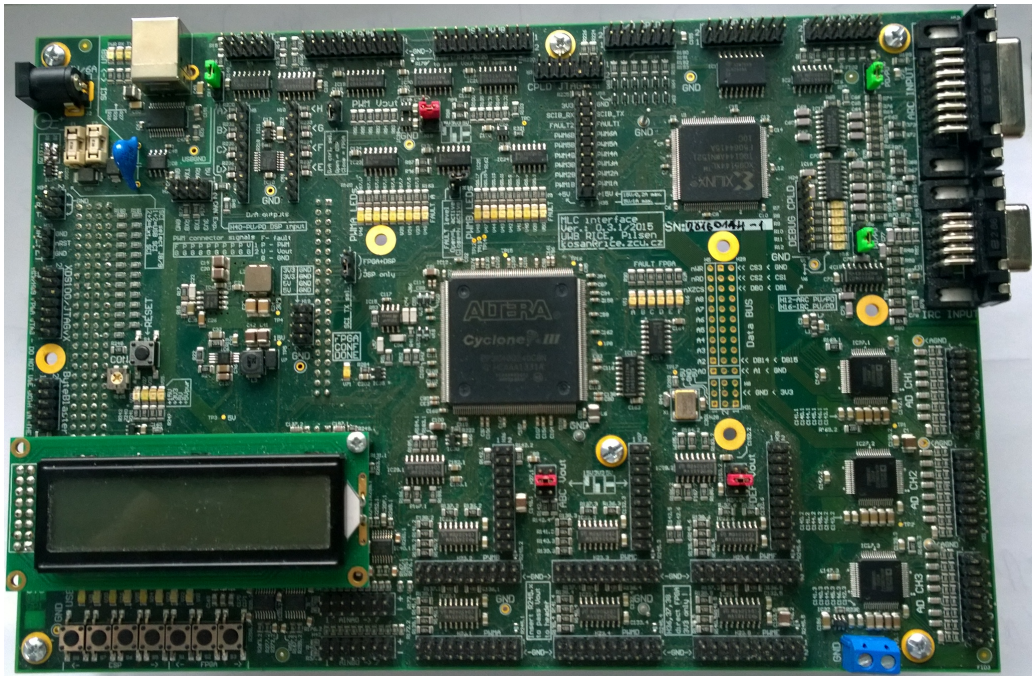

Figure A.1.: Control hardware

A.5. Laboratory PMSM drive

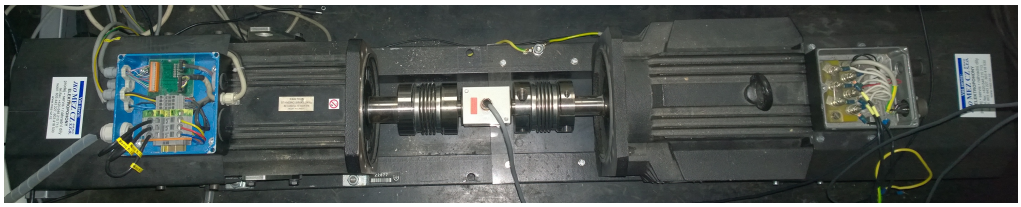

Figure A.2.: Laboratory PMSM of rated power $10.7\,kW$ (left machine) mechanically coupled with induction machine of rated power $14.5kW$ used as a loading machine (right machine)

A.6. Laboratory prototype of the traction drive with PMSM fed from DC catenary

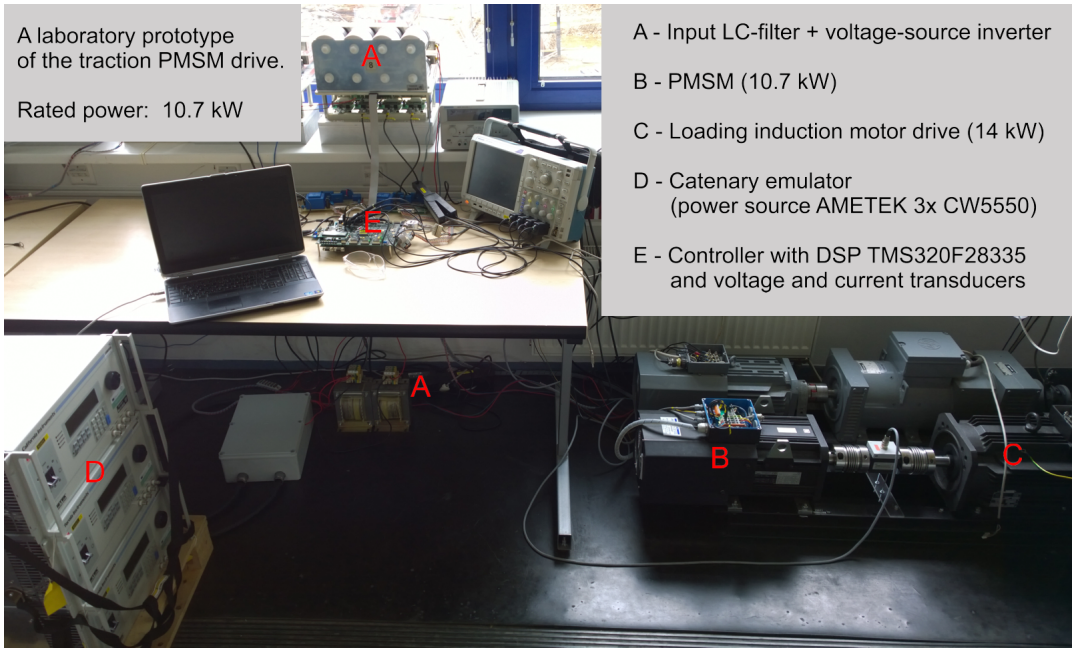

Figure A.3.: Laboratory prototype of the traction PMSM drive